PONTIFICIA
UNIVERSIDAD
CATÓLICA
DEL PERÚ

TECHNISCHE UNIVERSITÄT
ILMENAU

Technische Universität Ilmenau

Department of Computer Science and Automation
Control Engineering Group

Master Thesis

Practical Implementation of Fault Detection Scheme in a Three Tank System

To achieve the Degree:

Master of Science (M. Sc.)

in Technische Kybernetiks und Systemtheorie

Submitted by:	Fernando Córdova Ricapa
Date and Place of Birth:	21/09/1990 Lima, Perú
Responsible Tutor (TU Ilmenau):	Prof. Dr.-Ing. Johann Reger
Responsible Professor (TU Ilmenau):	Prof. Dr.-Ing. Johann Reger
Responsible Professor :	Prof. Javier Sotomayor Moriano
Date and Place:	31/03/2016, Ilmenau

Statement of the Authorship

The present work has been made independently without use other than those specified sources. All points were taken literally or in accordance with their published sources are identified as such. The work has not been submitted in the same or similar form, or in part, under one or other tests.

Ilmenau, 12/04/2016 Fernando Córdova Ricapa

Kurzfassung

Die vorliegende Masterarbeit präsentiert eine praktische Durchführung der Fehlerermittlung in einem realen System unter der Anwendung von "Residual Signals". Diese "Residuals" wurden mit Hilfe eines Verfahren der sogenannten modellbasierten Fehlerdiagnose erstellt. Es wurden verschiedene Techniken untersucht und die dazugehörigen Algorhithmen entwickelt. Der Schwerpunkt dieser Forschung liegt auf dem Drei-Tank-System, in welchem unterschiedliche Methoden der Fehlerermitlung angewendet wurden. Einige Situationen, die Fehler in Aktoren, Sensoren oder Komponenten simulieren, werden analysiert, wobei auch Rauschen berücksichtigt wird. Aufgrund der Eigenschaften des Systems stellt dieses vier mögliche Arbeitsbereiche dar, die normalerweise nicht in der Literatur, aber hier in dieser Arbeit genannt werden. Zudem werden Spezialfälle gezeigt, in denen das System von einem Bereich zu einem anderen übergeht und dabei kritische Punkte durchläuft, bei denen im System Singularitäten auftauchen. Es werden Fehler um den Zeitpunkt, in dem Systemzustände in der Nähe der kritischen Punkte liegen, festgestellt und die Hauptaufgabe ist es nun diese Singularitäten zu überwinden und eine erfolgreiche Fehlerermittlung zu erzielen.

Abstract

This thesis presents a practical implementation of fault detection scheme in a real system by using residuals signals. These residuals have been generated applying the method of a model-based fault diagnosis. Different approaches have been studied and the corresponding algorithms developed. The object of the investigation is the three tank system in which different kind of methods of fault detection were performed. Various scenarios in which faults are simulated in actuators, sensors or components are analyzed considering also the presence of noise. Due to the inherent system characteristics it presents four possible work regions which are usually not taken into account in literature, but studied in this thesis. Also special cases, when the system goes from one region to another through critical points in which the system presents singularities, are shown. Faults will be performed around the time when the system states lie in the neighborhood of the critical points and the main task is now to overcome these singularities and achieve successfully a fault detection.

Acknowledgment

First of all I would like to express my gratitude to my supervisor in Germany, Prof. Dr.-Ing. Johann Reger (TU-Ilmenau), for all his guidance throughout the research and development of this Master Thesis as well as for his support during the stay in Germany. Also, express my thanks to my supervisor in Perú, Dr. Javier Sotomayor Moriano (PUCP), due to all his help during the time of studying in Perú.

I would like to thank CONCYTEC of Peru for their support with the scholarship, which made it possible for me to complete the research and finish the Master Thesis . In the same way I thank DAAD for its financial support while in Germany as part of a double degree program between Pontificia Universidad Católica del Perú and Technische Universität Ilmenau.

I am also thankful to the Department of Computer Science and Automation of Technische Universität Ilmenau for providing the laboratory system which is studied in this work. Also I am thankful to the research group which works with it, for its help introducing and explaining the system.

Then I would like to express my sincerest gratitudes to my parents, who have supported me in every moment, even in the distance. Also to my friends and their suggestions during the accomplishment of this work. And I need to thank the person who supported and has accompanied me, Vera.

Abbreviations and Symbols

SISO	Single Input, Single Output System
MIMO	Multiple Inputs, Multiple Outputs System
SIMO	Single Input, Multiple Output System
MISO	Multiple Input, Single Output System
FDI	Fault Detection and Isolation
FD	Fault Detection
FDII	Fault Detection, Isolation and Identification
ARR	Analytical Redundancy Relation
TTS	Three Tank System

Contents

List of Figures

List of Tables

1 Introduction

1.1 Motivation

Currently, there is a large number of industrial processes and systems which are controlled by various control techniques in order to ensure optimum performance of such process or system. However, in the process control industry, there may occur very often failures in some process elements which are crucial for proper system control. Faults in some of these important components of the systems not only affect the performance of the process, but in the worst case they may eventually cause operational problems resulting in potential instability or even complete system failure. Therefore, troubleshooting has become one of the most important issues in the field of process control, being partly involved in the fault-tolerant control, which has become a basic and indispensable component in the field of process control.

Fault detection is the basis for a system or process to continue operating under certain circumstances where certain parts or elements of the system have submitted a fault. Once the fault is detected, a controller system with the ability to respond and adapt the control in the presence of a fault can be implemented.

These failures can cause delays in the production lines of certain industrial processes and as a result it can lead to delays which are reflected as economic losses to businesses. At the same time, some faults may cause damages like accidents which involves operators or users in particular processes[4]. Then, because the presence of faults is an important problem, several approaches have been taken in order to implement a system of reliable detection of failures. Therefore, it is intended to design and implement fault detection algorithms using different methods applied to a laboratory system: the three tank system in which individual cases of that system are also discussed.
Also, an important scenario is considered. The fault detection will be performed

not in only one of the working regions of the system but it will be performed for the four working regions. In the jump from one working region to another, the system goes through certain *critical points* in which the three tank system presents singularities.

1.2 Objectives

1.2.1 Main Objective

Design and implementation of a fault detection system by using different residual generation approaches in a laboratory Three Tank System.

1.2.2 General Objectives

In order to achieve this goal it is necessary to make the following research and development:

- Study of techniques applied to the fault detection based on the system model.
- Study of residual generation methods, which are then analyzed in order to perform failure detection.
- Obtaining a general model of a Three Tank System, which was proposed as an object of study because it is quite a problem discussed in the literature and which may make future comparisons between different detection methods applied in this Thesis work.
- Analysis of possible faults that could occur in the system of three tanks: failure due to independent leaks in each of the three tanks, faults in the interconnecting valves between tanks, variations of the system, which produce changes in the modeled system's parameters.
- Residual generation and fault detection in the system by various methods presented in the literature.
- Analysis of residual generation in the four possible working regions of the system and for the particular case in which stable tank levels are equal and with the presence of noise in the sensors; due to singularities in these cases and problems that are generated in the fault detection system.

- Perform a residual generation by using a finite simultaneous parameter and states estimation which will be carried out applying a modulating functions approach.
- Implementation of the developed methods on the real system of three tanks.

1.2.3 Resources, Materials and Equipment

- The tasks of modeling and simulation methods of fault detection are carried out with use of Matlab and Simulink program.
- The Three Tank System where the developed methods will be applied is provided by the Department of Computer Science and Automation of Technische Universität Ilmenau.

2 Fault Diagnosis System

2.1 Introduction

Nowadays, control systems are becoming more complex and control algorithms are more sophisticated with in course of time. As a consequence, issues like availability, reliability or operating safety are of major importance [6]. This issues are not only important in safety-critical systems such as nuclear reactors, chemical processes plants or aircrafts, but also to other advances systems used in cars or other industrial processes. For safety-critical system, the presence of a fault can be extremely serious in terms of human mortality or environmental impact [6]. Consequently, there is a growing demand of on-line fault detection systems in order to increase the reliability of such safety-critical systems. For systems which are not safety-critical, fault detection scheme involve an improve in plant's efficiency, higher product quality, safety and operational reliability.
Since some decades ago, fault detection and diagnosis fields have been deeply studied and its application demand has been grown. This development was and still is stimulated by the side of modern control theory, with the development of powerful techniques of modeling, state estimation and parameter identification methods, observing techniques and a notable progress of computer technology [7].

2.1.1 Definitions

By taking a look in the literature, one realizes that the terminology in this field is not totally consistent. In order to make the terminology consistent, the SAFEPROCESS Technical Committee discussed this matter in the SAFEPROCESS 2000 conference. Below, some important definitions in this field are presented [11]:

- **Fault**: an unpermitted deviation of at least one characteristic property or parameter of the system from the acceptable / usual / standard condition.

- **Failure**: a permanent interruption of a system's ability to perform a required function under specified operating conditions.
- **Malfunction**: is an intermittent irregularity in the fulfillment of a system's desired behavior.
- **Error**: A deviation between a measured or computed value (of an input variable) and the true, specified or theoretically correct value.
- **Disturbance**: An unknown (and uncontrolled) input acting in the system.
- **Perturbation**: An input acting on the system, which results in a temporary departure from the current state.

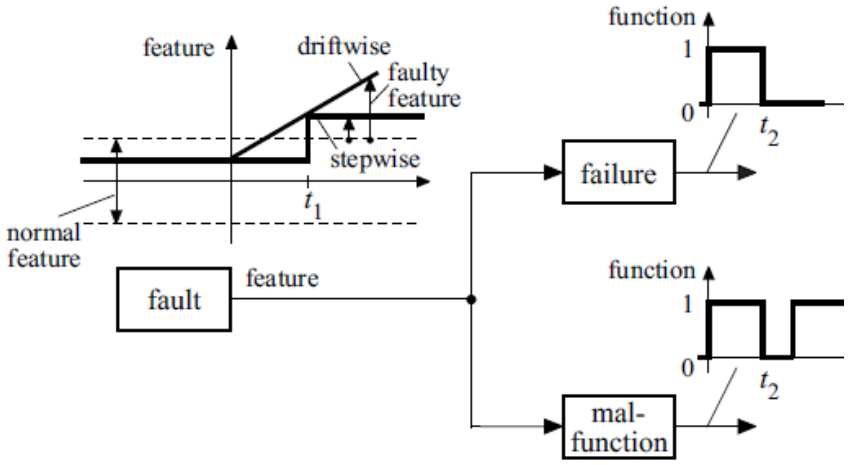

Figure 2.1: Development of event „failure" and „malfunction" from a fault which causes a stepwise or a driftwise change in the feature [1]

After these definitions, it is possible to make some relations and differences between a fault, failure and malfunction. A fault can develop abruptly, like a step function, or incipiently, like a drift function. The response of the system in front of the fault is assumed to be proportional to the fault development. Once the tolerance of the normal values is exceeded, the feature indicates a fault. Dependent on the size of the fault, a failure or a malfunction in a system may occur at time t_e[1]. Figure 2.1 shows the relations mentioned above.

2.1.2 Functions

A system which is able to detect faults and diagnose their location and significance in a particular system is called a „Fault Diagnosis System". These systems normally concerns the following tasks [4]:

- Fault detection: The system decides whether or not a fault occurs. Also, the time at which a fault has appeared in the system is determined.
- Fault isolation: The system determines the location of the fault, e.g. which sensor or actuator has become faulty.
- Fault identification: In this last task the system determines the intensity and nature of the fault and its severity.

2.1.3 System Properties

With regard to the overall functioning of elements, components, processes and systems, the terms reliability, availability and safety play an important role. These terms are defined as follows [4],[1]:

- Safety: is the ability of a system not to cause danger to persons, equipment or the environment. A safety system is a part of the control equipment which protects a system from permanent damage.
- Reliability: is the ability of a system to perform a required function under stated conditions, within a given scope, during a given period of time.
- Availability: is the probability that a system or equipment will operate satisfactorily and effectively at any point of time when its needed.

2.1.4 Faults

Faults are events which may take place in any part of the whole system. In literature, faults can be classified according to: the location of their occurrence and their behavior in time.

- **Location of occurrence**
  Faults can take place in different parts of the system such as actuators, sensor or components of the plant.

a. Actuator faults:
These kind of faults represent partial or total loss of control action. A completely lost actuator is for example a “stuck” actuator that produces no (controllable) actuation regardless of the input applied to it. Total actuator fault can occur, for instance, as a result of a breakage, cut or burned wiring, shortcuts, or the presence of an outer body in the actuator[12]. Partially failed actuator produces only a part of the normal actuation under nominal operating conditions. It can result for example from hydraulic or pneumatic leakage, increased resistance in a pump or fall in the supply voltage[12].

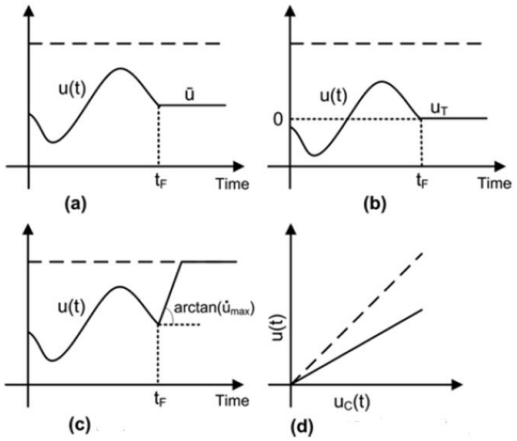

Figure 2.2: Common types of actuator faults [2]

b. Sensor faults:
These faults represent incorrect readings from the sensors that belong to the system. Sensor faults can also be subdivided into partial and total. Total sensor faults produce information that is not related to the value of the measured physical parameter in cases such as broken wires, lost contact with the surface, etc. Partial sensor faults produce reading that is related to the measured signal in such a way that useful information could still be retrieved. This can, for instance, be a gain reduction so that a scaled version of the signal is measured, a biased measurement resulting in an offset in the reading, or increased noise[3]. Figure 2.3 shows a summarize of the fault impact in sensor reading $Y(t)$ for the measured value $Y_o(t)$.

Due to their smaller sizes sensors can be duplicated in the system to

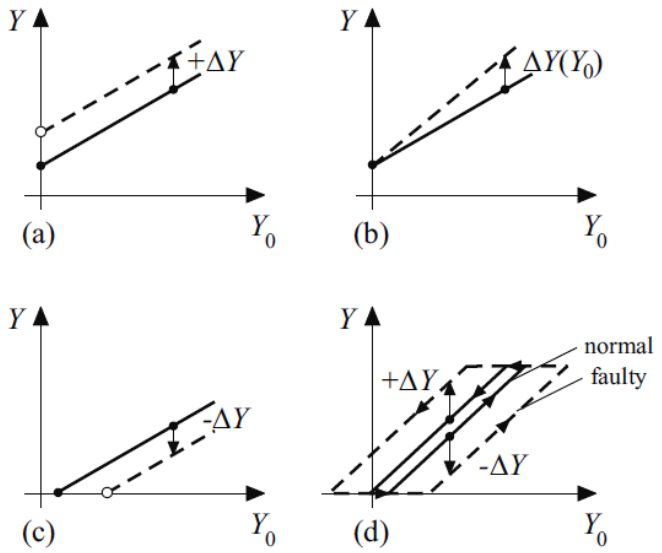

Figure 2.3: (a)zero offset, (b)change of gain, (c)change of response value, (d)change of hysteresis [3]

increase the fault tolerance. Consequently, using more than one sensor (two or three), to measure the same signal, the system can use these reading and compare them in order to detect a fault. However, this approach implies a significantly increase in terms of costs[12].

c. Component or plant faults:
These are faults in the components of the plant itself, that means, all faults that cannot be categorized as sensor or actuator faults will be referred to as component faults. These faults represent changes in the real physical parameters of the systems such as mass, damping constant, viscosity constant, etc., which are often due to structural damages. They often result in a change in the dynamical behavior of the controlled system[12]. Due to their diversity, component faults cover a very wide class of unanticipated situations, and as such are the most difficult ones to deal with[12].

A distinction between each fault mentioned before is showed in Figure 2.4

To make an example, consider a process which is a Linear Time Invariant (LTI) system:

$$\begin{aligned} \dot{x}(t) &= Ax(t) + Bu(t) \\ y(t) &= Cx(t) + Du(t) \end{aligned} \tag{2.1}$$

with the state matrices $A \in \mathbb{R}^{nxn}$, $B \in \mathbb{R}^{nxm}$, $C \in \mathbb{R}^{lxn}$, $D \in \mathbb{R}^{lxm}$, the state

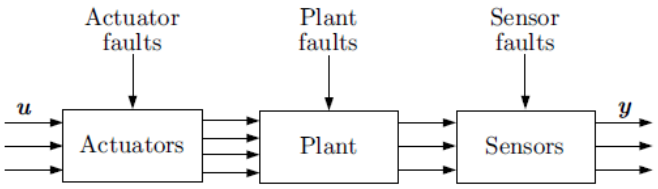

Figure 2.4: Distinction between actuator, sensor and component or plant fault [4]

vector $x \in \mathbb{R}^n$, the vector $u \in \mathbb{R}^m$ and the vector $y \in \mathbb{R}^l$.
An actuator fault can be perceived as a faulty control signal that has an influence in the state vector x and in the output vector y, consequently matrices B and D are affected. In the same way, a sensor fault can be perceived as a wrong reading and a faulty vector y affecting state matrices C and D. Finally, a component fault is perceived as a fault in any component of the plant. It may denote a change in the dynamics of the physical process and has a direct influence on the state matrix A.

- **Behavior in time**
  According to time characteristics, faults are classified as abrupt, incipient and intermittent. An abrupt fault presents a step-like behavior, as is illustrated in Figure 2.5. In this case, a signal which is affected directly by a fault, changes abruptly from the nominal value to the faulty value. It is usually produced by a hardware damage and may have a severe effect in the performance of the system[1]. An incipient fault presents a drift-like behavior. In this case, the fault term has a slow and gradual change to the faulty value, that means, in a linear way. This kind of faults may represent changes in the system parameters and because of their slow change, are usually difficult to detect. An intermittent fault appears and disappears repeatedly. In this case, the fault term changes continuously from the nominal value to the faulty value and return to the nominal value after a short period of time. It may be produced by a partially damage wire[1].

2.2 Fault Diagnosis Techniques

As it was be mentioned before, the concept of a FDS (Fault Diagnosis System) consists in the following three tasks, which have been already defined in the section

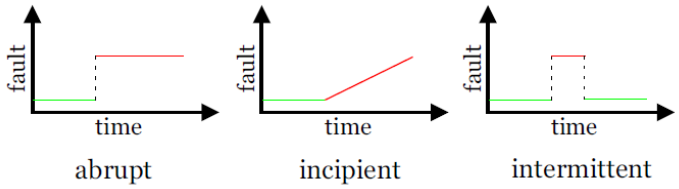

Figure 2.5: Time dependency of fault [2]

above: Fault detection, Fault isolation and Fault identification.
Fault detection(FD) is the first step in a FDS where another signal is triggered in order to indicate the occurrence of a fault. Fault detection and isolation (FDI) and Fault detection, isolation and identification (FDII) systems not only indicate if whether or not a fault occurs, the first one is able to deliver a specified signal to indicate which fault has occurred and in which part of the system[13][5]. The second one, additionally, delivers a signal which indicates the type and magnitude of the fault.
Nowadays, exist different approaches about Fault diagnosis techniques and they can be classified as shown in Figure 2.6.

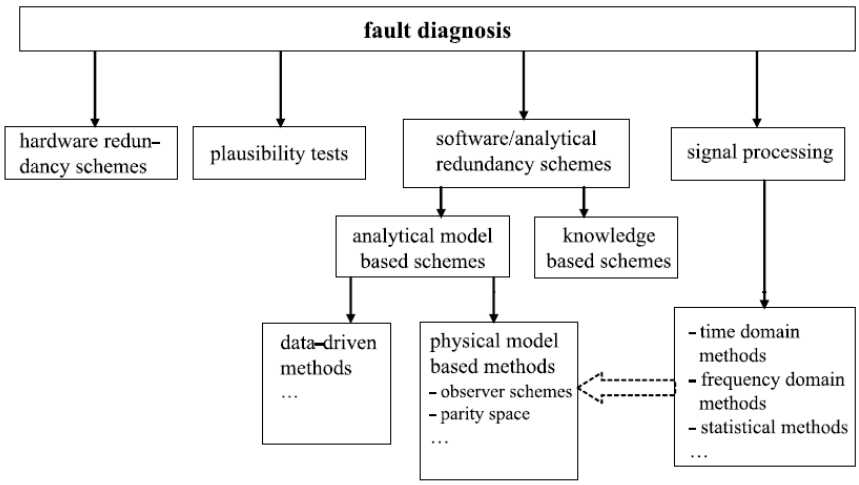

Figure 2.6: Fault diagnosis methods [5]

Since in this thesis a model based fault diagnosis is used, it will be explained in the following. The first idea of this method consists in the reconstruction of the system like in the hardware redundancy based fault diagnosis, but without the use of physical redundant components[5]. The main idea of the model based scheme is to replace the hardware redundancy by a process model which is implemented in

software. A process model is a quantitative or qualitative description of the dynamic and steady behavior of the real system. This model can be obtained using mathematical expressions that describes the behavior of a component based in physical laws and also using process modeling techniques. In this sense, it is possible to reconstruct the process behavior, which is called *software redundancy concept* or *analytical redundancies*[5]. As in hardware redundancy scheme, the process model and the real system run at the same time, in parallel, and both are driven by the same input signals. The reconstructed process variables, which are delivered by the process model, will be the same as the corresponding real system variables only in the fault-free case and will show a deviation respect to the real ones when any fault occurs. In order to obtain this information, a comparison

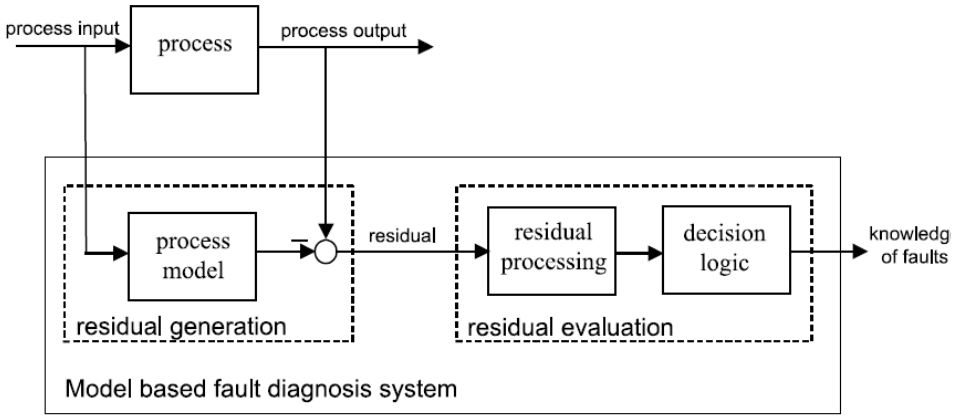

Figure 2.7: Model based fault diagnosis [5]

(difference) between the output signals of the real systems and the estimated by the process model will be made. This comparison is called *residual*[5], which carries the most important information for a successful fault diagnosis. Figure 2.7 illustrates the main idea of this technique.

If $residual \neq 0$, then fault occurs, otherwise free-of-fault

2.3 Model-Based Fault Diagnosis

As mentioned in the brief description before, the main idea of model based diagnosis consists in the reconstruction of the real process and make a comparison between the real outputs or variables and the variables delivered by the model process, in order

to create a residual, which carries the most important information to achieve a fault diagnosis. If residuals are properly generated, then fault detection is really near to be achieved. Once fault detection is successfully made, it is possible to perform a fault isolation and consequently, a fault identification. In this sense, residual generation is a very important task in model based fault diagnosis scheme [14],[15].
Model based diagnosis comprise two main stages: residual generation and decision making or residual evaluation, which are showed in Figure 2.7. These two stages were first proposed by Chow and Willsky (1980) and now they are widely accepted by the fault diagnosis community. The main stages are described as follows[6]:

- Residual Generation:
  The main task in this stage is generate an auxiliary fault indicating signal, using inputs and available sensed output signals. This auxiliary called residual, is generated for the purpose of reflecting the presence of a possible fault in the real system. When there is no presence of any fault, the residual should be normally zero, close to zero, or less than a fixed or variable threshold. In the other hand, when a fault occurs, the residual clearly presents a different value from zero or exceeds significantly the threshold.
  The algorithm or system used to generates residual is called a *residual generator*. Residual generation is thus a procedure for extracting fault symptoms from the system, with the fault symptom represented by the residual signal. The residual should ideally carry only fault information. To ensure reliable FDI, the loss of fault information in residual generation should be as small as possible [6].

- Decision Making or Residual Evaluation:
  In this stage, residuals are examined for the purpose of knowing whether or not any fault has occurred. In order to determine if a fault occurs, a decision rule is applied to the residual. A decision process may consists in a threshold test applied on the residual behavior. This threshold may be a fixed value or an adaptive one depending on the knowledge about the behavior of the signal which has been used to generate the residual. The decision process can also consist of methods of statical decision theory, such as generalized likelihood ratio (GLR) testing or sequential probability ratio testing (SPRT) [6],[4].
  Additionally, the residual is evaluated in order to know where the fault has been occurred and which elements are faulty, actuator or sensor.

The most of works in literature in the field of model-based fault diagnosis have been

focused in the residual generation problem or in the fault detection, because once the residuals have been well designed, decision making is a little easier.

2.3.1 On-line Fault Diagnosis

Model based fault detection and isolation (FDI) is mostly familiar with on-line fault diagnosis. Residual generation is carried out during the system operation. The main reason is that model-based fault diagnosis scheme request information for input and output which is only available while the system is in operation. Open loop tests in the system or supplying test signal leading to incorrect behavior of the system is not admissible to achieve a successful fault detection [6]. Model based fault diagnosis is usually performed in closed loop. Figure 2.8 illustrates the relationship between the real system control loop with the Fault Diagnosis.
Fault Diagnosis system requires information about the measured output from the sensor and input to the actuators[6]. The measured outputs are also needed by the controller and then are used in order to generate the required control action which is represented as the input to the actuator.

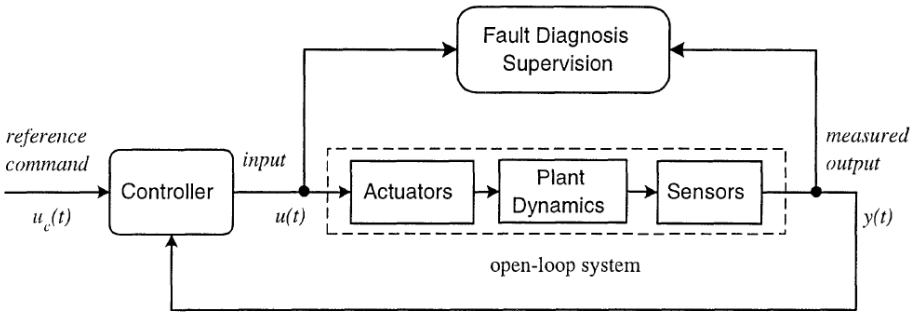

Figure 2.8: Faul Diagnosis and close loop [6]

The process model needed by the model based fault diagnosis is reconstructed using only the open loop system, as it is shown in Figure 2.8. However, when the fault diagnosis is performed, the system is considered in closed loop. This is because the input and output required in model based fault diagnosis is related to the open loop system, but these input and output have to be generated in closed loop, while the system is in operation. Nevertheless, the controller design is not necessarily considered in the design of the fault diagnosis system. This fact takes consistency with the control theory in the sense that fault diagnosis can be treated as an observation problem[6].

In the case when it is not possible to have access to the input signal $u(t)$, the process model has to be designed using the reference or tracking signal $u_c(t)$. As a consequence, the model considers relationship between the output $y(t)$ and the reference $u_c(t)$, that is to say, the model is designed using the closed loop system. In this case, the controller has a very important role in the fault diagnosis scheme. To give an example, a robust controller can attenuate the presence of faults, making them to be less perceived and the fault diagnosis may turns more difficult.

2.3.2 Modeling of Faulty Systems

The first step in model based diagnosis approach is, as mentioned before, the reconstruction of process model of the system that will be monitored. In this way, it is important to know how a fault can be modeled and represented according to its influence in the system. Faults can be represented as additional external signals or as parameter deviations. The first ones are called additive faults, because in the model these faults are represented by an unknown input that enters in the model equation. It can be produced, in a physical sense, by sensor or an actuator offset. The second ones are called multiplicative faults because the system parameters depending on the fault size are multiplied with the input or system state. In physical sense, it can be caused by a degradation in any actuator or sensor. This kind of faults may also describe a component fault, like a change in the parameters of the plant. Figure 2.9 shows the representation of an additive and a multiplicative fault.

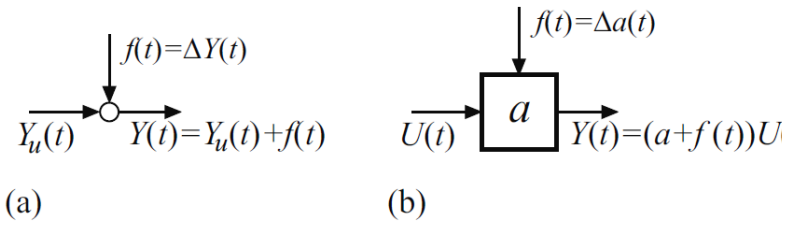

Figure 2.9: (a) Additive fault, (b) Multiplicative fault [3]

As explained before, the process model is reconstructed using the open loop system model, which for purposes of modeling, may be separated in three parts as it is illustrated in Figure 2.10: actuator, system or plant dynamics and sensors.[6] Then, faults corresponding to each of the parts mentioned above, can be modeled as additive or multiplicative faults according to how these faults influence

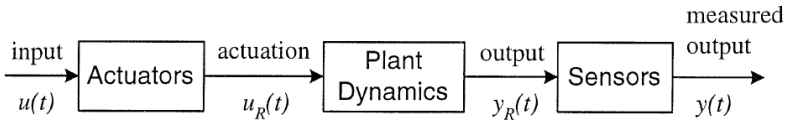

Figure 2.10: Open loop system [6]

actuators, sensors or system dynamics behavior. Considering the system dynamics in (2.2), which represents the situation in Figure 2.11:

$$\begin{aligned} \dot{x}(t) &= Ax(t) + Bu_R(t) \\ y_R(t) &= Cx(t) + Du_R(t) \end{aligned} \tag{2.2}$$

where the state vector $x \in \mathbb{R}^n$, the input vector to the actuator $u_R \in \mathbb{R}^r$ and the real system output vector $y \in \mathbb{R}^m$. Matrices A, B, C and D are known with appropriate dimensions; faults can be modeled as follows.

- System dynamic Faults
  A component fault affects directly the system dynamics as shown in Figure 2.11. It may represents a change in the plant conditions, leading to an invalid dynamic relation, for example, a water leakage in a tank system. In this case, the fault is modeled as an additive fault and the model of the faulty system may be described as:

$$\dot{x}(t) = Ax(t) + Bu_R(t) + f_c(t)$$

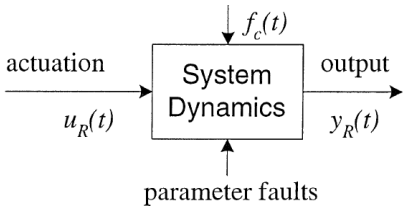

Figure 2.11: System dynamics [6]

  Also, the fault can express a change in the system parameters and it is modeled as a multiplicative fault. For example, a change in the i^{th} row and j^{th} column element of the matrix A, the dynamic equation of the system can be described as in [6]:

$$\dot{x}(t) = Ax(t) + Bu_R(t) + I_i \Delta_{ij} x_j(t)$$

where $x_j(t)$ is the j^{th} element of the vector $x(t)$ and I_i is an n-dimensional vector with all zero elements except an 1 in the i^{th} element[6].

For a nonlinear system, a change in the plant conditions may be modeled as

$$\dot{x}(t) = f(x,t) + g(x,t)u_R(t) + f_c(t)$$

and when a change in the parameter system occurs, the dynamics of the system is described as follows:

$$\dot{x}(t) = \bar{f}(x,t) + g(x,t)u_R(t)$$

with

$$\bar{f}(x,t) = f(x,t) + f_c(x,t)$$

where $f_c(x,t)$ represents the parameter change in the system.

- Sensor Faults
  In a real system, outputs of the plant ($y_R(t)$) are not directly accessible, hence, they are measured using sensors. Figure 2.12 illustrates the relations between the output signals, the sensor, the measured signal and a sensor fault.

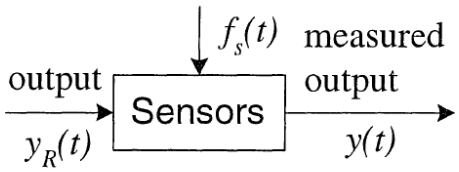

Figure 2.12: Sensor dynamics and presence of a fault [6]

The measured signal of the output system and the influence of the sensor fault can be described as

$$y(t) = y_R(t) + f_s(t)$$

where $f_s(t) \in \mathbb{R}^m$ is the sensor fault vector. The vector $f_s(t)$ may describe different fault situations[6]. The first situation is when the sensor value is stuck at a particular value, for example a constant „a", the measured value $y(t) = a$ and in this case $f_s(t) = a - y_R(t)$. Another situation is when there exists a deviation in the gain or scalar factor of the sensor. This fault is represented as a multiplicative fault and the measured value $y(t)=(1+\Delta)y_R$. In this case the fault is modeled as $f_s(t)=\Delta y_R(t)$.

- Actuator Faults
  In the same way as the plant outputs, the action $u_R(t)$ of the system is not directly accessible. In the most of the real systems, the action $u_R(t)$ is the actuator response to a control signal $u(t)$ generated by a controller system[6]. Figure 2.13 illustrates the actuator dynamic in presence of a fault and it is described by

$$u_R(t) = u(t) + f_a(t)$$

  where $f_a(t) \in \mathbb{R}^r$ is the actuator fault vector and $u(t)$ is the known control signal generated by the controller. As in the sensor fault situation, $f_a(t)$ can

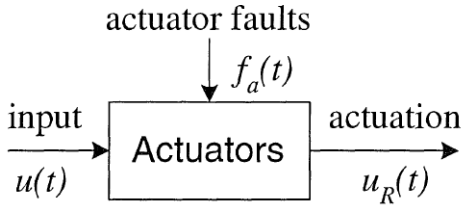

Figure 2.13: Actuator dynamic [6]

  describes different actuator fault situations. In the first situation, $f_a(t)$ may represents a external disturbance in the actuator input and it is modeled as an additive fault as in the equation above. In the second situation, a change in the actuator behavior or in the actuator parameters may be represented. In this case the fault is modeled as a multiplicative fault, leading the actuator dynamics as follows:

$$u_R(t) = (1 + \Delta)u(t)$$

  where $f_a(t)$=$\Delta u(t)$.

Additionally, there are other kinds of signals which change the plant behavior, such as disturbances and model uncertainties. These two kinds of signals have similar effects on the system. Disturbances are usually represented as unknown inputs signal which have to be added to the system output and as consequence can be modeled as additive faults. Model uncertainties change the model parameters in a similar way as multiplicative faults [4].

To summarize, when the system presents all the possible situations: actuator, sensor

and component faults, the total system model is represented as[6]:

$$\begin{aligned} \dot{x}(t) &= Ax(t) + Bu(t) + Bf_a(t) + f_c(t) \\ y(t) &= Cx(t) + Du(t) + Df_a(t) + f_s(t) \end{aligned} \tag{2.3}$$

Considering a general case, system may also be described as the following state model:

$$\begin{aligned} \dot{x}(t) &= Ax(t) + Bu(t) + R_1 f(t) \\ y(t) &= Cx(t) + Du(t) + R_2 f(t) \end{aligned} \tag{2.4}$$

where $f(t) \in \mathbb{R}^g$ is the fault vector and each $f_i(t)$ with $i = 1, 2..., g$ correspond to a specific fault. Matrices R_1 and R_2 are called „fault entry matrices" and represent the influence and effect of each fault in the system. In the state space shown in (2.4), $u(t)$ is the input to the actuator and $y(t)$ is the measured signal, although for FDI purpose in the course of literature they are just called input and output of the monitored system. Both vectors are supposed known for FDI purpose [6].
The system described in (2.4) can be also described as an input-output transfer matrix as follows[6]:

$$y(s) = G_{yu}(s)U(s) + G_{yf}(s)f(s) \tag{2.5}$$

where s denotes the frequency domain and transfer matrices G_{yu} and G_{yf} are defined as:

$$\begin{aligned} G_{yu} &= C(sI - A)^{-1}B + D \\ G_{yf} &= C(sI - A)^{-1}R_1 + R_2 \end{aligned} \tag{2.6}$$

General models presented in time and frequency domain as shown in (2.4) and (2.5), respectively, have been widely accepted in fault diagnosis literature [6].
For nonlinear systems, faults are modeled similarly, as additive or multiplicative faults. The representation of a nonlinear faulty systems may be described as follows:

$$\begin{aligned} \dot{x}(t) &= f(x,t) + g(x,t)u(t) + g(x,t)f_a(t) + f_c(t) \\ y(t) &= h(x,t) + f_s(t) \end{aligned} \tag{2.7}$$

where $f_a(t)$, $f_c(t)$ and $f_s(t)$ denote actuator, component and sensor faults, respectively. Additionally, it is possible to model disturbances or unknown inputs in the state vector $x(t)$ or noise in the sensor signal $y(t)$ as additive faults.

2.3.3 Residual Generation General Structure

The most frequently used FDI approaches in practice involve *a priori* knowledge of the system behavior and certain signal characteristics. For example, the previous knowledge about the dynamic range of a certain signal or its spectrum in order to be able to check variations on its behavior. The main deficiencies of this kind of approaches are the necessity of a priori knowledge of the monitored signals characteristics and the dependence of these characteristics on certain operation states which are not known a priori[7][16].

In order to avoid these deficiencies, modern model based fault diagnosis approaches have made a significant contribution related to the introduction of *symptons or residual signals*[7]. These residuals signals are independent of the system operation states and have a direct dependence on faults. Residuals represent the inconsistency between the real measured signals and the corresponding process model signals. It is possible to make different invariant relations according to different system variables and any inconsistency or violation of these relations represent a variation in residual signal, which may be represented as the presence of a fault.

The general residual generator block is illustrated in Figure 2.14. Residual generation may be carried out in terms of a redundant signal structure. As showed in Figure 2.14, the redundant signal $z(t)$ is generated by the function $F_1(u, y)$ and then it is used with the measured signal $y(t)$ by the function $F_2(z, y)$ to generate the residual signal $r(t)$[6]. In a free fault case, the followings relations are fulfilled:

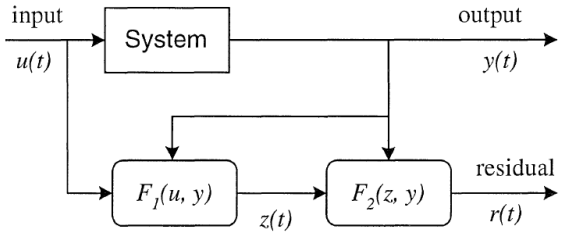

Figure 2.14: Redundant signal structure in residual generation [6]

$$\begin{aligned} z(t) &= F_1(u(t), y(t)) \\ r(t) &= F_2(z(t), y(t)) = 0 \end{aligned} \tag{2.8}$$

In the presence of a fault, relation presented in (2.8) is not satisfied and the residual $r(t)$ is different from zero.

The simplest residual generation approach is to use a completely identical model of the real system, that means the function F_1 mentioned before is an identical model of the system[6]. In this case signal $y(t)$ is not necessary and only the input $u(t)$ is used in the simulator system: $F_1{=}F_1(u(t))z(t)$. Then, the residual is generated by computing the difference between the simulated output signal and the real output signal: $F_2(z(t), y(t)){=}y(t){-}z(t){=}r(t)$. The simplest approach is illustrated in Figure 2.15. Its simplicity is the most important advantage, but the disadvantage is that the

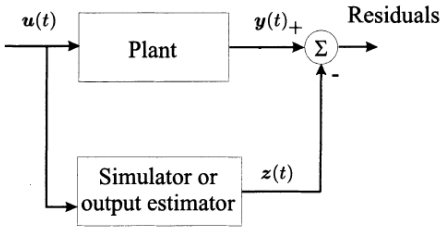

Figure 2.15: Residual generation simplest approach [7]

simulator system may become unstable when the real system becomes also unstable. On the purpose of avoiding, as possible, the disadvantage mentioned before, an extension of the model based residual generation has been made. This extension consists in replacing function $F_1(u(.))$ by $F_1(u(.), y(.))$ and using now an output estimator which required both, input and output from the real system. So now, function F_1 estimates a linear function of the output y, $F_1(u(.), y(.)){=}\mathrm{M}y$, and function F_2 defined by $F_2(z(.), y(.)){=}\mathrm{W}(z - \mathrm{M}y)$, with W being a weighted matrix. In conclusion, no matter which residual generation method is used, the process is nothing more but a linear mapping whose inputs consist of both, input and output of the system being monitored[7][6]. Figure 2.16 describes a general structure for a residual generator. With equations presented in (2.5) and (2.6) as reference, residual generation structure can be represented mathematically as:

$$r(s) = \begin{bmatrix} H_u(s) & H_y(s) \end{bmatrix} \begin{bmatrix} u(s) \\ y(s) \end{bmatrix} = H_u(s)u(s) + H_y(s)y(s) \tag{2.9}$$

where H_u and H_y are transfer matrices that can be designed using stable linear systems. Signals $u(s)$, $y(s)$, $r(s)$ and $f(s)$ are the Laplace Transform of the corresponding continuous time signals[7]. According to the definition in (2.8), residual $r(t)$ is designed in order to become zero in the fault free case and differs

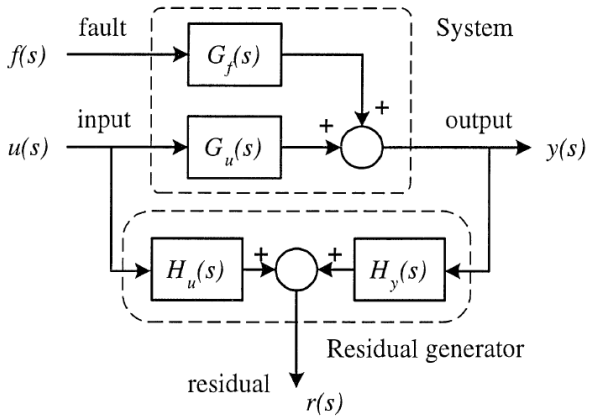

Figure 2.16: General residual generation structure [6]

from zero when a fault occurs, that means:

$$r(t) = 0 \quad \Longleftrightarrow \quad f(t) = 0 \tag{2.10}$$

To satisfy condition mentioned above, matrices H_u and H_y have to fulfill the following constraint conditions:

$$H_u(s) + H_y(s)G_{yu}(s) = 0 \tag{2.11}$$

Since equation (2.9) represents the general structure of residual generation system, the design of it involves a good choice of functions $H_u(.)$ and $H_y(.)$, which must satisfy condition in (2.11). As mentioned in [7], different residual generators can be designed by using different parameterizations of matrices $H_u(.)$ and $H_y(.)$.
Once the residual signal $r(t)$ has been generated, the fault detection is achieved comparing the residual signal $r(t)$ or an evaluation function of the residual $J(r(t))$ with a fixed threshold T or a function of time of it $T(t)$ as follows[6][7]:

$$\begin{aligned} J(r(t)) < T(t) \quad for \quad f(t) = 0 \\ J(r(t)) > T(t) \quad for \quad f(t) \neq 0 \end{aligned}$$

where $f(t)$ is the fault general vector. If the evaluation function of the residual exceeds the threshold, it is possible that a fault has occurred.
The evaluation given above works well with a fixed threshold when the system operates in a steady state and it reacts after relatively large features. On the other hand, a function threshold which depends on the system operating conditions may

be used. To give an example, the threshold function $T(t)$ may be expressed as a function of system inputs [7].

3 Model Based Residual Generation Techniques

3.1 Introduction

Residual generation is the most important issue in Model based Fault Diagnosis and as a consequence, different approaches based in mathematical models have been developed in the last decades, as for example in ([7],[6],[5],[3],[1],[17],[7],[14],etc). The main task consists in the detection of faults in a particular system. These faults may be occur in any part of the system: process, actuators or sensors. Fault detection is achieved by using the *dependencies between different measurable signals* [1] which are expressed with the use of mathematical process models. The general structure of model based fault detection is showed in Figure 3.1.

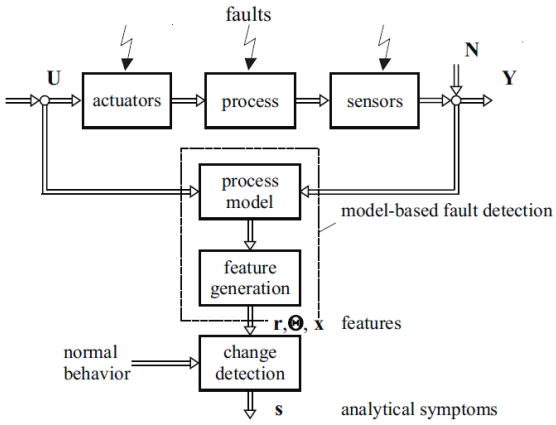

Figure 3.1: Basic structure in Model based fault detection [1]

As Figure 3.1 explains, using the measured outputs signals of the system Y and the input signals U, the fault detection system may generates parameter estimates $\hat{\theta}$ and states estimates $\hat{\mathbf{x}}$. In a general sense, parameter estimates and states estimates can be named *features*. Once these features have been generated, by a comparison with the nominal features values (i.e. nominal parameters and real or

measured states), features changes are detected, leading to analytical symptoms s or residuals r.

$$r(t) = \Omega(t) - \hat{\Omega}(t)$$

where $\Omega(t)$ and $\hat{\Omega}(t)$ represent the nominal and the estimated features respectively. For the application of model based fault detection methods, it is really necessary to distinguished between the different process configuration as shown in Figure 3.2. Considering the importance of the inherent dependencies used for fault detection, and the possibilities to isolate faults, the situation becomes greatly better from case (a) to (b) or (c) or (d), because of the availability of more measured output signals and input signals[1].

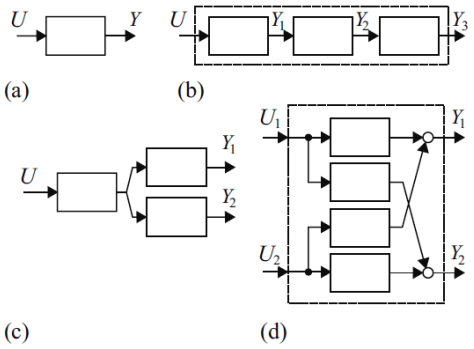

Figure 3.2: Process configuration: (a) SISO system, (b) SISO system with intermediate measurements, (c) SIMO system, (d) MIMO system [1]

In the last decades, there have been many developments concerning model based fault detection, leading to a residual generation. These developments have took place in both context, theoretical and real system applications. The most common approaches can be classified in three categories[10]:

- Observer-based
- Parameter estimation
- Parity relations

The approaches mentioned, all of them somehow, use the mathematical system description to generated the model process and then generate the residual signals. Then, the first two categories and additionally another approach which also uses redundancy relationships to generate residuals will be developed generally.

3.2 Observer Based Approach

The basic idea of the observer based approach is to estimate the output signals of the system by using an observer which has as inputs the measured output signals or a subset of them (in case all the outputs are not available for be measured) and the control signal. The observer used in the estimation can be a linear or a nonlinear observer depending on the monitored system. In the linear case, the observer used for Fault detection scheme may be either a Luenberger obsevers or Kalman filters when exists the presence of noise in the environment. Linear case have been deeply studied as in [6],[7] and since the object of study is a nonlinear system, only this case will be addressed.

Observer based residual generation for nonlinear systems is a topic that has been studied a lot in the last decades and different types of observers have been developed depending on the system. Some of the developed observers which can be found in literature will be now mentioned briefly.

- Extended Luenberger observer
  The main idea of this observer consists in the linearization of the nonlinear system around the current estimated state and not around a fixed point. A widely explanation is presented in [18]. For the fault detection scheme a similar approach is presented in [18] and a case for MIMO system is presented in [19]. Since not every nonlinear system has the same characteristics, in some cases, because of linearization errors, the proper design of the filter gain matrix turns out difficult in practice.

- Nonlinear identity observer approach
  The main idea of identity observer approach is to linearize the estimation error dynamic around the estimated state and neglect the higher order terms. In this approach, the design of the filter gain is determined in the way that the equilibrium point of the estimation error is asymptotically stable, that means, $e(t) = 0$.

- Unknown input observer
  In the same way as for linear systems, the unknown input observer approach consists in designing the residual generator system so the unknown inputs are decoupled from the residual $r(t)$. A study of this approach is shown for example in [10]. An important advantage of this technique involves the

possibility of transforming the structure of the nonlinear model into a new form which is suitable. Also, existence conditions of UIO proposed for linear systems are restrictive for nonlinear cases.

- Disturbance decoupling nonlinear observer
  The idea is the same as UIO approach but, disturbance decoupling nonlinear observer approach is applicate for a more general form of nonlinear systems. The aim in the observer design is to make an state transformation in order to obtain a new form where disturbances have been decoupled. Some problems appear when the disturbances distribution matrix depends explicitly on the inputs.

- Adaptive nonlinear observer
  These observers have been developed in order to overcome the difficulty of less performance detecting slowly developing faults in nonlinear uncertain systems, specially when uncertainties are dominant [13]. At the same time, using this technique it is possible to estimate some uncertainties online and use these estimations for a robustness design against model uncertainties.

- High gain observer
  High gain observers have been developed with the aim task of overcoming model uncertainties. An inherent characteristic of this observer is the peaking phenomenon at the begin of the observation. High gain observer approach has been used in different applications related to fault detection scheme as shown in [20][21].

- Geometric approach
  The main idea consists in the detection filter design for linear system using geometric approach. A deeper explanation can be found in [16]. In the fault detection scheme, residual generator system is designed as the residual signal depends trivially on faults but non trivially on disturbances which may be decoupled. In this way, disturbance decoupling may lead to a undetectability of the faults if and only if these faults lie in the same subspace of disturbances. An application of geometric approach in fault detection is shown in [22].

- Sliding mode observer
  Widely applicated have been sliding mode observers in the fault detection

and isolation scheme. Inherent property of being robust to uncertainties and external disturbances makes this observer very suitable for FDI, specially for residual generation. Some application for some class of nonlinear systems have been made in [23],[24],[25],[26].

Now, before applying the observer based approach, it is important to know about some concepts of high utility in observer approach, which will be briefly explained.

3.2.1 Observability

As in linear systems, observability of the monitored system must be proved in order to be able to implement the observer based approach. Considering a class of nonlinear system described as follows:

$$\begin{aligned} \dot{x}(t) &= f(x(t)) + g(x(t))u(t) \\ y(t) &= h(x(t)) \end{aligned} \tag{3.1}$$

where $x \in \mathcal{M} \subset \mathbb{R}^n$, $u : [0, T] \to \mathcal{U} \subset \mathbb{R}^r$, $y \in \mathcal{N} \subset \mathbb{R}^m$, are the state vector, input vector and the output vector respectively, which are defined on open sets.
Different notions about observability in nonlinear systems have been developed, from fundamental observability [27] to uniform observability [28], which is closely related to observer design. The following definition is equivalent but less formal than[28]:

Definition 3.1 (*Uniform observability* [29]):
The system presented in (3.1) is said to be uniformly observable if every $x \in \mathcal{M}$ can be uniquely determined on the basis of y, which is $\mathcal{C}^\infty$ from $\mathcal{M}$ in $\mathbb{R}$, for all $u \in \mathcal{U}$.

A test to check uniform observability is proposed in the following proposition.

Proposition 3.1 [30]: The system in (3.1) is uniformly observable if for some

positive integer k the set of equations

$$\begin{bmatrix} y \\ \dot{y} \\ . \\ . \\ . \\ y^{(k-1)} \end{bmatrix} = \begin{bmatrix} q_{0,v}(x,u) \\ q_{1,v}(x,u,\dot{u}) \\ . \\ . \\ . \\ q_{k-1,v}(x,u,...,u^{(k-1)}) \end{bmatrix} \tag{3.2}$$

denoted by $\mathrm{Y} = q_v(x,v)$ with $v = u,...,u^{(k-1)}$ defines an injective map on $\mathcal{M} : x \mapsto \mathrm{Y}$ for arbitrary v, where $\mathcal{M} \subset \mathbb{R}^n$ is the open set defined in (3.1).
For a special case, considering system in (3.1) may be decoupled from its inputs, that means it is possible that $u = 0$, the same test mentioned as *Proposition 3.1* but less formal, is presented. Differentiating the output $y(t)$:

$$\begin{aligned} &y(t) = h(x(t)) \\ &\dot{y}(t) = \frac{d}{dt}h(x(t)) = \tfrac{\partial h(x)}{\partial x}\dot{x}(t) = \tfrac{\partial h(x)}{\partial x}f(x(t)) := L_f h(x) \\ &\ddot{y}(t) = \tfrac{\partial L_f h(x)}{\partial x}\dot{x}(t) = \tfrac{\partial L_f h(x)}{\partial x}f(x) := L_f^2 h(x) \\ &. \\ &. \\ &. \\ &y^{(n-1)}(t) = \tfrac{\partial L_f^{n-2} h(x)}{\partial x}\dot{x}(t) = \tfrac{\partial L_f^{n-2} h(x)}{\partial x}f(x) := L_f^{n-1} h(x) \end{aligned} \tag{3.3}$$

where $L_f^k h(x)$ are Lie's derivatives of h along f [31]. Then, simplifying it is possible to obtain

$$\begin{bmatrix} y(t) \\ \dot{y}(t) \\ \ddot{y}(t) \\ . \\ . \\ . \\ y^{(n-1)}(t) \end{bmatrix} = \begin{bmatrix} h(x) \\ L_f h(x) \\ L_f^2 h(x) \\ . \\ . \\ . \\ L_f^{(n-1)} h(x) \end{bmatrix} := \mathcal{O}_n(x) \tag{3.4}$$

where $\mathcal{O}_n(x)$ is the Observability map.

Theorem [31]:

If the Observability map $\mathcal{O}_n(x)$ is injective (invertible), then the nonlinear system described in (3.1) is observable.

3.2.2 Observation Synthesis

By performing a nonlinear transformation of the nonlinear system $\dot{x} = f(x)$ using the observability map $\mathcal{O}_n(x)$, that means:

$$z = \mathcal{O}_n(x), \quad x = \mathcal{O}_n^{-1}(z)$$

the system can be represented in the observability form:

$$\begin{aligned}
&\dot{z}_1 = z_2 \\
&\dot{z}_2 = z_3 \\
&. \\
&. \\
&. \\
&\dot{z}_n = \phi(z_1, z_2, ..., z_n) \\
&y = h(z)
\end{aligned}$$

According to [28],[29],[30], considering the system in 3.1 and using the bijective map $z = \mathcal{O}_n(x)$, the new system is obtained:

$$\dot{z} = Az + \phi(z, u), \quad y = Cz \tag{3.5}$$

where

$$A = \left[\begin{array}{c|c} 0 & I_{(n-1)\times(n-1)} \\ \hline 0 & 0_{1\times(n-1)} \end{array}\right]$$

After the system transformation and using the following Proposition:
Proposition 3.2 [32]: The observability map $\mathcal{O}_n(x)$ is a local diffeomorphism $\forall x \in \mathcal{M}$ and both, the Jacobi matrix $\partial\mathcal{O}_n(x)/\partial x$ and the inverse Jacobi matrix $[\partial\mathcal{O}_n(x)/\partial x]^{-1}$ exist, that means $\partial\mathcal{O}_n(x)/\partial x$ is nonsingular.

According to results presented in [29],[32], the estimation error between the system in (3.5) and the following general estimator converges to zero.

$$\dot{\hat{z}} = A\hat{z} + \phi(\hat{z}, u) + L(y - C\hat{z}) \tag{3.6}$$

where $\hat{z}$ is the estimate of z. Matrices A and C are constants and since the pair (A, C) is observable, the gain matrix L may be designed such that $A - LC$ has only

stable eigenvalues.
Then, applying the inverse transformation using the observability map:

$$\dot{\hat{x}} = \left[\frac{\partial \mathcal{O}_n(x)}{\partial x}\right]^{-1}_{x=\hat{x}} \dot{\hat{z}}$$

The general observer in the original coordinates for the nonlinear system in (3.1) is described by:

$$\dot{\hat{x}}(t) = f(\hat{x}(t)) + g(\hat{x}(t))u(t) + \left[\frac{\partial \mathcal{O}_n(x)}{\partial x}\right]^{-1}_{x=\hat{x}} L(y(t) - h(\hat{x}(t))) \tag{3.7}$$

The observer presented in (3.7) represents a general case and matrix L may take different forms depending on the class of observer that is used in the monitored system, such as high gain observer, sliding mode observer or a super twisting observer.

3.2.3 Robust Nonlinear Observer

Since a good estimation of the states is important in the residual generation approach, it is necessary to design an observer which is robust against the presence of some uncertainties, disturbances or unknown inputs. So, considering the system in Equation (3.1) but adding a term which represents the presence of disturbances, the new system is described by:

$$\begin{aligned} \dot{x}(t) &= f(x(t)) + g(x(t))u(t) + \mathrm{P}d(x(t)) \\ y(t) &= h(x(t)) \end{aligned} \tag{3.8}$$

where the disturbances are represented by the function $d(x(t))$ and the matrix P is assumed to be known and indicates the distribution of the disturbances in the system.
Considering the existence of a diffeomorphism $\mathcal{O}(x)$, the system can be transformed in a triangular form and is described as follows[26]:

$$\dot{z} = Az + \phi(z, u) + \bar{\mathrm{P}}d(x, t)$$

with $\bar{\mathrm{P}} = (\partial \mathcal{O}(x)/\partial x)\mathrm{P}$.
Assumed that the disturbances are bounded, the nonlinear estimator presents now a term based on sliding mode theory which main task is to compensate the presence

of the disturbance. The nonlinear estimator is described as follows [32][26]:

$$\dot{\hat{z}} = A\hat{z} + \phi(\hat{z}, u) + L(y - C\hat{z}) + \bar{\mathrm{P}}d_s(t) \tag{3.9}$$

where $d_s(t)$ is a discontinuous term and is described by[26]:

$$d_s(t) = \rho sign(e_1) = \rho sign(h(\hat{x}) - h(x))$$

The error estimate is defined as $e = \hat{z} - z$, then the dynamics of the error is:

$$\dot{\hat{e}} = (A - LC)e + \phi(\hat{z}, u) - \phi(z, u) + \bar{\mathrm{P}}d(x, t) - \bar{\mathrm{P}}d_s(t)$$

Then the first term of the error estimation dynamics, corresponding to the sliding manifold e_1, is:

$$\dot{e}_1 = e_2 - l_1 e_1 + (\phi_1(\hat{z}, u) - \phi_1(z, u)) + d_s - d(x, t) \tag{3.10}$$

where l_1 represents the first term in the matrix L.
For the sliding mode term, when $e_1 = 0$, the estimated state converges to the real state, $\hat{z}_1 = z_1$, and the derivative of the error is $\dot{e}_1 = 0$. From Equation (3.10), considering that with the previous conditions, when $\hat{z}_1 = z_1$ then $\phi_1(\hat{z}, u) = \phi_1(z, u)$, and finally the equivalent control of d_s is described as follows [33]:

$$d_{s,eq} = d(x, t) - e_2$$

Once the estimated states converge to the real ones, the error dynamic becomes zero, that means $e_2 \approx 0$ and then the sliding mode term d_s may be used to estimate the unknown input or disturbance [32].

$$d(x, t) \approx d_{s,eq} = d_s(t) = \rho sign(h(\hat{x}) - h(x)) \tag{3.11}$$

Finally, the nonlinear robust observer in the original coordinates is described by:

$$\dot{\hat{x}}(t) = f(\hat{x}(t)) + g(\hat{x}(t))u(t) + \left[\frac{\partial \mathcal{O}_n(x)}{\partial x}\right]^{-1}_{x=\hat{x}} L(y(t) - h(\hat{x}(t))) + \mathrm{P}\rho\ sign(h(\hat{x}) - h(x)) \tag{3.12}$$

As mentioned before, additive faults can be represented as disturbances in the system and consequently, residuals can be generated by using the estimated disturbance as shown in Equation (3.11).

3.3 Parameter Estimation Approach

The term *parameter* is related to a scalar or vector value which is assumed to be time invariant. In some cases, this parameter may change with the time, and may be called "time-varying parameter", but this variation is considered very slow in comparison with the change of the system states [10].
Parameter estimation approach is another well known technique used in FDI and in the residual generation scheme. This approach is subtended on the idea that faults occurrence may be reflected in the physical parameter of the system. In this way, in order to achieve a fault detection, system parameters are estimated using different well known parameter estimation techniques. Once the parameters have been estimated, the residual signal is generated by the difference between the parameters in a fault free case and them corresponding on-line parameter estimates. The problem of parameter estimation p can be described as follows, in a general form, as in [2]: From measurements of the system outputs and considering the presence of the known input signals u and the possible presence of disturbances w, that is via

$$y(t) = \mathrm{G}(t, u(t), w(t), p) \tag{3.13}$$

it is possible to find a function that estimates the parameter p in function of the input signals and the measured output signals as

$$\hat{p}(t) = \hat{\mathrm{P}}(t, Z_0^t) \tag{3.14}$$

where $\hat{p}$ and $\hat{P}$ are the estimated parameter and the parameter estimation function, respectively. Z_0^t represents the values of the input and measured signals from the initial until the time t:

$$Z_0^t = [y_j, u_j]_0^t$$

From Equation (3.14) it is possible to note that the function $\hat{\mathrm{P}}$ requires all the past observed values. That is impractical and computationally unfeasible for on-line monitoring and fault detection because the dimension of the inputs in the estimator function increases with the time [2]. So, a formulation of a parameter estimation for a finite horizon T is proposed:

$$\hat{\alpha}(t) = \hat{\mathrm{A}}(Y_{t-T}^t, U_{t-T}^t, t) \tag{3.15}$$

where $\hat{\alpha}$ and $\hat{\mathrm{A}}$ are the estimated parameter and the parameter estimation function in a finite horizon, respectively. And Y_{t-T}^{t}=$[y_j]_{j=t-T}^{t}$, U_{t-T}^{t}=$[u_j]_{j=t-T}^{t}$.

The vector-valued function G presented in Equation 3.13 is the observation function and it is the linearity or nonlinearity of function G (or equivalently, function $f(.)$ in $\dot{x} = f(t, x, u, p)$) with respect to the parameters p which determines the linearity or nonlinearity of the parameter estimation problem [2].

3.3.1 Linear Parameter Estimation

In this case, the function G (or $f(.)$) is linear with respect to the parameter. The system may be represented in the following form:

$$y(t) = a_1 y(t-1) + a_2 y(t-2) + ... + a_n y(t-n) + b_1 u(t-1) + ... + b_n u(t-n) \quad (3.16)$$

The system may be simplified and rewritten in the matrix form:

$$y(t) = \psi^{\mathrm{T}} \theta \quad (3.17)$$

where:

$$\psi^{\mathrm{T}} = \begin{bmatrix} y(t-1) & ... & y(t-n) & u(t-1) & ... & u(t-n) \end{bmatrix}$$
$$\theta^{\mathrm{T}} = \begin{bmatrix} a_1 & ... & a_{(n-1)} & b_1 & ... & b_{(n-1)} \end{bmatrix}$$

are the data vector and the parameter vector, respectively.
The parameter estimation can be achieved by using Least Square Error(LSE) method. In the case when there are r measurements, the system take the following form [10]:

$$\begin{bmatrix} y_1 \\ . \\ . \\ . \\ y_r \end{bmatrix} = \begin{bmatrix} \psi_{1,1} & ... & \psi_{1,2n} \\ . & & \\ . & & \\ . & & \\ \psi_{r,1} & ... & \psi_{r,2n} \end{bmatrix} \begin{bmatrix} \theta_1 \\ . \\ . \\ . \\ \theta_{2n} \end{bmatrix}$$

Then, the error is the difference between the real and the estimated data

$$e = \begin{bmatrix} e_1 \\ . \\ . \\ . \\ e_r \end{bmatrix} = \begin{bmatrix} y_1 \\ . \\ . \\ . \\ y_r \end{bmatrix} - \begin{bmatrix} \psi_{1,1} & ... & \psi_{1,2n} \\ . & & \\ . & & \\ . & & \\ \psi_{r,1} & ... & \psi_{r,2n} \end{bmatrix} \begin{bmatrix} \hat{\theta}_1 \\ . \\ . \\ . \\ \hat{\theta}_{2n} \end{bmatrix} = \mathbf{Y} - \hat{\mathbf{Y}} = \mathbf{Y} - \mathbf{\Psi}\hat{\mathbf{\Theta}} \tag{3.18}$$

The cost function is defined by:

$$J = \sum_{i=1}^{r} e_i^2 = e^{\mathrm{T}} e = (\mathbf{Y} - \mathbf{\Psi\Theta})^{\mathrm{T}}(\mathbf{Y} - \mathbf{\Psi\Theta}) \tag{3.19}$$

From the minimization of the cost function J [10]:

$$\begin{aligned} \frac{\partial J}{\partial \mathbf{\Theta}} &= \frac{\partial}{\partial \mathbf{\Theta}}(\mathbf{Y}^{\mathrm{T}}\mathbf{Y} - \mathbf{Y}^{\mathrm{T}}\mathbf{\Psi\Theta} - \mathbf{\Theta}^{\mathrm{T}}\mathbf{\Psi}\mathbf{Y} + \mathbf{\Theta}^{\mathrm{T}}\mathbf{\Psi}^{\mathrm{T}}\mathbf{\Psi\Theta}) \\ &= -\mathbf{\Psi}^{\mathrm{T}}\mathbf{Y} - \mathbf{\Psi}^{\mathrm{T}}\mathbf{Y} + 2\mathbf{\Psi}^{\mathrm{T}}\mathbf{\Psi}\hat{\mathbf{\Theta}} \end{aligned}$$

And finally, the parameter estimates are calculated as follows:

$$\hat{\mathbf{\Theta}} = \left[\mathbf{\Psi}^{\mathrm{T}}\mathbf{\Psi}\right]^{-1}\mathbf{\Psi}^{\mathrm{T}}\mathbf{Y} \tag{3.20}$$

3.3.2 Nonlinear Parameter Estimation

Here it is proposed a method for nonlinear systems where the parameters may be decomposed. Considering a nonlinear system of the form:

$$\begin{aligned} \dot{x}(t) &= f(x, \theta, t) + g(x, t)\psi(u) \\ y(t) &= h(x, \theta, t) + \pi(t) \end{aligned} \tag{3.21}$$

where $x \in \mathbb{R}^n$ is the state vector, $u \in \mathbb{R}^q$ is the control input signal, $y \in \mathbb{R}^m$ is the output vector and $\theta \in \mathbb{R}^p$ represent the unknown parameter vector and $\pi(t)$ represents a disturbance in the measurements such as noise.
The function $f(x, \theta, t)$ must be or is assumed to be a smooth nonlinear function and must fulfill the following assumptions as in [34][35].
Assumption 3.1: Function $f(x, p, t)$ is decomposable in the form:

$$f(x, p, t) = \alpha^{\mathrm{T}}(\theta)\zeta(x, t) \tag{3.22}$$

with:

$$\alpha^{\mathrm{T}} = [\alpha_1, \alpha_2, ..., \alpha_p]$$
$$\zeta(x,t)^{\mathrm{T}} = [\zeta_1, \zeta_2, ..., \zeta_p]$$

where:

$\zeta_i = \zeta_i(x,t) \neq 0$ are known nonlinear functions and linearly independent. Function $\alpha_i = \alpha_i(t)$ is a combination of θ.

The unknown parameter vector belongs to a space $\boldsymbol{\Theta} : \{\theta_i \in [\theta_{imin}, \theta_{imax}], i = 1, 2, ..., p\}$. So, since the parameters are bounded, the function $\alpha(\theta)$ has to be also bounded.

Assumption 3.2 Uncertain parameters α_i satisfy the bounds:

$$\alpha_i \in [\alpha_{imin}, \alpha_{imax}], \forall \theta \in \boldsymbol{\Theta}$$

where:

$\hat{\alpha_i} \rightarrow$ uncertain parameter of the estimator.

$\hat{\alpha_o} \rightarrow$ time varying parameter which is calculated in terms of uncertain parameters and its bound are:

$$\hat{\alpha_o} = \begin{cases} \alpha_{imin}, & \hat{\alpha_i} < \alpha_{imin} \\ \hat{\alpha_i}(t), & \alpha_{imin} \leq \hat{\alpha_i} \leq \alpha_{imax} \\ \alpha_{imax}, & \hat{\alpha_i} < \alpha_{imax} \end{cases}$$

Now the third assumption is concerned with the system identifiability.

Assumption 3.3 This assumption is related to the identifiability of the system parameters. Since identifiability consists in identify the parameters of the system from its input-output map, it is possible to treat the parameter identifiability as an special case of observability by considering parameters as states, but with its time derivatives equal to zero, that means $\dot{\theta} = 0$[36]. The rank test condition is used to test observability of the system, which consists in determining the rank of the

observability Jacobian:

$$J_O = \begin{bmatrix} \frac{\partial L_f h_1}{\partial x_1} & \cdots & \frac{\partial L_f h_1}{\partial x_n} \\ \vdots & \ddots & \vdots \\ \frac{\partial L_f h_m}{\partial x_1} & \cdots & \frac{\partial L_f h_m}{\partial x_n} \\ \vdots & \ddots & \vdots \\ \frac{\partial L_f^{n-1} h_1}{\partial x_1} & \cdots & \frac{\partial L_f^{n-1} h_1}{\partial x_n} \\ \vdots & \ddots & \vdots \\ \frac{\partial L_f^{n-1} h_m}{\partial x_1} & \cdots & \frac{\partial L_f^{n-1} h_m}{\partial x_n} \end{bmatrix} \tag{3.23}$$

If the matrix J_O has a full rank, the system is algebraic observable [37]. In the same way, parameter identifiability can be determined by test rank condition. So, the identifiability Jacobian has to fulfill the following condition:

$$rank(J_I) = rank(\frac{\partial}{\partial \theta_j} L_f^k h_i) = n$$

where $i = 1, 2, ..., m$, $j = 1, 2, ..., p$, $k = 1, 2, ..., n-1$ and $L_f^k h$ is the Lie derivative. Additionally it is assumed that the nonlinear system described in 3.21 is a differentially flat system, as it is defined in [38].

Definition 3.2 (*Flat Systems*):

A dynamic system is said to be flat if any of its states, outputs or inputs can be represented as a function of flat outputs $y_f = L_f^0 h = h$ and their derivatives up to some finite order and if any component of the flat output can be written as a function of system variables and their derivatives up to some finite order such that

$$\begin{aligned} y &= h(x, u, \dot{u}, ..., u^{(r)}) \\ x &= \varphi_1(L_f^0 h, L_f^1 h, ..., L_f^m h) \\ u &= \varphi_2(L_f^0 h, L_f^1 h, ..., L_f^p h) \end{aligned} \tag{3.24}$$

where m and p are positive integers.

Flatness for linear and nonlinear systems using differential algebra is discussed widely in [38].

The parameter estimation is achieved using the properties of differential flat

systems [8][35]. Assumed that the parameter vector $\theta^{\mathrm{T}} = [\theta_1, \theta_2, ..., \theta_p]$ of the nonlinear flat system described in (3.21) satisfies the three assumptions presented before. Then, the parameters can be expressed in the following form:

$$\theta = \gamma(t, L_f^0 f, L_f^1 h, ..., L_f^k h, u, \dot{u}, ..., u^{(r)}) \tag{3.25}$$

What is the same

$$\theta_i = \gamma_i(t, y, \dot{y}, ..., y^{(k)}, u, \dot{u}, ..., u^{(r)}) \tag{3.26}$$

for each parameter θ_i, with $i = 1, 2, ..., p$. The function γ_i is a nonlinear function whose inputs are the input signals, flat outputs signals and their derivatives. Assuming that output signals are measurable and the input control signal is known, it is possible to estimate their corresponding derivatives. Consequently, with an accurate estimation of the derivatives and replacing them in Equation (3.26), an accurate estimate parameter vector may be calculated as follows [8][35][39]:

$$\hat{\theta}_i = \gamma_i(t, y, \hat{\dot{y}}, ..., \hat{y}^{(k)}, u, \hat{\dot{u}}, ..., \hat{u}^{(r)}) \tag{3.27}$$

The estimation of the derivatives of both, outputs and inputs, may be carried out with different methods such as using algebraic estimation techniques like iterated integrals as in [8] and [40] or using a high order differentiator like a Levant's differentiator observer as in [37],[35].

As in the other methods, once the parameter estimates have been calculated, the residual generation may be computed as a comparison between the real parameter or the estimated parameter in the fault free case (assuming that at the beginning any fault has occurred) and the on-line parameter estimated.

$$r_i(t) = \theta_i - \hat{\theta}_i(t) \tag{3.28}$$

3.4 Structural Analysis Approach

The structural analysis approach uses the structural properties of the system. This structural properties are analyzed by using a structural model which is an abstraction of the system behavior in the sense that only the structure of the constraints (existence of relations between the variables and parameters) is considered but not the constraints themselves [4]. The links between variables and parameters are represented by using a bi-partite graph, which describes, in a very

simple level, a model of the system behavior. In contrast with its relative simplicity, the structural model is very useful for fault diagnosis tasks because the structural analysis is able to give important information about the system components which may be or not monitorable, to provides information about analytical redundancy based residuals and others.
The main assumption of this approach is that every component is related to one or more constraints. In this way, if any constraint is not fulfilled or is violated, that may represents the presence of a fault. So, structural analysis allows residual generation by analytical redundancy.

3.4.1 Structural Model

As mentioned before, the structural model is represented by using a bi-partite graph where is possible to visualize the relations between the systems variables and constraints.
In order to check if a system is well represented by a set of constraints, the following assumption must be fulfilled.
Assumption 3.4 [4]:

- All constraints are compatible and there is no contradiction between the set of constraints.
- All constraints are independent and any constraint should not be include in another one.

Considering a system model which is defined by a pair ($\mathcal{C}$,$\mathcal{Z}$), where $\mathcal{Z}$ and $\mathcal{C}$ denote the set of variables or parameters and the set of constraints, the structural model is defined as follows.
Definition 3.3 (*Structural model*)[4]:
The structural model or the structure of the system ($\mathcal{C}$,$\mathcal{Z}$) is a bi-partite graph ($\mathcal{C}$,$\mathcal{Z}$,Γ) where $\Gamma \in \mathcal{C}x\mathcal{Z}$ is the set of edges defined by:

$$(c_i, z_j) \in \Gamma \; if \; the \; variable \; z_j \; appears \; in \; the \; constraint \; c_i$$

In the bi-partite graph, all the variables which are connected or have a relation with a particular constraint, have to satisfy the equation that this constraint represents. An example of a simple structural model is illustrated in Figure 3.3, where the circles represent the variables of the system and the bars represent the constraints.

It is simple to realize from the graphic, which variables have relations with which constraints.

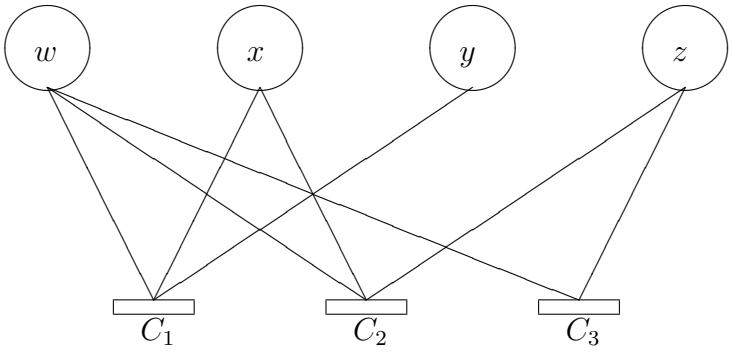

Figure 3.3: Simple bi-partite graph

Another way to represent the relation between variables and constraints is by using an incidence matrix which can be used in the construction of structural model. The incidence matrix makes a distinction between the known variables and the unknown variables. Known variables are for example, input control signals, output measured signals or known parameters of the system. On the other hand, unknown variables may be unmeasured signals, unknown parameters of the system or internal variables. The distinction in the incidence matrix is necessary because it will be used afterwards in the matching process. However, since it is assumed that known system parameters are fixed, it is not necessary to include them in the structural model. Table 3.1, from [4] gives an example of an incidence matrix of a tank system where both, unknown and known variables are distinguished. Then since parameters h_o, r and k are assumed to be fixed, they are not included in the structural model as is shown in Figure 3.4.

	Known Variables					**Unknown variables**			
	u	y	h_0	r	k	h	$\dot{h}$	q_{in}	q_{out}
C_1							1	1	1
C_2	1							1	
C_3					1	1			1
C_4		1				1			
C_5	1	1	1	1					
C_6						1	1		

Table 3.1: Example of incidence matrix

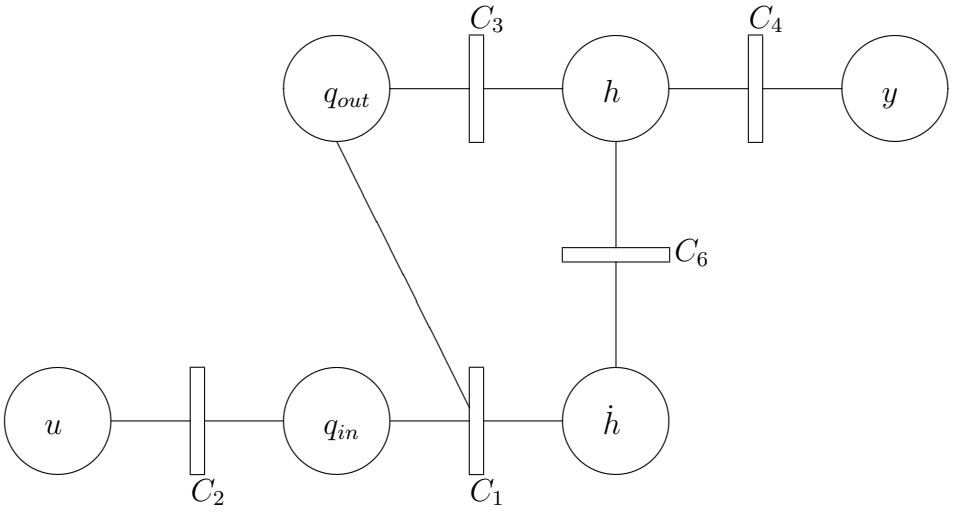

Figure 3.4: Example of Structural model of the tank system

3.4.2 Matching Process

Matching is the main tool of the structural analysis approach in the residual generation scheme. This concept consists in the association between unknown variables and the system constraints and these associations will be used then to calculate a particular unknown variable. In terms of matching, the unknown variables which have been matched, will be able to be calculated, otherwise the variable cannot be computed. In contrast, if a variable has more than one matching, it may be calculated in different ways and these additional ways (redundancies) will be used for purpose of fault detection and residual generation. Considering the bi-partite graph $(\mathcal{C}, \mathcal{Z}, \Gamma)$ and $e = (\alpha, \beta) \in \Gamma$ be an edge who links the variable β with the constraint α and p_c,p_z two projections:

$$\begin{aligned} p_c \quad &: \quad \Gamma \rightarrow \mathcal{C} \\ &: \quad p_c(e) = \alpha \\ p_z \quad &: \quad \Gamma \rightarrow \mathcal{Z} \\ &: \quad p_z(e) = \beta \end{aligned}$$

Definition 3.4 (*Matching*)[4]:
A matching $\mathcal{M}$ is a subset of Γ such that he restrictions of p_c and p_z to $\mathcal{M}$ are injective, i.e.:

$$\forall e_1, e_2 \in \mathcal{M} : \; e_1 \neq e_2 \quad \rightarrow \quad p_c(e_1) \neq p_c(e_2) \; \textit{and} \; p_z(e_1) \neq p_z(e_2)$$

That means, in a matching process it is not possible that two different edges have the same node, a variable or a constraint.

Once the matching has been carried out successfully, it is possible to know, which unknown matched will be calculated by using the constraint, where the unknown variable belongs, and the others variables that belong to the same constraint. In this way, appears a kind of orientation in the bi-partite graph. The matched unknown variable will be calculated by using its corresponding matched constraint and the others non-matched variables. The orientation of the bi-partite graph is made by using the following rules [4]:

- Matched constraint: All the variables which belong to the constraint have an orientation:
  - from the non-matched variables to the constraint. That means that the non-matched variables are considered as inputs of the constraint.
  - from the constraint to the matched variable. In the same sense, the matched variable is considered as an output of the constraint.

  In other words, the matched variable will be compute using the constraint and the other variables:
  $$x = \gamma(\mathcal{C}, \mathcal{Z} - \{x\}) \tag{3.29}$$
- Non-matched constraint: In this case, all the variables are considered as inputs, i.e. all the variable are orientated to the constraint.
  In that situation, since there is any "output", it is equal to zero and the constraint may be represents as follows:
  $$\gamma(\mathcal{C}, \mathcal{Z}) = 0 \tag{3.30}$$

The non-matched constraint represented in (3.30) receives the label of *ZERO*.
In the matching process, in order to avoid structural model or bi-partite graphs without the presence of any loops, a "Ranking algorithm" is used. When this algorithm is applied, the matching is made in a way that the ranking of each constraint indicates the flow of the computation of the unknown variables. In a general sense, the lower rank "0" denotes the known variables (inputs or measured signals) and the following ranks indicate the order in which the unknown variables will be computed. An explanation of the ranking algorithm may be found in [4].

3.4.3 Residual Generation

The basis for residual generation in the structural analysis approach is the matching process. The idea is to obtain a complete matching (see [4] for a complete explanation)) respect to the unknown variables and a non-complete matching respect to the constraints. In the first case, the complete matching indicates that all the unknown variables are able to be computed as a function of the known variables and the unknown ones which have been already computed. In the second case, the non-complete matching indicates that at least one constraint is non-matched. Consequently, non-matched constraints will be equal to *ZERO*, as in (3.30) and it results in an analytical redundancy relation. This AAR's (analytical redundancy relations) will be used as a residual signal, which may be represented as:

$$r_i(t) = ZERO_i(t) = \gamma_i(\mathcal{C}, \mathcal{Z}, t) \tag{3.31}$$

A violation of any non-matched constraint implicates a deviation of the residual signal from the value zero and consequently it may represent a fault occurrence.
A deeper and wider explanation of the structural analysis and other important concepts related to this approach are explained in [4].

4 Three Tank System

4.1 Three-Tank System Model

The system that will be studied in this thesis is a Three Tank System. The Three Tank System has typical characteristics of tanks, pipes, and pumps that are used very often in different processes and in the industry. That is the reason why this system serves as a benchmark in laboratories of process control. Also, because this system is a benchmark, there is some literature about the topic of this work and all that makes it possible to compare the methods of fault detection that will be development in this thesis and other methods used in the literature. The schematic diagram of the system is shown in figure 4.1.

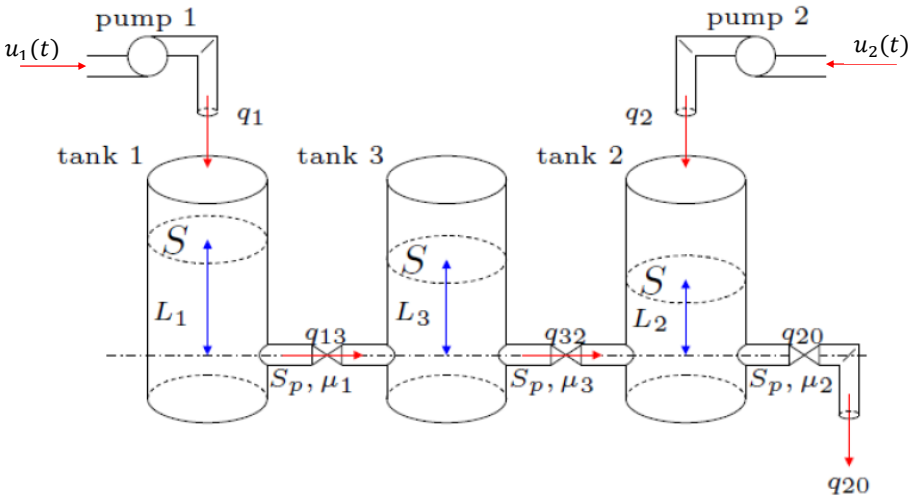

Figure 4.1: Three Tank System model [8]

Under considerations of Torriceli's law and applying the incoming and outcoming

mass flows, dynamics of the system model illustrated in Figure 4.1 described by [9]:

$$\begin{aligned} S\dot{h_1}(t) &= q_1 - q_{13}, \\ S\dot{h_2}(t) &= q_2 - q_{32} - q_{20}, \\ S\dot{h_3}(t) &= q_{13} - q_{32}. \end{aligned} \tag{4.1}$$

The water flows from tank i to j, represented as q_{ij}, are obtained as follow:

$$q_{ij} = \mu_i S_p sign(h_i - h_j)\sqrt{2g|h_i - h_j|}, \quad where i, j = 1, 2, 3 \tag{4.2}$$

and the outgoing flow from tank 2 is described by:

$$q_{20} = \mu_2 S_p sign(h_2)\sqrt{2g|h_2|} \tag{4.3}$$

where:

- μ_i, S_p are the flow coefficients of viscosity and the cross sectional areas of interconnecting pipes.
- h_i are the water levels of each tank.
- S is the transversal area of each tank.

Additionally, q_1 and q_2 are flow rates into tank 1 and tank 2, respectively. These flows are delivered by pump 1 and pump 2 using $u_1(t)$ and $u_2(t)$, which are the control signals of the input flow rates.
Then, the full system model is described as follows:

$$\begin{aligned} \dot{x_1} &= -C_1 sign(x_1 - x_3)\sqrt{|x_1 - x_3|} + \tfrac{u_1}{S} \\ \dot{x_2} &= C_3 sign(x_3 - x_2)\sqrt{|x_3 - x_2|} - C_2 sign(x_2)\sqrt{|x_2|} + \tfrac{u_2}{S} \\ \dot{x_3} &= C_1 sign(x_1 - x_3)\sqrt{|x_1 - x_3|} - C_3 sign(x_3 - x_2)\sqrt{|x_3 - x_2|} \\ y &= \begin{bmatrix} x_1 & x_2 & x_3 \end{bmatrix}^{\mathrm{T}}. \end{aligned} \tag{4.4}$$

where $x_i(t)$ is the water level in each tank i and $C_i = \frac{1}{S}\mu_i S_p\sqrt{2g}$.
The typical parameters of the benchmark system that will be used are given in table 4.1 [9].

PARAMETER	DESCRIPTION	UNITS	NOMINAL VALUES
S	Cross section area of tanks	m^2	0.0154
S_n	Cross section area of pipes	m^2	$5x10^{-5}$
u_{1max}, u_{2max}	Maximun flow rate of pumps	$\frac{cm^3}{sec}$	100
$h_{i,max}, i = 1, 2, 3$	Maximun height of tanks	m	0.60
μ_1	Viscosity or flows coefficients	-	0.46
μ_2		-	0.6
μ_3		-	0.45

Table 4.1: Typical Parameters of the system model [9]

4.2 Possible Faults

There are three types of faults, which are often studied in the present benchmark system [9]:

- **Component Faults**
  In this kind of fault there are two possible cases:
  - Leaks in the three tanks, which can be described as additional mass flows out of the tank and can be modeled by:

$$\begin{aligned} q_{L1} &= \theta_{A1}\sqrt{2gh_1}, \\ q_{L2} &= \theta_{A2}\sqrt{2gh_2}, \\ q_{L3} &= \theta_{A3}\sqrt{2gh_3} \end{aligned} \tag{4.5}$$

    where $\theta_{A1}, \theta_{A2}, \theta_{A3}$ are unknown and depend on the size of the leaks.
  - Pluggings between two tanks and in the outlet pipe by tank 2, which cause changes in the flows q_{13}, q_{32} and q_{20}. These changes can be modeled by:

$$\begin{aligned} q_{P13} &= \theta_{A4}\mu_1 S_p sign(h_1 - h_3)\sqrt{2g|h_1 - h_3|}, \\ q_{P32} &= \theta_{A6}\mu_3 S_p sign(h_3 - h_2)\sqrt{2g|h_3 - h_2|}, \\ q_{P20} &= \theta_{A5}\mu_2 S_p sign(h_2)\sqrt{2g|h_2|} \end{aligned} \tag{4.6}$$

    where $\theta_{A4}, \theta_{A5}, \theta_{A6} \in [-1, 0]$ are unknown.

  The influences of these faults can be integrated into the system model

presented in (4.1) and the new form is described below:

$$\begin{aligned} S\dot{h_1}(t) &= q_1 - q_{13} + (q_{P13} - q_{L1}), \\ S\dot{h_2}(t) &= q_2 - q_{32} - q_{20} + (q_{P20} - q_{L2}), \\ S\dot{h_3}(t) &= q_{13} - q_{32} + (q_{P32} - q_{L3}). \end{aligned} \tag{4.7}$$

- **Sensor Faults**
  In this case, there is a possibility of an error in the sensor's lectures that can be modeled as additive faults in the three sensors or a presence of Gaussian noise. The influence of these faults in the output signals of the model can be modeled as:

$$y = \begin{bmatrix} x_1 \\ x_2 \\ x_3 \end{bmatrix} + \begin{bmatrix} \epsilon_1 \\ \epsilon_2 \\ \epsilon_3 \end{bmatrix} + \eta \tag{4.8}$$

  where:
  - x_1, x_2 and x_3 are the real height values.
  - $\begin{bmatrix} \epsilon_1 & \epsilon_2 & \epsilon_3 \end{bmatrix}^{\mathrm{T}}$ are additive faults that correspond to the i^{th} sensor.
  - η is the Gaussian noise.

- **Actuator Faults**
  It is important to note that an actuator fault corresponds to the variation of the global control input applied to the system [10]. In this case, there are possible faults in each pump:

$$\begin{bmatrix} U_1 \\ U_2 \end{bmatrix} = \lambda \begin{bmatrix} u_1 \\ u_2 \end{bmatrix} + \begin{bmatrix} u_{f1} \\ u_{f2} \end{bmatrix} \tag{4.9}$$

  where:
  - u_1 and u_2 are the global input applied to the system.
  - U_1 and U_2 are the global faulty control signal.
  - $\lambda = diag(\alpha_1, \alpha_2)$ denotes multiplicative faults.
  - u_{f1} and u_{f2} denote additive faults in each control signal.

  So, the i^{th} actuator is faulty if $\alpha_i \neq 1$ or $u_{fi} \neq 0$ [10]. In Table 4.2, different types of actuator faults are represented.

	Constant offset $\mathbf{u_{fi}} = \mathbf{0}$	**Constant offset $\mathbf{u_{fi}} \neq \mathbf{0}$**
$\alpha_\mathbf{i} \neq \mathbf{1}$	Fault-free case	Bias
$\alpha_\mathbf{i} \in <\mathbf{0};\mathbf{1}>$	Loss of effectiveness	Loss of effectiveness
$\alpha_\mathbf{i} = \mathbf{0}$	Out of order	Actuator blocked

Table 4.2: Actuator faults [10]

4.3 Diagnosability Analysis

In order to analyze either or not a system diagnosable, it is necessary to include a definition based on [17].

Definition 4.1 (*Diagnosable System*)

A system is considered diagnosable if it is possible to estimate the faults of the system by using the system model equations and the data obtained from the measured output signals y and the input signal u.

In other words, faults have to be observable respect to the input and output signals and that will be fulfilled if each fault is algebraic observable by using signals u and y. An algebraic observability can be achieved when each fault f_i is able to be written as a solution of a polynomial equation f_i by using the signals u, y and their respective finite time derivatives, i.e.

$$\mathrm{H}(f_i, u, ..., u^{(n)}, y, ..., y^{(n)}) = 0 \tag{4.10}$$

where n is a finite positive number.

Now, since the measured output signals y are needed in the algebraic observability of the faults, a common question is about the number of measured outputs that is necessary in order to make a system diagnosable. In this way another definition is needed:

Definition 4.2 (*Differential output rank*)[17]

The differential output rank ρ of a system represents the maximum number of outputs which are related by a differential polynomial equation.

In order to calculate the differential output rank ρ, a practical technique has been developed in [17]. It consists in determine the possible polynomial equations which involves the possible system outputs and which have the following form:

$$P(y, \dot{y}, ..., y^{(n)}) = 0 \tag{4.11}$$

Then, the number of independent polynomials of the form in (4.11) are found and considering that there is κ independent polynomials, the differential output rank is calculated as follows[17]:

$$\rho = m - \kappa \tag{4.12}$$

where m is the number of the available measured outputs. So, the minimum number of outputs that are necessary to make a system diagnosable have to be the same as the number of faults that may appear or that are considered in the faulty system [17].

Now, the three tank system is analyzed. Since the main idea of differential output rank consists in finding the maximal number of outputs which are related by a differential equation, for the three tanks system, it is considering to talk about differential functions instead of differential polynomial equations.
Assuming that the faults mentioned may be represented as additives, independent of the kind of fault, two scenarios are presented:

(a) First scenario:
Three faults are considered and each one has a direct influence on a state. The system, summarizing the possible faults as an additive one, is described as:

$$\begin{aligned} \dot{x}_1 &= \tfrac{1}{S}(-q_{13} + u_1 + f_1) \\ \dot{x}_2 &= \tfrac{1}{S}(q_{32} - q_{20} + u_2 + f_2) \\ \dot{x}_3 &= \tfrac{1}{S}(q_{13} - q_{32} + f_3) \\ y &= \begin{bmatrix} x_1 & x_2 & x_3 \end{bmatrix}^{\mathrm{T}} \end{aligned} \tag{4.13}$$

In this case there is no function in the form (4.11) in which the outputs appear. Then, the differential output rank $\rho = 3$ and consequently the system is diagnosable only if the three outputs are measured.
According to this diagnosability analysis, in the case when only two measurements are available, it won't be possible to diagnose the three faults which are considered. This idea makes sense since, for example from the observer based approach, the residuals are generated as a difference between the measured and the estimated signals, and when only two outputs can be measured, only two residual may be generated (each one for a corresponding state).

(b) Second scenario:

In this scenario the considered faults have direct influence on two states, which are x_1 and x_2. This selection has been made because these states present the influence of the actuators (input signals) in their dynamic equation and as a consequence actuator faults can also be considered in the summarized additive faults. The system is described now by:

$$\begin{aligned} \dot{x}_1 &= \tfrac{1}{S}(-q_{13} + u_1 + f_1) \\ \dot{x}_2 &= \tfrac{1}{S}(q_{32} - q_{20} + u_2 + f_2) \\ \dot{x}_3 &= \tfrac{1}{S}(q_{13} - q_{32}) \end{aligned} \tag{4.14}$$

In this scenario exists one function in the form (4.11) in which the outputs appear.

$$P(y, \dot{y}, ..., y^{(n)}) = \dot{y_3} - C_1\sqrt{|y_1 - y_3|} + C_3\sqrt{|y_3 - y_2|} = 0$$

So, two or more measured outputs are needed in order to make the system diagnosable and it leads to four different cases:

- Case 1:
  The three states are measured. This is the simplest case and it is the most common in the literature. Since the differential output rank $\rho = 2$ and the three states are available, the system is diagnosable. The faults are observable with respect to the input and output signals and may be expressed as follows:

$$\begin{aligned} f_1 &= S\dot{y}_1 + C_1 sign(y_1 - y_3)\sqrt{|y_1 - y_3|} - u_1 \\ f_2 &= S\dot{y}_2 - C_3 sign(y_3 - y_2)\sqrt{|y_3 - y_2|} + C_2 sign(y_2)\sqrt{|y_2|} - u_2 \end{aligned} \tag{4.15}$$

- Case 2:
  In this case, the states x_1 and x_3 are measured. Now, the observability respect to the inputs and measured signals will be tested. From equation (4.14), it is possible to calculates x_2:

$$x_2 = y_3 - \frac{(-S\dot{y}_3 + C_1 sign(y_1 - y_3)\sqrt{|y_1 - y_3|})^2}{C_3^2\sqrt{2g}}$$

  Replacing x_2 in equation (4.15), faults can be represented as a function

of the input and output signals.

$$H_1(f_1, y_1, \dot{y}_1, y_3, \dot{y}_3) = 0$$
$$H_2(f_2, y_1, \dot{y}_1, y_3, \dot{y}_3) = 0$$

Also, a system with two equations and two unknown variables, f_1 and f_2 is obtained. That means, the faults are diagnosable using the proposed outputs.

– Case 3:
Now the considered outputs are $y_2 = x_2$ and $y_3 = x_3$. As in the previous case, from 4.14, x_1 can be computed as:

$$x_1 = y_3 + \frac{(S\dot{y}_3 + C_3 sign(y_3 - y_2)\sqrt{|y_3 - y_2|})^2}{C_1^2\sqrt{2g}}$$

In the same way, faults can be represented as a function of the two considered outputs:

$$H_1(f_1, y_2, \dot{y}_2, y_3, \dot{y}_3) = 0$$
$$H_2(f_2, y_2, \dot{y}_2, y_3, \dot{y}_3) = 0$$

and a solvable system is obtained. In this case, faults are diagnosable too, with the considered outputs.

– Case 4:
The last case considers outputs $y_1 = x_1$ and $y_2 = x_2$. State x_3 can be represented by:

$$x_3 = y_1 - \frac{(-S\dot{y}_1 + f_1 + u_1)^2}{C_1^2\sqrt{2g}}$$

Unlike the previous cases, replacing x_3 in the system equation (4.15), only one differential equation with two unknown variables f_1 and f_2 has been obtained. In this sense, it is not possible to diagnose the two considered faults, i.e. system is not diagnosable with the two considered outputs.

4.4 Controller Design

In order to be able to implement the algorithms of the methods of residual generations that are studied in this Thesis, a controller will be designed to control

the system and reach a desired level of the tanks, and then faults will be simulated in the stable system. The controller that will be implemented is a standard first order sliding mode controller.
Standard sliding mode control provides high accuracy and robustness against various kinds of internal or external disturbances. However, it suffers from chattering phenomena associated with high frequency vibrations of the controlled system leading to wear out of actuators and the system itself.
In standard sliding mode control, sliding surfaces are defined as a hyperplane [41]. This approach has two stages, the first one is a reaching phase where states are driven to a stable manifold using appropriate control law and the second one is sliding phase where states slide to a stable equilibrium point [41][33]. The sliding manifolds may be designed to ensure a finite time convergence of sliding variables in order to track desired trajectories.
Sliding manifolds are designed based on error of the dynamic, that means, a difference between the real value and the desired value of the variable or the equilibrium point. The error is defined as follows:

$$e = x - x_{eq} \tag{4.16}$$

where x is the measured real value and x_{eq} is the equilibrium point. Considering that all the heights may be measured, but only two of them are controlled, the system present three errors that are defined by:

$$\begin{aligned} e_1 &= x_1 - x_{1d} \\ e_2 &= x_2 - x_{2d} \\ e_3 &= x_3 \end{aligned} \tag{4.17}$$

where x_{id} is the desired value of the height h_1 and h_2, $i = 1, 2$.
Then, the manifolds are defined as a function of the errors as follows [42]:

$$s = \begin{bmatrix} s_1 \\ s_2 \end{bmatrix} = \begin{bmatrix} f(e_1, e_3) \\ f(e_2, e_3) \end{bmatrix} \tag{4.18}$$

where:

$$\begin{aligned} f(e_1, e_3) &= a_1 e_1 + a_2 e_3 \\ f(e_2, e_3) &= b_1 e_2 + b_2 e_3 \end{aligned} \tag{4.19}$$

The system will stabilize in the equilibrium point if $s = 0$ after a finite transient

process and the rate of convergence is governed by the sliding manifold dynamics, which are defined by coefficients a_i and b_i.
The designed control laws that make the system converge at $s = 0$ are defined by [43][42]:

$$u(t) = \begin{bmatrix} u_1 \\ u_2 \end{bmatrix} = \begin{bmatrix} u_{1eq} - k_1 sign(s_1) \\ u_{2eq} - k_2 sign(s_2) \end{bmatrix} \tag{4.20}$$

u_{1eq} and u_{2eq} are the equivalent control for both input flow rates and are obtained making the dynamics of sliding manifolds mentioned in 4.18 equal to zero.

$$\begin{aligned} \dot{s}_1 &= a_1\dot{e}_1 + a_2\dot{e}_3 = 0 \\ \dot{s}_2 &= b_1\dot{e}_2 + b_2\dot{e}_3 = 0 \end{aligned} \tag{4.21}$$

From equation (4.21) u_{1eq} and u_{2eq} are obtained as detailed below:

$$\begin{aligned} u_{1eq} &= \tfrac{S}{a_1}[-a_2(C_1 f(x_1, x_3) - C_3 f(x_2, x_3)) + a_1(C_1 f(x_1, x_3))] \\ u_{2eq} &= \tfrac{S}{b_1}[-b_2(C_1 f(x_1, x_3) - C_3 f(x_2, x_3)) + b_1(C_2 f(x_2) - C_1 f(x_1, x_3))] \end{aligned} \tag{4.22}$$

where:

$$\begin{aligned} C_1 f(x_1, x_3) &= C_1 sign(x_1 - x_3)\sqrt{|x_1 - x_3|} \\ C_2 f(x_2) &= C_2 sign(x_2)\sqrt{|x_2|} \\ C_3 f(x_2, x_3) &= C_3 sign(x_3 - x_2)\sqrt{|x_3 - x_2|} \end{aligned} \tag{4.23}$$

Both, the algorithm of the control laws and the system model are implemented in Simulink and the behavior of the tank levels is showed in Figure 4.2. The equilibrium points that have been chosen are $h_1 = 0.6m$ and $h_2 = 0.4m$. The state variables converge to desired trajectories in less than 1 second.

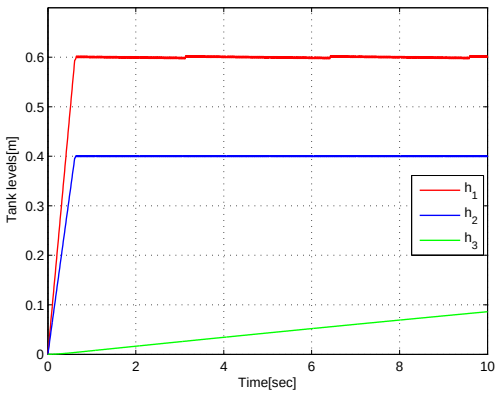

Figure 4.2: Performance of the First Order Sliding Mode Controller

It is possible to notice the presence of chattering, that is a feature of a first order sliding mode. Although, the states of the system are able to achieve their steady state. The chattering phenomena that was mentioned before is showed in Figure 4.3, which illustrates the behavior of the control signals $u_1(t)$ and $u_2(t)$.

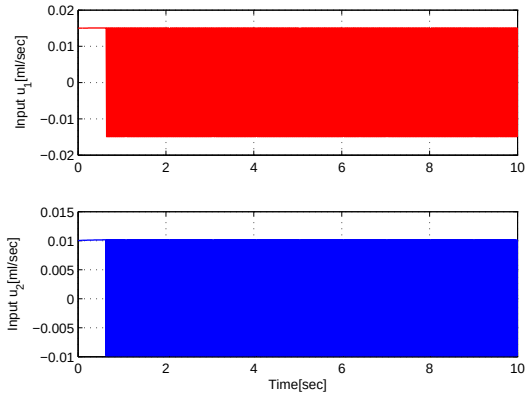

Figure 4.3: Behavior of the control signals with chattering phenomena

As it is described in Figure 4.2, the variables of the system reach the equilibrium point after a finite transient process where the manifold $s_i = 0$. Figure 4.4 illustrates the behavior of manifolds s_1 and s_2.

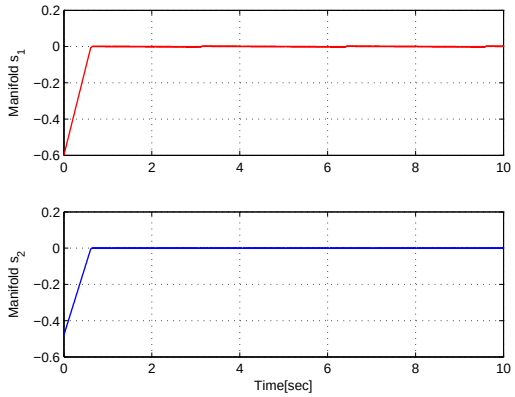

Figure 4.4: Behavior of the manifolds s_1 and s_2

In order to avoid the high frequency chattering that is present in the control laws, these can be performed by employing a saturation function $sat(s_i)$, defined as follows [42][32]:

$$\begin{aligned} sat(s_i) &= sign(\tfrac{s_i}{\epsilon}), \quad if \quad |\tfrac{s_i}{\epsilon}| > 1 \\ sat(s_i) &= \tfrac{s_i}{\epsilon}, \quad if \quad |\tfrac{s_i}{\epsilon}| < 1 \end{aligned} \tag{4.24}$$

The new control laws, including the saturation function, are defined by:

$$u(t) = \begin{bmatrix} u_1 \\ u_2 \end{bmatrix} = \begin{bmatrix} u_{1eq} - k_1 sign(sat(s_1)) \\ u_{2eq} - k_2 sign(sat(s_2)) \end{bmatrix} \tag{4.25}$$

The simulation results for tracking of systems trajectories using the modified control law are illustrated in Figure 4.5 and the control effort of the controller are showed in Figure 4.6 for $u_1(t)$ and $u_2(t)$.

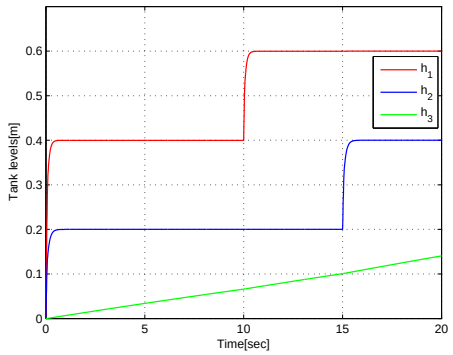

Figure 4.5: Tracking performance of the FOSM controller with Saturation function

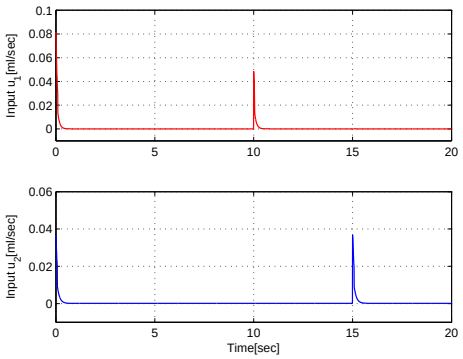

Figure 4.6: Control effort of the signals u_1 and u_2

The chattering phenomenon in the systems trajectories and control effort has been removed by using the saturation function. The desired trajectories to be tracked for the simulations are given by the following equations:

$$h_{1d} = \begin{cases} 0.4, & t \leq 10 \\ 0.6, & t > 10 \end{cases}$$
$$h_{2d} = \begin{cases} 0.2, & t \leq 15 \\ 0.4, & t > 15 \end{cases} \tag{4.26}$$

Additionally, Figure 4.7 illustrates the manifolds converge to zero.

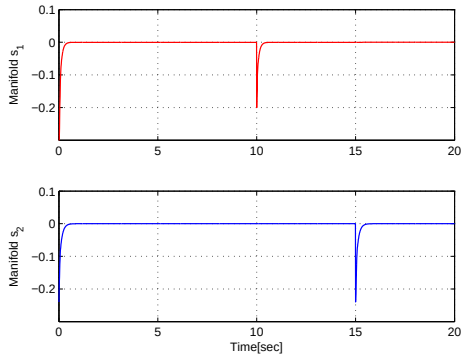

Figure 4.7: Behavior of the manifolds with Saturation function

The gain coefficients, manifolds parameters and saturation coefficient used in the simulations are given in Table 4.3.

PARAMETER	**VALUES**
a_1, a_2	1, $1x10^{-3}$
b_1, b_2	1.2, $1x10^{-3}$
k_1, k_2	$1.5x10^{-2}$ $1x10^{-2}$
ϵ	0.09

Table 4.3: Coefficients and parameters used in the First Order Sliding Mode Controller

Manifolds parameters a_i define the overshoot of the states and parameters b_i define the precision of the desired state, that means, it defines the error between the real and the desired height in stable state, like an integrator behavior. Additionally, Coefficients k_i define the convergence speed of the states.
As it is shown in Figure 4.5, states converge to the desired values in less than 1 second and also they do not have presence of noise or chattering due to the chattering phenomenon in the control signals. Additionally, another important fact which can be notice from Figure 4.6 is that control signals now have not presence of chattering phenomenon. This is very relevant since model-based fault diagnosis requires input and output signals. So, in case an input signal with presence of chattering is used for the residual generation, these residuals may also have a coupled chattering behavior and the fault detection process may be not achieved properly.

5 Residual Generation Implementation and Simulation

In this chapter, some approaches which have been mentioned before will be used in the residual generation process. The algorithms will be developed in Matlab and Simulink. The simulations are done on the three tank system and for different kind of faults. For the majority of approaches, the three outputs will be considered as measurable.

5.1 Observer Based Approach

The main idea of this approach is to generate the residual signals by the comparison between the output signals and their corresponding estimates, i.e. the estimated states of the system.
Since estimates of the states are directly use in this approach, the first step is about a successful state vector estimation. The three tank system model, as described in 4.4, can be reorganized in the following form:

$$\dot{x} = f(x,t) + g(x,t)u(t) \tag{5.1}$$

where x is the state vector which represents the three heights and $u = \begin{bmatrix} u_1 & u_2 \end{bmatrix}^{\mathrm{T}}$. The function $f(x,t)$ and $g(x,t)$ are defined as:

$$f(x,t) = \begin{bmatrix} -C_1 sign(x_1 - x_3)\sqrt{|x_1 - x_3|} \\ C_3 sign(x_3 - x_2)\sqrt{|x_3 - x_2|} + C_2 sign(x_2)\sqrt{|x_2|} \\ C_1 sign(x_1 - x_3)\sqrt{|x_1 - x_3|} - C_3 sign(x_3 - x_2)\sqrt{|x_3 - x_2|} \end{bmatrix} \quad g(x,t) = \begin{bmatrix} \frac{1}{S} & 0 \\ 0 & \frac{1}{S} \\ 0 & 0 \end{bmatrix} \tag{5.2}$$

5.1.1 Observability Analysis

Assuming that the output $h(x) = x_1$, the uniformly observability is analyzed according to Definition 3.2. The matrix of the output and its derivatives is [29]:

$$\begin{bmatrix} y \\ \dot{y} \\ \ddot{y} \end{bmatrix} = \begin{bmatrix} x_1 \\ -C_1 sign(x_1 - x_3)\sqrt{|x_1 - x_3|} + \frac{u_1}{S} \\ C_1^2 sign(x_1 - x_3)\sqrt{|x_1 - x_3|} - \frac{C_1 C_3}{2}\frac{sign(x3-x2)\sqrt{|x_3-x_2|}}{\sqrt{|x_1-x_3|}} - \frac{u_1}{2S\sqrt{|x_1-x_3|}} + \frac{\dot{u_1}}{S} \end{bmatrix} \tag{5.3}$$

From 5.3 it is possible to note that the system is uniformly observable and that can be shown since the states can be calculated from the measured output and the input signal:

$$\begin{aligned} x_1 &= h_1 \\ x_3 &= x_1 + \tfrac{(\dot{x}_1 - u_1/S)^2}{C_1^2} \\ x_2 &= x_3 + \tfrac{4}{C_1^2 C_3^2}[sign(x_1 - x_3)\sqrt{|x_1 - x_3|}(\ddot{x}_1 - \tfrac{\dot{u}_1}{S} - C_1^2) - \tfrac{C_1 u_1}{2S}]^2 \end{aligned}$$

In the same way, it is possible to make the same analysis considering the other two outputs $h(x) = x_2$ or $h(x) = x_3$ and conclude that the system is uniformly observable when any of the other outputs is considered as measurable.

Now, in order to design the observer, it is necessary to computed the observable mapping $\mathcal{O}(x)$ and check if it is a diffeomorphism. So, using the output signal $h(x) = x_1$, the observable mapping is described as:

$$\mathcal{O}_1(x) = \begin{bmatrix} h(x) \\ L_f h(x) \\ L_f^2 h(x) \end{bmatrix} = \begin{bmatrix} x_1 \\ -C_1 sign(x_1 - x_3)\sqrt{|x_1 - x_3|} \\ C_1^2 sign(x_1 - x_3) - \frac{C_1 C_3}{2}\frac{sign(x3-x2)\sqrt{|x_3-x_2|}}{\sqrt{|x_1-x_3|}} \end{bmatrix} \tag{5.4}$$

And the Jacobi matrix of the observability map is described by:

$$\frac{\partial \mathcal{O}_n(x)}{\partial x} = \begin{bmatrix} 1 & 0 & 0 \\ -\frac{C_1}{2}\alpha & \frac{C_1}{2}\alpha & 0 \\ \frac{C_1 C_3}{4}\beta & -\frac{C_1 C_3}{4}(\omega + \beta) & \frac{C_1 C_3}{4}\omega \end{bmatrix} \tag{5.5}$$

where:

$$\alpha = \frac{1}{\sqrt{|x_1 - x_3|}}$$
$$\beta = \frac{sign(x_3 - x_2)\sqrt{|x_3 - x_2|}}{sign(x_1 - x_3)|x_1 - x_3|^{3/2}}$$
$$\omega = \frac{1}{\sqrt{|x_1 - x_3|}\sqrt{|x_3 - x_2|}}$$

It is important to note that since functions $sign(x)$ and $\sqrt{(x)}$ are not differentiable at $x = 0$, the system is also non-differentiable when $x_1 = x_3$ or $x_2 = x_3$. In this points, the system is said to have a singularity[29].

The determinant of Jacobi Matrix is different to zero and its range $Rank(\frac{\partial \mathcal{O}_n(x)}{\partial x})$ is equal to three. That means, the Jacobi matrix is invertible and its inverse is described by:

$$\left[\frac{\partial \mathcal{O}(x)}{\partial x}\right]^{-1} = \begin{bmatrix} 1 & 0 & 0 \\ 1 & \frac{2}{C_1}\frac{1}{\alpha} & 0 \\ 1 & \frac{2}{C_1}(\frac{1}{\omega} + \frac{\beta}{\alpha\omega}) & \frac{4}{C_1 C_3}\frac{1}{\omega} \end{bmatrix} \tag{5.6}$$

Since the Jacobi matrix of the observability map $\mathcal{O}(x)$ and its inverse exist, the mapping $\mathcal{O}$ is a diffeomorphism and the system is observable with the considered output $h(x) = x_1$ but only for the exception for the points of non-differentiability . It is possible to make the same calculations for the two remaining outputs and the results show that an observability map $\mathcal{O}_2(x)$ and $\mathcal{O}_3(x)$ exists (for each corresponding output h_2 and h_3) and they are diffeomorphism since their Jacobi matrix and its inverse exists.

However, from equation (5.4) one can note the existence of a singularity since $L_f^2 h(x)$ is not well defined when $x_1 = x_3$. Also, in the inverse Jacobi matrix of the observability map, the term $\frac{1}{\omega} = 0$ when $h_1 = h_3$ or $h_3 = h_2$ and then there is a complete column of zeros. As a consequence, the matrix $(\partial \mathcal{O}/\partial x)^{-1}$ presents a rank deficiency and that may leads to a divergence or oscillation of the observer when x_1 is very close to x_3 or when x_3 is very close to x_2 [29]. In the same way, when the measured output is h_2 or h_3, by analyzing the observable map and the inverse of its Jacobian matrix, it is possible to see that there also exist cases when the Lie derivative is not well defined and cases of rank deficiency. Then, the observers also present singularities when states are close to each other, specially when x_1 is very close to x_3 or when x_3 is very close to x_2.

5.1.2 Observer Design

Once the existence of a diffeomorphism has been checked, the system can be transformed into a triangular form and consequently, an observer of the form in equation (3.7) may be designed. From equation (3.7), considering the output h_1, an observer for the system will have the form as described below [26]:

$$\dot{\hat{x}} = f(\hat{x}(t)) + g(\hat{x}(t))u(t) + \left[\frac{\partial \mathcal{O}_1(x)}{\partial x}\right]^{-1}_{x=\hat{x}} L(y(t) - h(\hat{x}(t)))$$

The observer showed above has a general form, where matrix L can take different form according to the kind of observer that has being designed. In that way, by using a high gain observer, the matrix L can be represented in the following form[29][31]:

$$L = \begin{bmatrix} LK_1 \\ L^2K_2 \\ L^3K_3 \end{bmatrix}$$

where K_1, K_2 and K_3 are positive gains selected in order to guarantee a convergence in the absence of perturbation and $L > 0$ is a constant which guarantee convergence for any large perturbation [31].
Now, as mentioned before in Chapter 4, faults can be summarized and be represented as additive faults in the following form [26]:

$$\dot{x} = f(x(t)) + g(x(t))u(t) + Pf_d(x(t)) \tag{5.7}$$

where $f_d(x(t))$ is the fault vector and matrix P represents the distribution and the effect of the faults in the system. From equation (5.7) can be noted that the system has a similar form as system described in equation (3.8). So, it is possible to consider additive faults as disturbance or unknown inputs, and by using a sliding mode term, residual signals may be generated as a reconstruction of the disturbances.
According to the Diagnosability analysis made previously, the three outputs will be considered as measured signals, however the Observability map and the diffeomorphism has been made using only the output x_1. For the three tank

system, the nonlinear observer has the following state space[26]:

$$\dot{\hat{x}} = f(\hat{x}(t)) + g(\hat{x}(t))u(t) + \left[\frac{\partial \mathcal{O}_1(x)}{\partial x}\right]^{-1}_{x=\hat{x}} L(y(t) - h(\hat{x}(t))) + P\rho \begin{bmatrix} sign(\hat{x_1} - x_1) \\ sign(\hat{x_2} - x_2) \\ sign(\hat{x_3} - x_3) \end{bmatrix} \tag{5.8}$$

where the matrix $P = diag(1, 1, 1)$ and the constant $\rho = diag(\rho_1, \rho_2, \rho_3)$. In order to avoid the chattering phenomenon, as in the controller design in Chapter 4, a saturation function will be used instead of using directly the $sign(.)$ function.

$$sat(e_i) = sign(e_i), \quad if \quad |e_i| > \epsilon$$
$$sat(e_i) = e_i, \quad if \quad e_i < \epsilon$$

where $e_i = \hat{x}_i - x_i$ and ϵ is a positive constant.
Figure 5.1 shows the performance of the designed observer for a desired level tank $h_1 = 0.6m$ and $h_2 = 0.45m$ and it is possible to notice that the estimated states converge very fast to the real outputs.

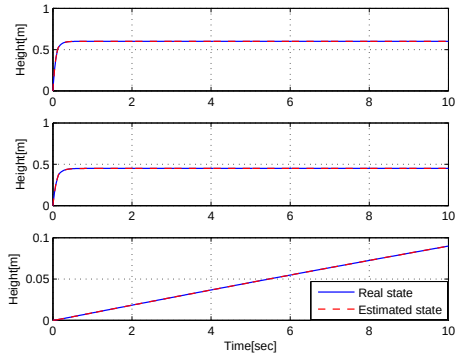

Figure 5.1: Real and estimated states

5.1.3 Residual Generation

Residuals are generated as the estimated disturbances and from equation (3.11) they are calculated as follow:

$$r_i(t) = \hat{d}_i(x, t) = \rho_i sat(e_i) \tag{5.9}$$

Now, some simulations will be shown for different kind of faults. The first simulation shows the free fault case where, as is shown in Figure 5.2 the residual is very close or

practically equal to zero. Another considered possible fault is a leakage in any tank

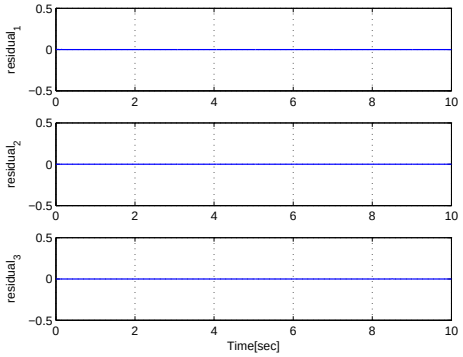

Figure 5.2: Residual signals

and Figure 5.3 illustrates the residual behavior when there is a presence of a leak in the tank system. The leakages are not constant, they occur only for an interval of time. Additionally, in Figure 5.4 is shown the behavior of the estimated states in presence of faults. The leakages behavior in time is described as follows:

$$q_{L1} = \begin{cases} 0, & for\ t < 15 \\ \neq 0, & for\ 15 \leq t \leq 20 \\ 0, & for\ t > 20 \end{cases} \qquad q_{L2} = \begin{cases} 0, & for\ t < 25 \\ \neq 0, & for\ 25 \leq t \leq 35 \\ 0, & for\ t > 35 \end{cases}$$

$$q_{L3} = \begin{cases} 0, & for\ t < 40 \\ \neq 0, & for\ 40 \leq t \leq 45 \\ 0, & for\ t > 45 \end{cases} \tag{5.10}$$

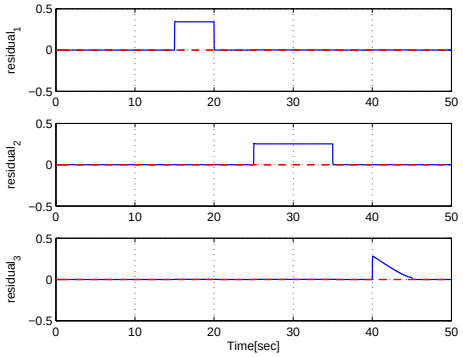

Figure 5.3: Residual behavior

Figure 5.4 shows that the estimated states converge to the real states even in presence of disturbances or in this case, in presence of faults and that indicates that the

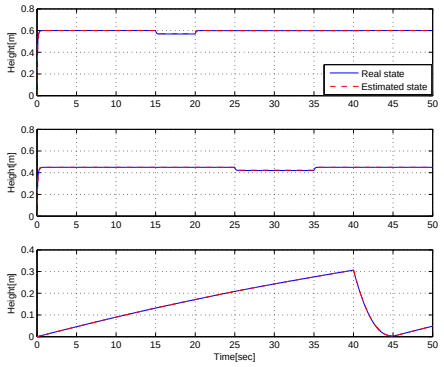

Figure 5.4: Real and estimated states in presence of faults

sliding mode term makes the nonlinear observer robust in front of unknown inputs. In Figure 5.3 it can be seen that residuals are different from zero when the leaks have occurred. Also, since the residuals are generated from the reconstruction of the disturbances which are considered to have an direct effect in each state, it is possible to associate each residual directly with a corresponding fault in that state. This means that, for example, r_1 shows a deviation from zero when a fault has occurred in the tank 1 and in the same way with residuals r_2 and r_3 and their corresponding states. So, from these residual signals one can isolate the faults and know in which tank or component a fault has occurred.

The next simulated fault is an actuator fault that affect the control signal and consequently affect the input flow q_1 and q_2. Figure 5.5 illustrates the way how the input flows are affected by the actuator faults. The green lines represent the normal input flows and the blue ones represent the input flows when are affected by the faults.

$$q_1 = \begin{cases} u_1(t), & for\ \ t < 20 \\ u_1(t) - f_{u1}, & for\ \ 20 \leq t \leq 30 \\ u_1(t), & for\ \ t > 30 \end{cases} \quad ; \quad q_2 = \begin{cases} u_2(t), & for\ \ t < 35 \\ u_2(t) - f_{u2}, & for\ \ 35 \leq t \leq 45 \\ u_2(t), & for\ \ t > 45 \end{cases} \tag{5.11}$$

In this case, as it is shown in Figure 5.6, residuals have a non-zero value at the moment when the faults have occurred. Only r_1 and r_2 are affected because actuators has direct influence only in the corresponding states x_1 and x_2. As in the previous fault case, here is also possible to isolate the fault since each residual corresponds to an actuator. However, comparing with the residual response in the previous case, when an actuator fault occurs the residual amplitude is lower than when a leakage

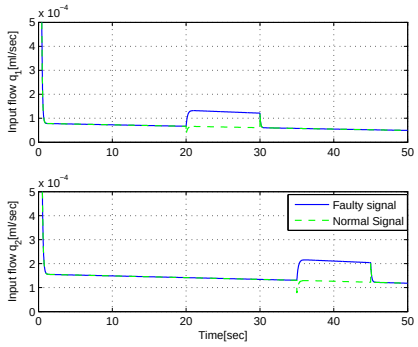

Figure 5.5: Input flows q_1 and q_2

occurs. That could occur because of the amplitude of the own fault. In terms of amplitude, the effect of a leakage is greater than the effect of a deviation in the actuator.

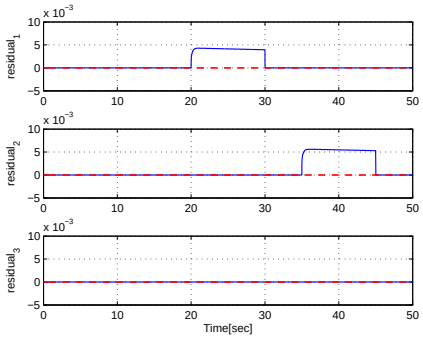

Figure 5.6: Residual signals in presence of actuator faults

In the next simulation the faults from equation (5.10) are considered again but now a Gaussian noise in the reading of the sensors is considered. Figure 5.7 illustrates the response of the residual and as can be seen, they present a coupled Gaussian noise. However, it is still possible to note when the faults have occurred by using a threshold which is a function of the amplitude of the estimated states in a interval of time when it is assumed that the system is in a fault free case.
Although one can still recognize the presence of a fault, there is a probability of false detection. Hence, it is possible to work in the sensed signals by filtering them. Then, Figure 5.8 shows the residual generation by filtering the measured signals but only in the observer inputs.

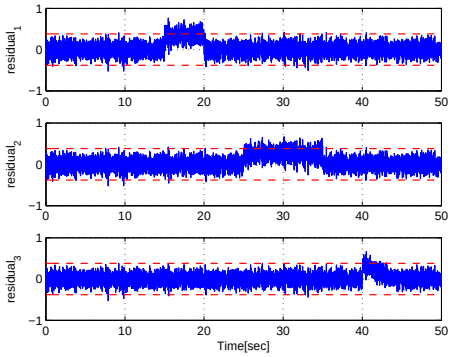

Figure 5.7: Residual signals in presence of Gaussian noise

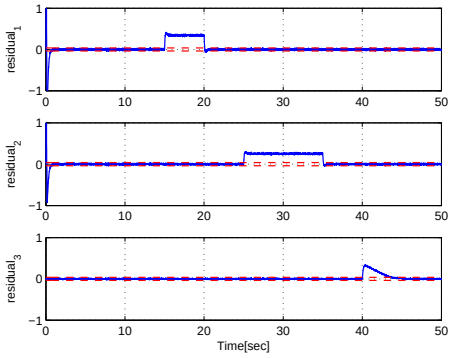

Figure 5.8: Residual signals with a filtering sensor reading

5.2 Structural Analysis

As mentioned in Chapter 3, this approach uses the structure graph to describe the relations between the signals and constraints. The structural model is used to analyze the redundancies which can be exploited for fault diagnosis. In this approach, the faults are interpreted as a violation of the constraints which describes the system. The analysis shows how component faults, which imply the violation of a single constraint, can be found by defining and utilizing appropriate redundancy relations.

The first step in this method is to set the model equations in order to use them to set the constraints. The model equations have to include the possible faults that can occur in the system. In this case there are considered faults that occur because of the presence of some leakages in the tanks, which are denoted by q_{L1}, q_{L2} and q_{L3}, respectively. The model equations are shown as follows:

$$
\begin{aligned}
\dot{x}_1 &= \tfrac{1}{S}(-q_{13} - q_{L1} + q_1) \\
\dot{x}_2 &= \tfrac{1}{S}(-q_{32} - q_{L2} + q_2 - q_{20}) \\
\dot{x}_3 &= \tfrac{1}{S}(q_{13} - q_{32} - q_{L3}) \\
q_{13} &= \mu_1 S_n sign(x_1 - x_3)\sqrt{2g|x_1 - x_3|} \\
q_{32} &= \mu_3 S_n sign(x_3 - x_2)\sqrt{2g|x_3 - x_2|} \\
q_{20} &= \mu_2 S_n sign(x_2)\sqrt{2g|x_2|} \\
q_{L1} &= C_{L1}\sqrt{|x_1|} \\
q_{L2} &= C_{L2}\sqrt{|x_2|} \\
q_{L3} &= C_{L3}\sqrt{|x_3|}
\end{aligned}
\tag{5.12}
$$

Now using the model equations, the constraints are computed:

$$
\begin{aligned}
C_1 &: \dot{x}_1 = \tfrac{1}{S}(-q_{13} - q_{L1} + q_1) \\
C_2 &: \dot{x}_1 = \tfrac{dx_1}{dt} \\
C_3 &: \dot{x}_2 = \tfrac{1}{S}(q_{32} - q_{L2} + q_2 - q_{20}) \\
C_4 &: \dot{x}_2 = \tfrac{dx_2}{dt} \\
C_5 &: \dot{x}_3 = \tfrac{1}{S}(q_{13} - q_{32} - q_{L3}) \\
C_6 &: \dot{x}_3 = \tfrac{dx_3}{dt} \\
C_7 &: q_{13} = \mu_1 S_n sign(x_1 - x_3)\sqrt{2g|x_1 - x_3|} \\
C_8 &: q_{32} = \mu_3 S_n sign(x_3 - x_2)\sqrt{2g|x_3 - x_2|} \\
C_9 &: q_{20} = \mu_2 S_n sign(x_2)\sqrt{2g|x_2|} \\
C_{10} &: q_1 = u_1(t) = f(x_1) \\
C_{11} &: q_2 = u_2(t) = f(x_2) \\
C_{12} &: q_{L1} = C_{L1}\sqrt{|x_1|} \\
C_{13} &: q_{L2} = C_{L2}\sqrt{|x_2|} \\
C_{14} &: q_{L3} = C_{L3}\sqrt{|x_3|} \\
C_{15} &: x_1 = h_1 km_1 \\
C_{16} &: x_2 = h_2 km_2 \\
C_{17} &: x_3 = h_3 km_3
\end{aligned}
\tag{5.13}
$$

where km_i is the constant gain of each level sensor and h_i are the measured signals. Once the constraints have been calculated, the incidence matrix is built. The incidence matrix, which is illustrated in Table 5.1, shows the relations between the constraints and of the variables of the system. The first row of the table shows the variables and the system and its relationship with each constraint is denoted by a number "1".

CONSTRAINTS	$\dot{x}_1$	q_1	q_{13}	x_1	$\dot{x}_2$	x_2	q_2	q_{32}	q_{20}	$\dot{x}_3$	x_3	q_{L1}	q_{L2}	q_{L3}
1	1	1	1									1		
2	1			1										
3					1		1	1	1				1	
4					1	1								
5			1					1		1				
6										1	1			
7			1	1							1			
8						1		1			1			
9						1			1					
10		1		1										
11						1	1							
12				1								1		
13						1							1	
14											1			1
15				1										
16						1								
17											1			

Table 5.1: Incidence Matrix

Once the incidence matrix is built and the relations between variables and constraints have been set, the matching process can be performed by using a ranking algorithm as mentioned in Chapter 3. From the ranked incidence matrix, shown in Table 5.2, it is possible to know which variable is found from each constraint. The variable which will be computed using each constraint is denoted by a $\boxed{1}$ and the other "1"'s are used to compute this variable. Then, the analytical redundancy relations (ARR's) are defined by the highest rank constraints, denoted by a ②, which are called *ZERO*. These *ZERO* constraints are equal to zero in case the system do not have presence of faults, otherwise these constraints present a deviation from the value zero. In this way, residual signals are calculated from the *ZERO* constraints 1, 3 and 5, and are defined by:

$$\begin{aligned} r_1 &= ZERO_1 = S\dot{h}_1 + q_{13} + q_{L1} - q_1 \\ r_2 &= ZERO_2 = S\dot{h}_2 + q_{32} + q_{L2} - q_2 + q_{20} \\ r_3 &= ZERO_3 = S\dot{h}_3 - q_{13} + q_{32} + q_{L3} \end{aligned} \tag{5.14}$$

The simulation results of the generation of residuals are illustrated in Figure 5.9. For these simulations the equilibrium points are fixed to $0.6m$ and $0.45m$ for the level of Tank 1 and Tank 2, respectively. Figure 5.9 shows that each fault has a relation with each residual, so it is possible to isolate each fault and the system is able to know the location and where the fault has occurred. The faults in the tanks, assumed as leakages, have the following behavior and are shown in Figure 5.10.

$$\begin{aligned} q_{L1} &= \begin{cases} 0, & for\ t < 15 \\ \neq 0, & for\ 15 \leq t \leq 20 \\ 0, & for\ t > 20 \end{cases} \\ q_{L2} &= \begin{cases} 0, & for\ t < 25 \\ \neq 0, & for\ 25 \leq t \leq 35 \\ 0, & for\ t > 35 \end{cases} \\ q_{L3} &= \begin{cases} 0, & for\ t < 40 \\ \neq 0, & for\ 40 \leq t \leq 45 \\ 0, & for\ t > 45 \end{cases} \end{aligned} \tag{5.15}$$

CONS	$\dot{x}_1$	q_1	q_{13}	x_1	$\dot{x}_2$	x_2	q_2	q_{32}	q_{20}	$\dot{x}_3$	x_3	q_{L1}	q_{L2}	q_{L3}		RANK	RESIDUAL
1	1	1	1									1				②	**ZERO**
2	[1]			1												1	
3					1		1	1	1				1			②	**ZERO**
4					[1]	1										1	
5			1					1		1						②	**ZERO**
6										[1]	1					1	
7			[1]	1							1					1	
8						1		[1]			1					1	
9						1			[1]							1	
10		[1]		1												1	
11						1	[1]									1	
12				1								[1]				1	
13						1							[1]			1	
14											1			[1]		1	
15				[1]												0	
16						[1]										0	
17											[1]					0	

Table 5.2: Ranked Incidence Matrix

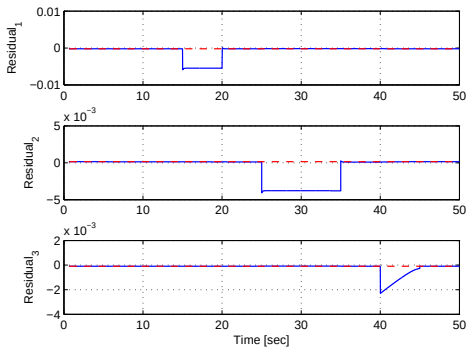

Figure 5.9: Residual behavior in front of leakage faults

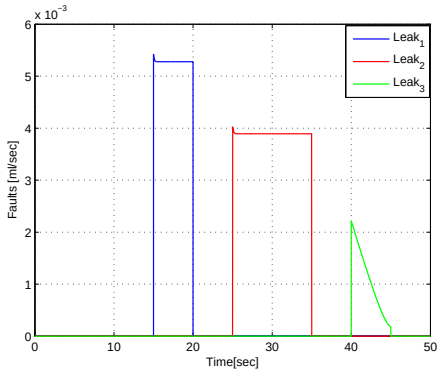

Figure 5.10: Behavior of the faults for each tank

The next simulation is suited for the same leakage faults and for the same equilibrium points, but in this simulation a Gaussian noise is assumed in the sensor readings. Figure 5.11 shows the behavior of the system in front of presence of the faults mentioned before. It is possible to notice the presence of noise in each level sensor reading. At the same time, Figure 5.12 illustrates the residual generation when it exists presence of noise in the sensor readings and it is still possible to notice the time at which the fault occurs for the residual 1 and 2, but it is not really clearly for the residual 3.

It is possible to deal with this issue adding a low pass filter to the outputs sensor readings. As is showed in Figure 5.13, after the filter addition, residuals still present a little noise, although fault detection may be done and it is feasible to notice when and where have the faults occurred.

Another kind of fault that is considered in the three tank system is presented in the next simulation. In this case, there are faults in the actuators, which may be produced because of disturbances or unknown inputs in the system. The behavior

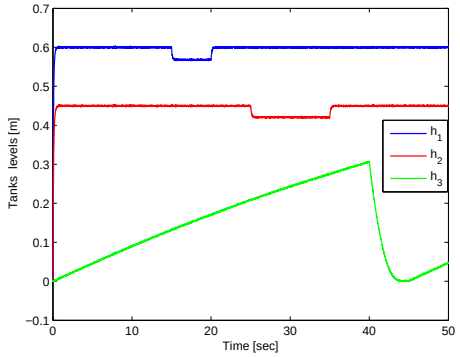

Figure 5.11: Response of the system in front of faults and noise in the sensors

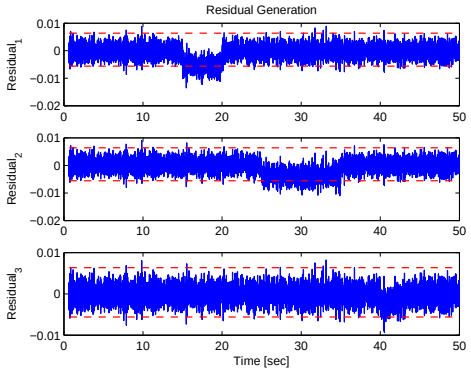

Figure 5.12: Residual generation with noise

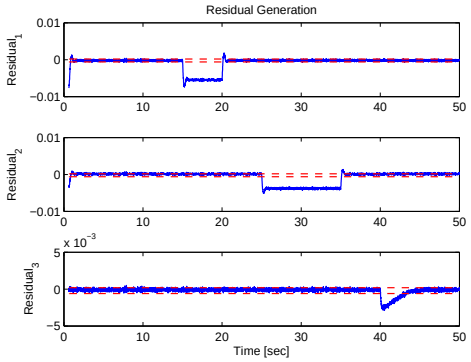

Figure 5.13: Residual generation using a low pass filter in sensor readings

of input flows are showed in the Figure 5.14. The blue lines are the normal input flow generated by the first order sliding mode controller and green lines are the real

input flow incoming to the tanks because of the presence of actuator faults.

$$q_1 = \begin{cases} u_1(t), & for\ t < 20 \\ u_1(t) - f_{u1}, & for\ 20 \leq t \leq 30 \\ u_1(t), & for\ t > 30 \end{cases} \quad ; \quad q_2 = \begin{cases} u_2(t), & for\ t < 35 \\ u_2(t) - f_{u2}, & for\ 35 \leq t \leq 45 \\ u_2(t), & for\ t > 45 \end{cases} \tag{5.16}$$

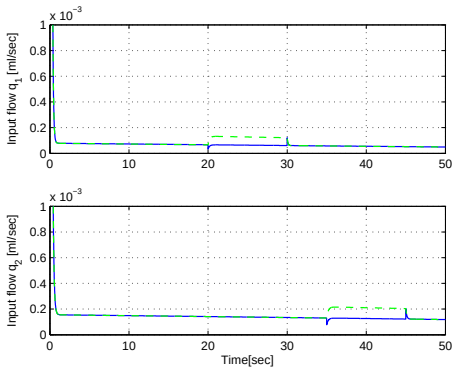

Figure 5.14: Normal input flow vs. real input flow of each actuator

The generated residuals are illustrated in Figure 5.15 and it can be noticed that residual behaviors do not give a clear idea about the presence of the actuator faults, but there are little changes of the residual 1 when the fault in the actuator occurs. This behavior can be presented because these faults are not included in the model equations that were used to generate the constraints which lead to the residuals signals. In this kind of method the model equations have to include every fault that may occur in the system.

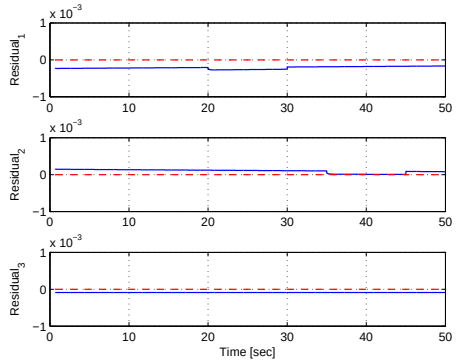

Figure 5.15: Normal input flow vs. real input flow of each actuator

5.3 Parameter Estimation Approach

The parameter estimation approach used in the three tank system is the one described in Chapter 3 for uncertain nonlinear systems by using an estimator of the derivatives of the output signals. The parameters of the nonlinear system are estimated using an algebraic method. The estimated parameters carry information about system and actuator faults. A fault signal or residual describes the behavior of the fault using the parameters that are estimated in presence of faults and comparing them with the nominal parameters of the system, in other words in a fault free case. For free fault case the residuals are close to zero but in presence of a fault in the system, residuals become non zero and have to cross a pre-fixed threshold that indicate the presence of a fault. Also, the technique used here is established on the estimation of robust time derivatives.

5.3.1 Identifiability Analysis

The current parameter estimation technique is applied to the three tank system. The system model, as defined in the previous Chapter, is described by the following equations:

$$
\begin{aligned}
\dot{x_1} &= -\tfrac{1}{S}\mu_1 S_p sign(x_1 - x_3)\sqrt{2g|x_1 - x_3|} + \tfrac{u_1}{S} \\
\dot{x_2} &= \tfrac{1}{S}\mu_3 S_p sign(x_3 - x_2)\sqrt{2g|x_3 - x_2|} + \tfrac{1}{S}\mu_2 S_p sign(x_2)\sqrt{2g|x_2|} + \tfrac{u_2}{S} \\
\dot{x_3} &= \tfrac{1}{S}\mu_1 S_p sign(x_1 - x_3)\sqrt{2g|x_1 - x_3|} - \tfrac{1}{S}\mu_3 S_p sign(x_3 - x_2)\sqrt{2g|x_3 - x_2|} \\
y &= \begin{bmatrix} x_1 & x_2 & x_3 \end{bmatrix}^{\mathrm{T}}.
\end{aligned}
$$

First, to be able to apply this technique, it is necessary to verify the identifiability of the three tank system[34][35]. In order to check its identifiability, the system must satisfy the three assumptions mentioned before in the respective section of Chapter 3.

It is relatively easy to notice that *Assumption 3.1* and *Assumption 3.2* are satisfied by the system. For the first assumption, the system may be decomposed as in (3.22) as follows:

$$
f(x,t) = \begin{bmatrix} -\mu_1 & 0 & 0 \\ 0 & -\mu_2 & \mu_3 \\ \mu_1 & 0 & -\mu_3 \end{bmatrix} \begin{bmatrix} \frac{1}{S} S_p sign(x_1 - x_3)\sqrt{2g|x_1 - x_3|} \\ \frac{1}{S} S_p sign(x_2)\sqrt{2g|x_2|} \\ \frac{1}{S} S_p sign(x_3 - x_2)\sqrt{2g|x_3 - x_2|} \end{bmatrix}
$$

with the following parameters matrix:

$$\alpha^{\mathrm{T}}(\mu) = \begin{bmatrix} -\mu_1 & 0 & 0 \\ 0 & -\mu_2 & \mu_3 \\ \mu_1 & 0 & -\mu_3 \end{bmatrix}$$

For the second assumption, considering that the uncertain parameters are physical parameters, as viscosity or flows coefficients, they are necessary bounded.

In order to check if assumption 3 is fulfilled, it is possible to reorganize the system like (3.21). Now, the system has the new following form:

$$\begin{aligned} \dot{x} &= f(x,t) + g(x,t)u(t); \\ y(t) &= h(x,t) \end{aligned}$$

where:

$$f(x,t) = \begin{bmatrix} -\frac{1}{S}\mu_1 S_p sign(x_1 - x_3)\sqrt{2g|x_1 - x_3|} \\ \frac{1}{S}\mu_3 S_p sign(x_3 - x_2)\sqrt{2g|x_3 - x_2|} - \frac{1}{S}\mu_2 S_p sign(x_2)\sqrt{2g|x_2|} \\ \frac{1}{S}\mu_1 S_p sign(x_1 - x_3)\sqrt{2g|x_1 - x_3|} - \frac{1}{S}\mu_3 S_p sign(x_3 - x_2)\sqrt{2g|x_3 - x_2|} \end{bmatrix}$$

$$g(x,t) = \begin{bmatrix} 1/S & 0 \\ 0 & 1/S \\ 0 & 0 \end{bmatrix}, \quad u(t) = \begin{bmatrix} u_1 \\ u_2 \end{bmatrix}, \quad and \quad h(x,t) = \begin{bmatrix} y_1 \\ y_2 \\ y_3 \end{bmatrix} = \begin{bmatrix} x_1 \\ x_2 \\ x_3 \end{bmatrix}$$

Then, identifiability Jacobi matrix is described as [35]:

$$J_I = \frac{\partial}{\partial \mu_j} L_f^k h_i$$

$$J_I = \begin{bmatrix} \frac{d}{d\mu_1} L_f h_1 & \frac{d}{d\mu_2} L_f h_1 & \frac{d}{d\mu_3} L_f h_1 \\ \frac{d}{d\mu_1} L_f h_2 & \frac{d}{d\mu_2} L_f h_2 & \frac{d}{d\mu_3} L_f h_2 \\ \frac{d}{d\mu_1} L_f h_3 & \frac{d}{d\mu_2} L_f h_3 & \frac{d}{d\mu_3} L_f h_3 \end{bmatrix}$$

Computing Lie derivatives:

$$L_f h_1 = -\frac{1}{S}\mu_1 S_p sign(x_1 - x_3)\sqrt{2g|x_1 - x_3|}$$

$$L_f h_2 = \frac{1}{S}\mu_3 S_p sign(x_3 - x_2)\sqrt{2g|x_3 - x_2|} - \frac{1}{S}\mu_2 S_p sign(x_2)\sqrt{2g|x_2|}$$

$$L_f h_3 = \frac{1}{S}\mu_1 S_p sign(x_1 - x_3)\sqrt{2g|x_1 - x_3|} - \frac{1}{S}\mu_3 S_p sign(x_3 - x_2)\sqrt{2g|x_3 - x_2|}$$

Then, computing derivatives respect to each uncertain parameter $\begin{bmatrix} p_1 & p_2 & p_3 \end{bmatrix} = \begin{bmatrix} \mu_1 & \mu_2 & \mu_3 \end{bmatrix}$, some of them are zero as is shown:

$$\frac{\partial}{\partial \mu_2} L_f h_1 = \frac{\partial}{\partial \mu_3} L_f h_1 = \frac{\partial}{\partial \mu_1} L_f h_2 = \frac{\partial}{\partial \mu_2} L_f h_3 = 0$$

The Jacobian identifiability matrix is:

$$J_I = \begin{bmatrix} \frac{\partial}{\partial \mu_1} L_f h_1 & 0 & 0 \\ 0 & \frac{\partial}{\partial \mu_2} L_f h_2 & \frac{\partial}{\partial \mu_3} L_f h_2 \\ \frac{\partial}{\partial \mu_1} L_f h_3 & 0 & \frac{\partial}{\partial \mu_3} L_f h_3 \end{bmatrix} \tag{5.17}$$

To verify if the J_I matrix is a full rank matrix, its determinant is calculated, yielding:

$$det(J_I) = (-\frac{\partial}{\partial \mu_2} L_f h_2)(\frac{\partial}{\partial \mu_1} L_f h_1)(\frac{\partial}{\partial \mu_3} L_f h_3)$$

$$det(J_I) = -(\frac{S_p\sqrt{2g}}{S})^3 (sign(x_2)\sqrt{|x_2|})(sign(x_1{-}x_3)\sqrt{|x_1 - x_3|})(sign(x_3{-}x_2)\sqrt{|x_3 - x_2|}) \tag{5.18}$$

It is possible to notice that $det(J_I) \neq 0$ when $x_1{\neq}x_2{\neq}x_3$. Consequently, the Jacobian matrix has full rank, so that ensure identifiability of the parameters μ_1, μ_2 and μ_3. However, when $x_1{=}x_2{=}x_3$, $det(J_I) = 0$ and that means, parameter estimation will not be able to achieve when the level tanks are the same.

5.3.2 Parameter Estimation

Since the system is assumed to be a flat system, according to equation (3.27), the parameter estimation is achieved using the properties of differential flat systems and an algebraic method. Then, from the model equation of the system, parameters can

be calculated using the estimated derivatives of the sensed signals as follows:

$$\begin{aligned}\hat{\mu}_1 &= \frac{-S\hat{y_1}+u_1}{S_p sign(y_1-y_3)\sqrt{2g|y_1-y_3|}} \\ \hat{\mu}_2 &= \frac{-S\hat{y_1}-S\hat{y_2}-S\hat{y_3}+u_1+u_2}{S_p sign(y_2)\sqrt{2g|y_2|}} \\ \hat{\mu}_3 &= \frac{-S\hat{y_1}-S\hat{y_3}+u_1}{S_p sign(y_3-y_2)\sqrt{2g|y_3-y_2|}}\end{aligned} \tag{5.19}$$

As mentioned previously, derivatives are not calculated because of the possible presence of noise in the sensors reading. The estimation of robust time derivatives is achieved by using a variable structure differentiator observer. So, the output derivatives will be estimated using a Levant's differentiator observer that has the following form [35]:

$$\begin{aligned}&\dot{z_0} = v_0, \quad v_0 = z_1 - L_k|z_0 - f(t)|^{\frac{k}{k+1}} sign(z_0 - f(t)) \\ &\dot{z_1} = v_1, \quad v_1 = z_2 - L_{k-1}|z_1 - v_0|^{\frac{k-1}{k}} sign(z_1 - v_0) \\ &. \\ &. \\ &. \\ &\dot{z_{k-1}} = v_{k-1}, \quad v_{k-1} = z_k - L_1|z_{k-1} - v_{k-2}|^{\frac{1}{2}} sign(z_{k-1} - v_{k-2}) \\ &\dot{z_k} = -L_0 sign(z_k - v_{k-1})\end{aligned} \tag{5.20}$$

Applying the Levant's differentiator presented in (5.20) to the three tank system, the output derivatives are estimated using the differentiator described by [35]:

$$\begin{aligned}&\dot{z_{0i}} = v_{0i}, \quad v_{0i} = z_{1i} - k_1 L_i^{\frac{1}{2}}|z_{0i} - y_i|^{\frac{3}{4}} sign(z_{0i} - y_i) \\ &\dot{z_{1i}} = v_{1i}, \quad v_{1i} = z_{2i} - k_2 L_i^{\frac{1}{2}}|z_{1i} - v_{0i}|^{\frac{2}{3}} sign(z_{1i} - v_{0i}) \\ &\dot{z_{2i}} = -k_3 L_i^{\frac{1}{2}} sign(z_{2i} - v_{1i})\end{aligned}$$

Since z_{1i} converges to $\dot{y_i}$, this will be the estimated value of the derivative: $z_{1i} = \hat{\dot{y}}_i$.

Figure 5.16 illustrates the performance of the Levant's differentiator. The estimated derivative converges to the real derivative in less than 1.5 seconds and consequently, as it is shown in Figure 5.17, the parameter estimation is achieved after the same time when the estimated derivative has already converged and the system states have reached their stable values.

Figure 5.18 shows a zoomed view of the estimated parameters and it shows that the estimated parameters are very close or almost equal as the nominal parameters in Table 4.1

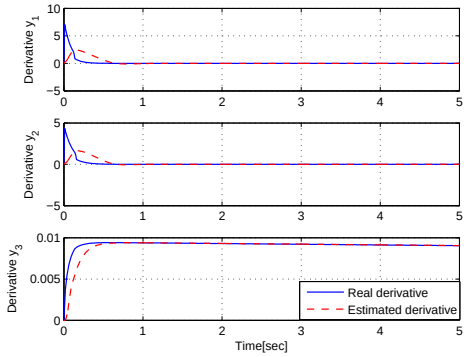

Figure 5.16: Estimated state derivatives

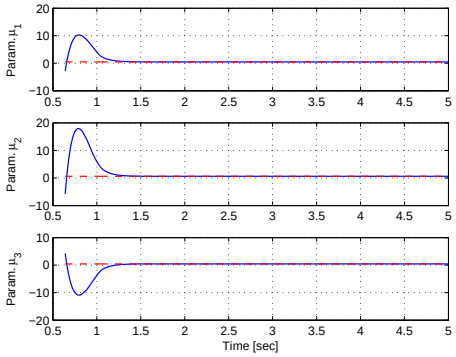

Figure 5.17: Parameter estimation

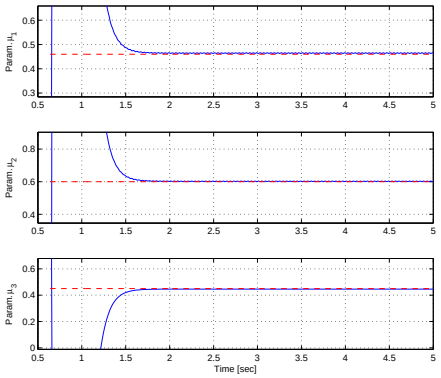

Figure 5.18: Parameter estimation zoomed view

5.3.3 Residual Generation

Once the derivatives are obtained it is possible to calculate the estimated parameters and after a finite time, it can be used as a nominal parameter assuming that in this initial time the system was in a free fault case. This nominal parameters will be used

with the normal estimated parameters to generate the residuals. Then the residuals are defined by:

$$r_i = \mu_i - \hat{\mu}_i \tag{5.21}$$

where μ_i is the nominal uncertain parameter and $\hat{\mu}_i$ becomes the estimated parameter.

Figure 5.19 shows the residual generation for a free fault case. Each residual signal, corresponding to a particular parameter, is equal to zero because no fault has occurred.

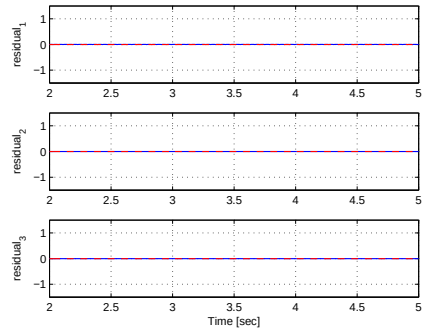

Figure 5.19: Residual signals in free fault case

Now, the first simulation has made in presence of some leaks in each tank which are considered as component faults. The leakages have the same behavior as in equation (5.10) and are shown in Figure 5.20.

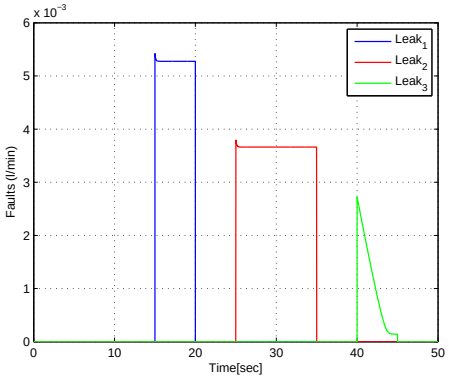

Figure 5.20: Leakages behavior in time

In this case, as it is shown in Figure 5.21, residuals present a deviation from zero when a fault occurs. However, when a leakage in the tank 1 appears, the three residuals are different from zero. That becomes clear since a leak in the first tank leads to a different flow between the first and the next one and in the same way the

flow between the center and the last tank changes. The same behavior is noticed when there is a presence of a leak in the last tank. So, by using the parameter estimation approach it is not possible to isolate the faults directly as in the previous approaches but they are still able to be detected.

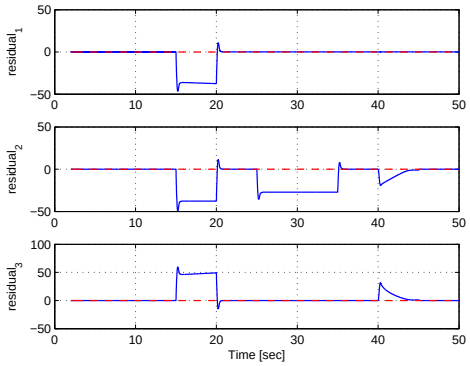

Figure 5.21: Residual signals in presence of leaks

In the case when the system is affected by actuator faults, as in the presence of leaks, more than one residual present a deviation from zero when only one fault occurs. Figure 5.22 illustrates the residual behavior in front of actuator faults which are the same as in equation (5.11). In this approach, the residuals generated due to actuator

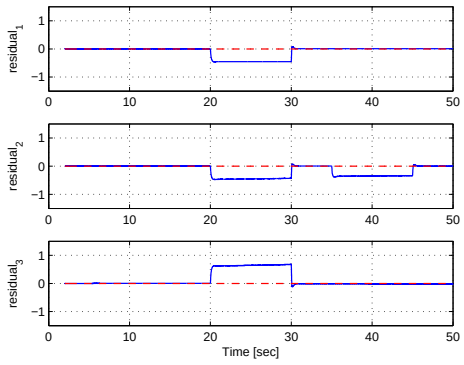

Figure 5.22: Residual in presence of actuator faults

faults present the same amplitude characteristic as in the observer based approach. That means, in term of amplitude, leakages faults have a greater influence compared with the influence of actuator faults.

The following considered fault is about a variation of the parameter of the system. In the three tank system, these parameters are related to viscosity or flow coefficients of the pipes which interconnect the tanks. The variation of parameters is usually

considered to be slow in time and the changes are not like a step but as a ramp function. Figure 5.23 shows the variation of the system parameters and the behavior of the residuals in front these variations. Parameters behavior are described as follows:

$$\mu_1 = \begin{cases} 0.46, & for\ t < 40 \\ \mu_1 + \Delta\mu_1, & for\ 40 \leq t \leq 45 \\ 58, & for\ t > 45 \end{cases}$$
$$\mu_2 = \begin{cases} 0.60, & for\ t < 25 \\ \mu_2 + \Delta\mu_2, & for\ 25 \leq t \leq 35 \\ 0.80, & for\ t > 35 \end{cases} \tag{5.22}$$
$$\mu_3 = \begin{cases} 0.45, & for\ t < 15 \\ \mu_3 + \Delta\mu_3, & for\ 15 \leq t \leq 20 \\ 0.60, & for\ t > 20 \end{cases}$$

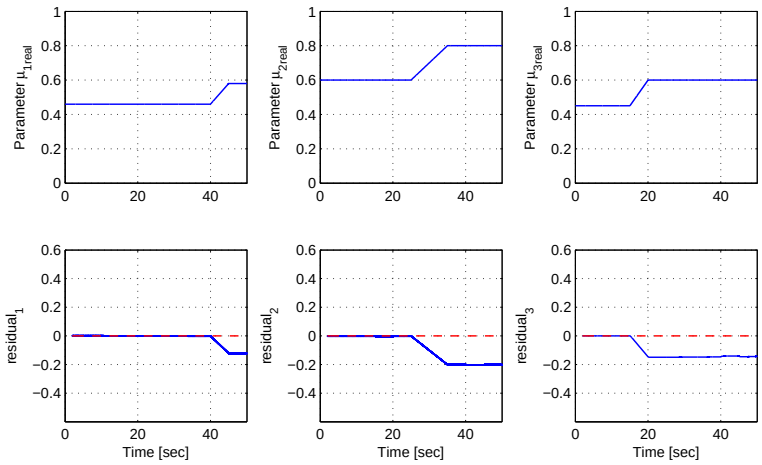

Figure 5.23: Residual signals in presence of parameter deviations

Now, Gaussian noise is considered in the sensor readings. The simulation has been made considering leakages as fault in the system. The leaks used are the same which were used before and are described in equation (5.10). From Figure 5.24 it can be seen that even in presence of noise which is coupled in residual, it is still possible to detect when a fault has occurred. In this case, also a fixed threshold which is a function based on the amplitude of the estimated parameters has been used. The noise has not too much influence in the residual generation due to the use of Levant's differentiator, since the derivatives are not calculated directly from the sensed signals, the effect of the noise does not increase when the signal is derivated.

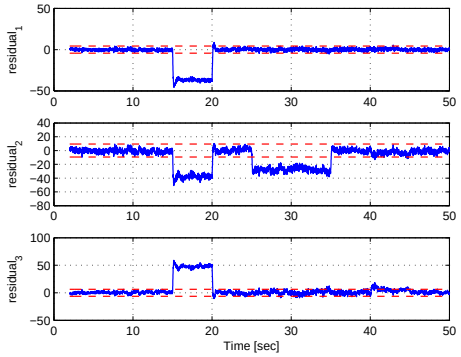

Figure 5.24: Residual in presence of Gaussian noise

Figure 5.25 shows the estimated derivative in presence of noise and it can be seen that the estimated derivatives present less presence of noise than the direct derivative.

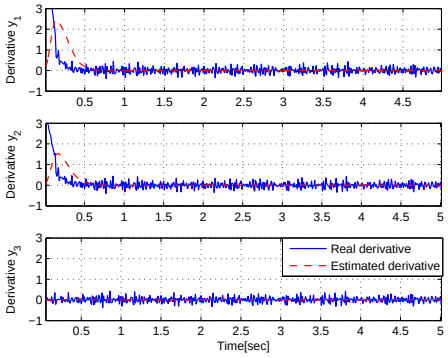

Figure 5.25: Estimated derivatives in presence of Gaussian noise

5.4 Special Cases

From the system model which is described in 4.4 by the following equations:

$$\begin{aligned}
\dot{x_1} &= -C_1 sign(x_1 - x_3)\sqrt{|x_1 - x_3|} + \tfrac{u_1}{S} \\
\dot{x_2} &= C_3 sign(x_3 - x_2)\sqrt{|x_3 - x_2|} + C_2 sign(x_2)\sqrt{|x_2|} + \tfrac{u_2}{S} \\
\dot{x_3} &= C_1 sign(x_1 - x_3)\sqrt{|x_1 - x_3|} - C_3 sign(x_3 - x_2)\sqrt{|x_3 - x_2|} \\
y &= \begin{bmatrix} x_1 & x_2 & x_3 \end{bmatrix}^{\mathrm{T}}.
\end{aligned} \tag{5.23}$$

Since there exists a function $sign(.)$ and absolute value function $|.|$, it is possible to notice that the system equations changes according to the tank levels. Hence the system presents four possible state locations or working regions which are illustrated

in Figure 5.26. Most of the literature studies the case indicated in Figure 5.26 with the dashed square in which the states present the following behavior $x_1 > x_3$ and $x_3 > x_2$. This case is usually studied because it is the most common situation and, in control scheme, due to its simplicity implementation in a real system. The simulations which have been shown before, have been all made in this working area.

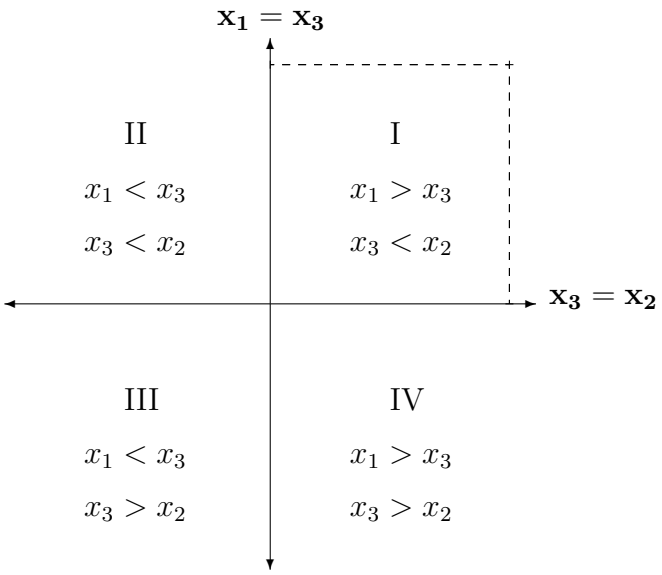

Figure 5.26: Possible working regions of states

In the following parts, some special cases related to different state locations will be considered.

5.4.1 Changing Regions

In this case, „jumps" from one working region to another one will be performed. With these jumps, the system will go through *critical points*, $x_1 = x_3$ or $x_3 = x_2$, in which the system present singularities. The main idea is to analyze the behavior of the residual signals while the system is around the critical points mentioned above. Figure 5.27 illustrates the tank levels and its behavior considering the four different state locations which are indicated in the graphic in the following order: I, IV, III and II.

In order to do it practicality, only leakage faults will be considered in the following simulations. The leaks will be simulated in the way in which they will occur around the time when the critical points are reached. The leaks are described by

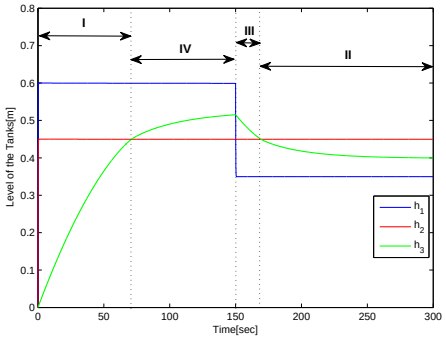

Figure 5.27: Tank levels in different working region

the following equations and they are depicted in Figure 5.28

$$q_{L1} = \begin{cases} 0, & for\ t < 160 \\ \neq 0, & for\ 160 \leq t \leq 180 \\ 0, & for\ t > 180 \end{cases} \qquad q_{L2} = \begin{cases} 0, & for\ t < 60 \\ \neq 0, & for\ 60 \leq t \leq 80 \\ 0, & for\ t > 80 \end{cases}$$

$$q_{L3} = \begin{cases} 0, & for\ t < 220 \\ \neq 0, & for\ 220 \leq t \leq 225 \\ 0, & for\ t > 225 \end{cases} \tag{5.24}$$

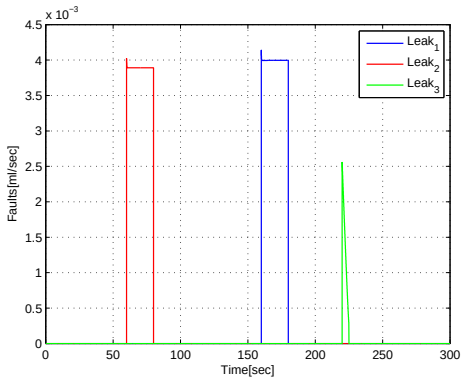

Figure 5.28: Leakages behavior in time

In Figure 5.29, 5.30 and 5.31 it can be seen the residual signals in front of the leakages by using the observer based, structural analysis and parameter estimation approach, respectively.

From the figures 5.29-5.31, one can notice that faults are detected even when the system „jump" from one region to another, so residuals can be used in the different state locations. However, in Figure 5.30, a peak in the first residual is presented, but that behavior is due to the control signal in order to follow the desired trajectory

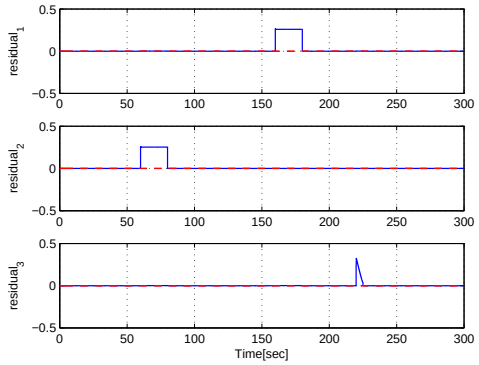

Figure 5.29: Observer based approach

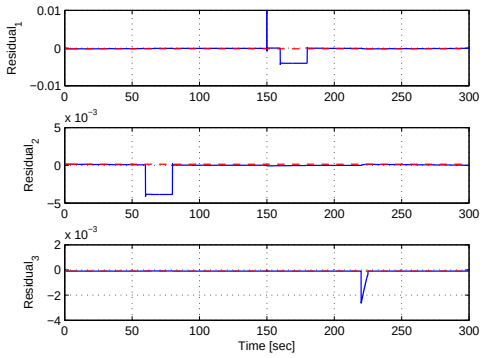

Figure 5.30: Structural analysis approach

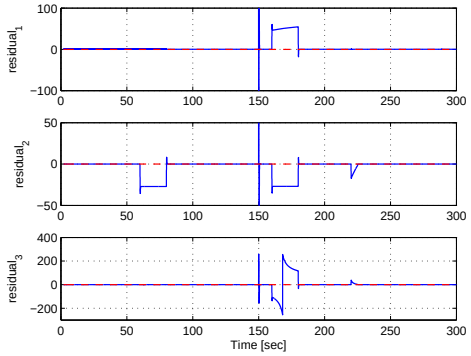

Figure 5.31: Parameter estimation approach

of the level tank 1. In the same way, in Figure 5.31 a peak is presented in the three residuals and it occurs at the same time as in previous case and because of the same reason.

The following simulations will be performed considering the same leaks described in 5.24 but now, with the presence of Gaussian noise in the sensor readings. The

results are shown in Figures 5.32, 5.33 and 5.34 which correspond to the residuals generated by using the observer based, structural analysis and parameter estimation approach. As shown in figures, although the presence of Gaussian noise, it is still possible to detect the faults, but in the case of the parameter estimation approach there is a coupled noise at the end of the first residual which can be considered as a false detection. However, it was noticed that the presented approaches may be used for a fault detection even in presence of noise and for any of the working regions of the system, but also it is necessary to consider some effects like the one generated by the control signal.

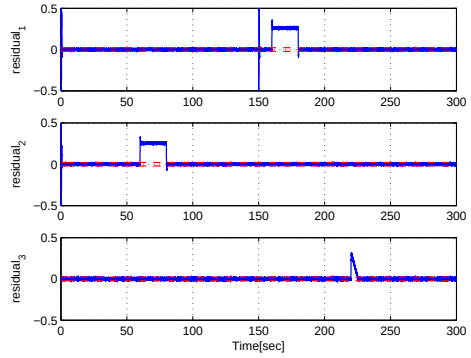

Figure 5.32: Observer based approach

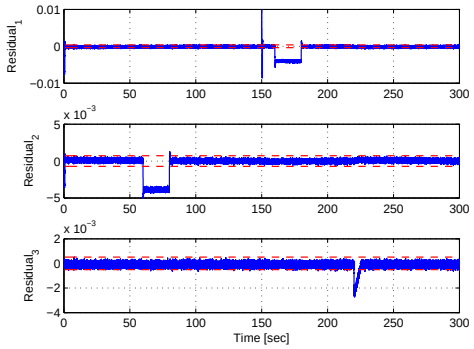

Figure 5.33: Structural analysis approach

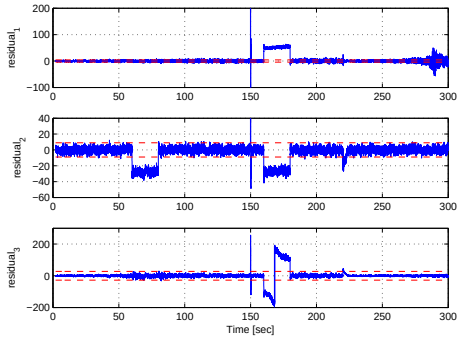

Figure 5.34: Parameter estimation approach

5.4.2 Axis Regions

In this section, the case when the system states are the same, i.e. the axis regions as depicted in Figure 5.27, is studied. The system desired equilibrium points are $x_1 = x_2 = x_3 = 0.45m$.

As it has been shown before, in these critical points exist a singularity in the system and the system is not observable or the parameter is also not identifiable.

In the two matrices presented id 5.6 and 5.17, related to the inverse of the Jacobian matrix of the Diffeomorphisms $\mathcal{O}$ and the Jacobian identifiability matrix J_I, it is possible notice that the system is not observable or the parameters are not identifiable (since matrix J_I is not full ranked) in the corresponding case, when the states are the same. In this way it is possible to avoid in some way the singularities making a numerical approximation of the denominator term as follows:

$$\begin{aligned} \frac{1}{sign(x_1-x_3)\sqrt{|x_1-x_3|}} &\approx \frac{1}{sign(x_1-x_3+\varepsilon)\sqrt{|x_1-x_3|+\varepsilon}} \\ \frac{1}{sign(x_3-x_2)\sqrt{|x_3-x_2|}} &\approx \frac{1}{sign(x_3-x_2+\varepsilon)\sqrt{|x_3-x_2|+\varepsilon}} \\ \frac{1}{sign(x_2)\sqrt{|x_2|}} &\approx \frac{1}{sign(x_2+\varepsilon)\sqrt{|x_2|+\varepsilon}} \end{aligned} \tag{5.25}$$

where ε is a positive considerably small value. With this approximation the observer will not present a rank deficiency and the Jacobian identifiability matrix keeps having a full rank ($n = 3$) since it determinant at critical points is different from zero. This approximation may make possible that the observer and estimation algorithm work continuously. Now, the residual generation using the approximation mentioned in equation (5.25) is illustrated in Figures 5.35, 5.36 and 5.37 for each corresponding approach. Additionally, leakages behavior in time is

illustrated in Figure 5.38.
As it can be seen from the residual depicted in the figures 5.35-5.37, faults can be detected due to the numerical approximation even when state locations are in the axis region.

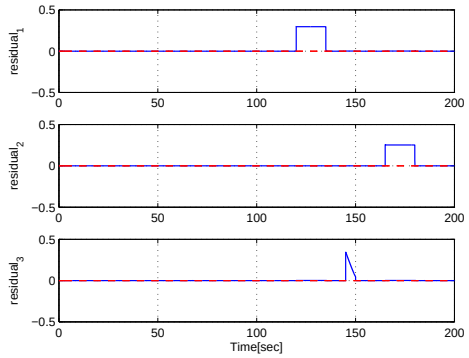

Figure 5.35: Observer based approach

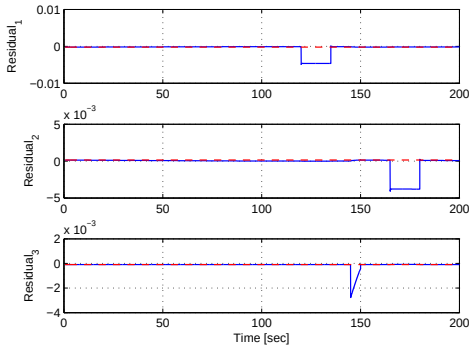

Figure 5.36: Structural analysis approach

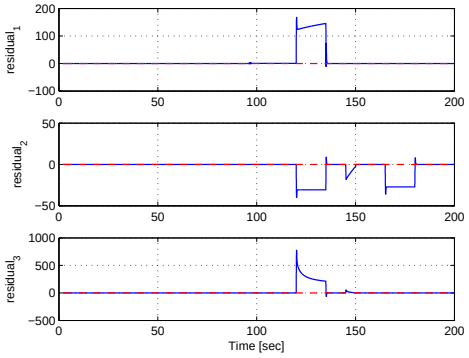

Figure 5.37: Parameter estimation approach

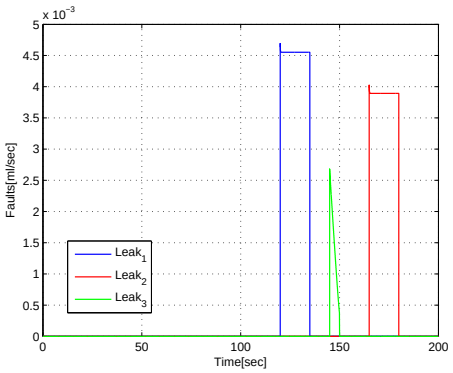

Figure 5.38: Leakage behavior in time

In the following simulation, a Gaussian noise is considered in the sensor readings and the leaks present the same behavior. Since there exists a presence of noise in the measured signals, there also exist many instants of time in which the stats are *jumping* from one working region to another one and consequently there also exist many critical points in which the states are equal to each other. Figure 5.39 illustrates the sensor readings and it can be seen the coupled noise in the measured signals.

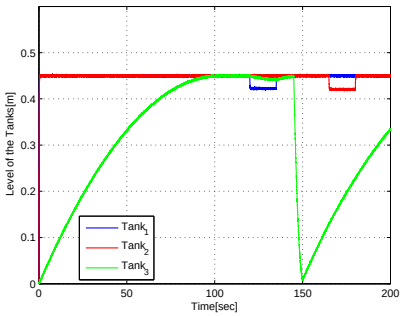

Figure 5.39: Sensor readings with presence of Gaussian noise

Then, in Figures 5.40, 5.41 and 5.42 one can see the residual signals for each approach. In the case of observer-based and structural analysis approaches due to the presence of noise, the residual are not well generated and they present a coupled noise. Although in the observer-based approach it is still possible to notice the instant when a fault has occurred, residual signals could also lead to a false fault detection. In Figure 5.42 the residual generated by using the parameter estimation approach is shown, and it can be seen that faults can be detected in presence of noise and around the axis region of the working regions. However, faults can not be isolated directly.

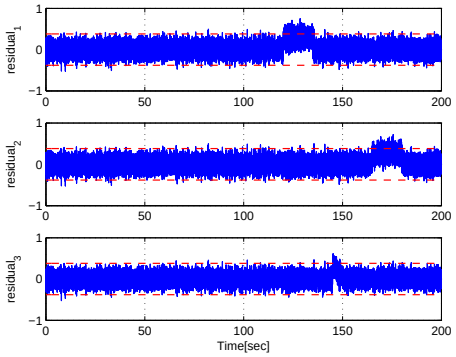

Figure 5.40: Observer based approach

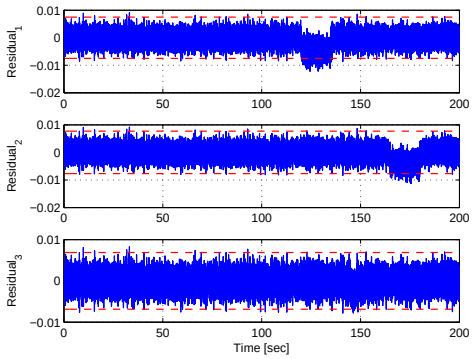

Figure 5.41: Structural analysis approach

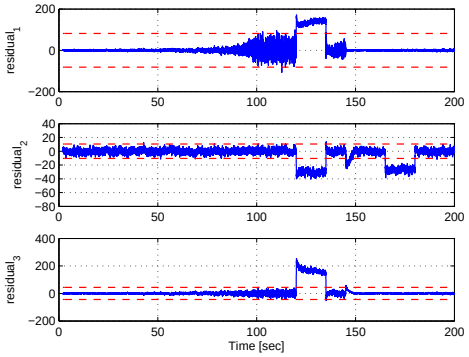

Figure 5.42: Parameter estimation approach

After a previous signal treatment in order to attenuate the noisy measured signals, the residual generation may be improved and now it is possible to notice when a fault has occurred. Figures 5.43 and 5.44 show the residual signals after the previous signal treatment using the observer based and structural analysis approach, respectively. In the case of the parameter estimation approach, the signal has not

been treated before due to the direct application of Levant's differentiator, which since it estimates the derivatives of the measured signals, the noise is attenuated and the residual generation is well performed.

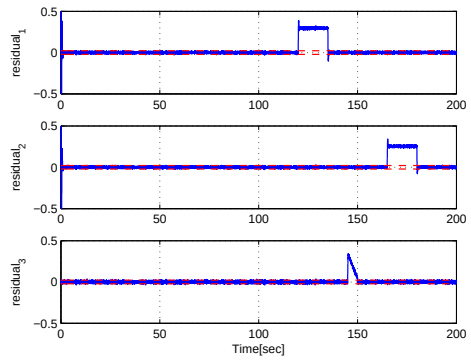

Figure 5.43: Observer based approach after a treatment of the signal

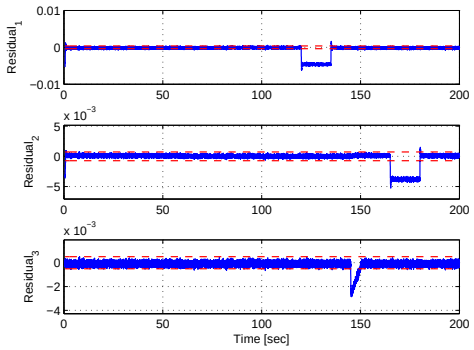

Figure 5.44: Structural analysis approach after a treatment of the signal

6 Modulating Functions

6.1 Introduction and Definitions

Modulating functions have been studied in the past decades and have been used in parameter estimation scheme. The first time this approach has been proposed was in 1957 by Shinbrot in [44]. This method is of considerable interest in the identification of nonlinear and time-varying systems and it has been used in different applications as in [45],[46],[47],[48].
In this thesis work, modulating fuctions are not only used to achieve a parameter estimation in finite time, but also to perform a simultaneous state estimation as described in [46].
Since parameter and state estimation can be performed at the same time, residual generation will be achieved by applying both approaches, parameter and observer based approach.
Now some basis facts about modulation functions will be recalled. In this way, a linear system of order n is considered and it is described as follows:

$$y^{(n)} + a_{n-1}y^{(n-1)} + ... + a_1\dot{y} + a_0 y = b_{n-1}u^{(n-1)} + ... + b_1\dot{u} + b_0 u \tag{6.1}$$

where y and u are the measured and control signal, respectively. The system can be also reorganized in a vector form as it is shown bellow:

$$y^{(n)} = \mathrm{Y}^{\mathrm{T}}\theta \tag{6.2}$$

where $\mathrm{Y} = [-y, -\dot{y}, ..., -y^{(n-1)}, u, \dot{u}, ..., u^{(n-1)}]^{\mathrm{T}}$ is the vector of signals y and u and their corresponding derivatives, and $\theta = [a_0, a_1, ..., a_{n-1}, b_0, b_1, ..., b_{n-1}]^{\mathrm{T}}$ is the parameter vector which will be identified. It is assumed that derivatives of the control signal are known for any instant t. In the same way, since y is a measured signal, it is possible to compute its derivatives. However, the directly computation of its derivatives should be as long as possible avoided because of the potential presence

of noise and issues related to it. One way to overcome the derivative problems in presence of noise is by using modulating functions.

A modulating function can be defined as follows [46][49]:

Definition 7.1 (*Modulating Functions*):

A function φ defined in a finite interval $[0, T]$ is called a modulating function if its is sufficiently smooth and if, for some fixed T, the following terminal conditions are satisfied:

$$\varphi^{(i)}(0) = \varphi^{(i)}(T) = 0 \tag{6.3}$$

for all $i = 1, 2, ..., k-1$; where k is the order of φ.

Considering the first derivative of the measured signal $\dot{y}(t)$, multiplying it by a modulating function $\varphi(t)$ and performing an integration by parts, one may obtain:

$$\int_0^T \varphi(\tau)\dot{y}(\tau)d\tau = [\varphi(\tau)y(\tau)]_0^T - \int_0^T \dot{\varphi}(\tau)y(\tau)d\tau$$

and then, applying the terminal conditions in equation 6.3, the integral can be expressed as follows:

$$\int_0^T \varphi(\tau)\dot{y}(\tau)d\tau = -\int_0^T \dot{\varphi}(\tau)y(\tau)d\tau$$

Performing the same operation repeatedly, the i derivative of some signal ξ can be:

$$\int_0^T \varphi(\tau)\xi^{(i)}(\tau)d\tau = (-1)^{(i)} \int_0^T \varphi^{(i)}(\tau)\xi(\tau)d\tau \tag{6.4}$$

This generalization is the main advantage of the modulating functions approach in which a directly derivative calculation is avoided and also it is not necessary to fix initial and final conditions.

There are different kinds of modulating functions, such as trigonometric or polynomial, which are shown below:

$$\varphi_k(t) = \left(sin\frac{k\pi t}{T}\right)^k$$
$$\varphi_k(t) = (T-t)^k t^k$$

6.1.1 Parameter Estimation

Considering the system described in equation (6.2) and applying the result shown in (6.4), the system can be replaced by [46]:

$$z = \mathbf{w}^{\mathrm{T}}\theta \tag{6.5}$$

with:

$$z = \int_0^T (-1)^{(n)}\, \varphi^{(n)}(\tau) y(\tau) d\tau \tag{6.6}$$

and the vector $\mathbf{w}$ is defined by:

$$w_i = \int_0^T (-1)^{(i-1)}\, \varphi^{(i-1)}(\tau) y(\tau) d\tau \tag{6.7}$$

for $i = 1, 2, ..., n$ and the next n terms as:

$$w_i = \int_0^T (-1)^{(i-n-1)}\, \varphi^{(i-n-1)}(\tau) u(\tau) d\tau \tag{6.8}$$

for $i = n+1, n+1, ..., 2n$.
Then, in order to obtain an estimation of θ, most of literature uses a set of equations $m \geq n$, each one using a different modulation function and the following equation is obtained [46]:

$$\mathbf{z} = \mathbf{W}^{\mathrm{T}}\theta \tag{6.9}$$

where $\mathbf{z} = (z_1, z_2, ..., z_m)^{\mathrm{T}}$ and $\mathbf{W} = (w_1, w_2, ..., w_m)$ are a set of z_k and w_k, which are calculated in the same way as explained in equations (6.6) to (6.8). Now, as usually done in literature, the parameter estimation is performed by an optimization problem using Least Square's Method as follows:

$$\hat{\theta} = \left(\mathbf{W}\mathbf{W}^{\mathrm{T}}\right)^{-1} \mathbf{W}\mathbf{z} \tag{6.10}$$

Another way to achieved the parameter estimation is, as mentioned in [46], to use a single modulating function in a fixed receding horizon and applying it in equation (6.5) it is obtained:

$$z(t) = \mathbf{w}^{\mathrm{T}}\theta \tag{6.11}$$

where $z(t)$ is defined by:

$$z(t) = \int_{t-T}^{t} (-1)^n \varphi^{(n)} (\tau - t + T)\, y(\tau) d\tau \tag{6.12}$$

and $w(t)$ is defined in the same way. Then, the estimated parameter vector $\hat{\theta}$ is obtained by applying the Gramian-based or L_2-norm-based estimator[46]:

$$\hat{\theta}(t) = \left(\int_{t-T'}^{t} \mathbf{w}(\tau)\mathbf{w}^{\mathrm{T}}(\tau) d\tau \right)^{-1} \int_{t-T'}^{t} \mathbf{w}(\tau) z(\tau) d\tau \tag{6.13}$$

where T' is the receding horizon of the estimation parameter vector θ. The horizon length used in equation (6.12) is not necessary equal to the length horizon used in the parameter estimation T'.

6.1.2 State Estimation

To achieve an state estimation, first of all it is necessary to introduce a new concept of modulating functions. It is related to a modulating function which fulfills partially the boundary conditions presented in equation (6.3) and it is called a right modulation function.
From [46], a right modulation function can be defined as follows:
Definition 7.2:
Considering a smooth function φ*:* $\mathbb{R} \times \mathbb{R} \to \mathbb{R}$ *and write one of its particle derivative as:*

$$\varphi^{(i)}(t, t_1) := \left[\frac{\partial^i \varphi}{\partial \tau^i} (\tau, t_1) \right]_{\tau = t} \tag{6.14}$$

Function $\varphi(.,.)$ *is called a modulating function if there exist* $t_0 < t_1$ *such that:*

$$\varphi^{(i)}(t_0, t_1) \cdot \varphi^{(i)}(t_1, t_1) = 0 \tag{6.15}$$

for all $i = 0, 1, ..., k-1$*; where* k *is the order of the function. A modulating function which satisfies* $\varphi^{(i)}(t_0, t_1) = 0$ *and* $\varphi^{(i)}(t_1, t_1) \neq 0$*, is called a left modulating function. If it satisfies* $\varphi^{(i)}(t_0, t_1 \neq 0$ *and* $\varphi^{(i)}(t_1, t_1) = 0$*, is called a right modulating functions and in the case it satisfies* $\varphi^{(i)}(t_0, t_1) = 0$ *and* $\varphi^{(i)}(t_1, t_1) = 0$*, it is called a complete modulating function.*
An example of a left modulating function and the same which will be used in the

implementation of the approach is described below:

$$\varphi_k(t) = t^k e^{-t} \tag{6.16}$$

To explain how the state estimation is performed, a simple case is considered:

$$\dot{y} + a_0 y = b_0 u \tag{6.17}$$

Assuming that parameters have been already calculated as in (6.10) or (6.13) and multiplying each side by a left modulating function, the following equation is obtained:

$$[\varphi(\tau)y(\tau)]_0^T - \int_0^T \dot{\varphi}(\tau)y(\tau)d\tau = -\hat{a}_0 \int_0^T \varphi(\tau)y(\tau)d\tau + \hat{b}_0 \int_0^T \varphi(\tau)u(\tau)d\tau \tag{6.18}$$

and then, using the left modulating function concept, the estimated state can be computed as:

$$\hat{y}(T) = \frac{\int_0^T \dot{\varphi}(\tau)y(\tau)d\tau - \hat{a}_0 \int_0^T \varphi(\tau)y(\tau)d\tau + \hat{b}_0 \int_0^T \varphi(\tau)u(\tau)d\tau}{\varphi(T)} \tag{6.19}$$

where $\hat{y}(T)$ is the estimated state after an horizon T.
A generalization and robust way to perform the state estimation has been done, as explained in [46], considering the following system:

$$\begin{aligned}
&\dot{x}_1 = x_2, \quad \dot{x}_2 = x_3, \quad ..., \\
&\dot{x}_{n-1} = -a_0 x_1 - ... - a_{n-1} x_n + b_0 u + b_{n-1} u^{(n-1)} \\
&\dot{a}_0 = 0, \quad \dot{a}_1 = 0, \quad ..., \quad \dot{a}_{n-1} = 0 \\
&\dot{b}_0 = 0, \quad \dot{b}_1 = 0, \quad ..., \quad \dot{b}_{n-1} = 0 \\
&y = x_1
\end{aligned} \tag{6.20}$$

and the estimated state is defined as:

$$\hat{\mathbf{x}}(t_1) = \left(\Delta\Delta^{\mathrm{T}}\right)^{-1} \Delta \left(\mathbf{U}^{\mathrm{T}}\hat{\mathbf{b}} - \mathbb{Q}^{\mathrm{T}}\hat{\mathbf{a}} - \gamma\right) \tag{6.21}$$

where $\hat{\mathbf{a}} = (\hat{a}_0, ..., \hat{a}_{n-1})^{\mathrm{T}}$ and $\hat{\mathbf{b}} = \left(\hat{b}_0, ..., \hat{b}_{n-1}\right)^{\mathrm{T}}$ are the estimated parameters and matrices Δ, $\mathbf{U}$, $\mathbf{Q}$ and γ are defined and explained in [46].

6.2 Simulation in the Three Tank System Model

Considering the system in the following form:

$$\begin{aligned}
\dot{x_1} &= -C_1 sign(x_1 - x_3)\sqrt{|x_1 - x_3|} + \tfrac{u_1}{S} \\
\dot{x_2} &= C_3 sign(x_3 - x_2)\sqrt{|x_3 - x_2|} - C_2 sign(x_2)\sqrt{|x_2|} + \tfrac{u_2}{S} \\
\dot{x_3} &= C_1 sign(x_1 - x_3)\sqrt{|x_1 - x_3|} - C_3 sign(x_3 - x_2)\sqrt{|x_3 - x_2|}
\end{aligned}$$

and assuming, as in the previous explained approaches, that the three tank levels are measured, that means $y = \begin{bmatrix} x_1 & x_2 & x_3 \end{bmatrix}^{\mathrm{T}}$., the system can be reorganized in the following from:

$$\begin{aligned}
\dot{x_1} - \tfrac{u_1}{S} &= -C_1 sign(x_1 - x_3)\sqrt{|x_1 - x_3|} \\
\dot{x_2} - \tfrac{u_2}{S} &= C_3 sign(x_3 - x_2)\sqrt{|x_3 - x_2|} - C_2 sign(x_2)\sqrt{|x_2|} \\
\dot{x_3} &= C_1 sign(x_1 - x_3)\sqrt{|x_1 - x_3|} - C_3 sign(x_3 - x_2)\sqrt{|x_3 - x_2|}
\end{aligned}$$

Applying three complete modulating functions of the form $\varphi_k(t) = (t - T)^k t^k$ and considering an horizon T, the system is expressed as in equation (6.11):

$$\mathbf{z}(t) = \mathbf{w}^{\mathrm{T}}\theta \tag{6.22}$$

with the matrices defined by:

$$\mathbf{z}(t) = \begin{bmatrix} -\int_{t-T}^{t} \dot{\varphi_1}(\tau)y_1(\tau)d\tau - \frac{1}{S}\int_{t-T}^{t} \varphi_1(\tau)u_1(\tau)d\tau \\ -\int_{t-T}^{t} \dot{\varphi_2}(\tau)y_2(\tau)d\tau - \frac{1}{S}\int_{t-T}^{t} \varphi_2(\tau)u_2(\tau)d\tau \\ -\int_{t-T}^{t} \dot{\varphi_3}(\tau)y_3(\tau)d\tau \end{bmatrix} \tag{6.23}$$

$$\mathbf{w}(t) = \begin{bmatrix} -\int_{t-T}^{t} \varphi_1(\tau)f_1(\tau)d\tau & 0 & 0 \\ 0 & -\int_{t-T}^{t} \dot{\varphi_2}(\tau)f_2(\tau)d\tau & \int_{t-T}^{t} \varphi_2(\tau)f_3(\tau)d\tau \\ \int_{t-T}^{t} \varphi_3(\tau)f_1(\tau)d\tau & 0 & -\int_{t-T}^{t} \varphi_3(\tau)f_3(\tau)d\tau \end{bmatrix} \tag{6.24}$$

where f_1, f_2, f_3 are described as below:

$$\begin{aligned} f_1 &= sign(x_1 - x_3)\sqrt{|x_1 - x_3|} \\ f_2 &= sign(x_2)\sqrt{|x_2|} \\ f_3 &= sign(x_3 - x_2)\sqrt{|x_3 - x_2|} \end{aligned}$$

and the vector of parameter $\theta = \begin{bmatrix} C_{13} & C_{20} & C_{32} \end{bmatrix}^{\mathrm{T}}$.
Then, the estimated parameters are calculated as:

$$\hat{\theta}(t) = \left(\int_{t-T}^{t} \mathbf{w}(\tau)\mathbf{w}^{\mathrm{T}}(\tau)d\tau \right)^{-1} \int_{t-T}^{t} \mathbf{w}(\tau)\mathbf{z}(\tau)d\tau$$

Once parameters are estimated, they are used to achieve the states estimation. In the same way as for parameters, three left modulating function of the form $\varphi_k(t) = t^k e^{-t}$ are used. The states are estimated by using the following equation:

$$\hat{y}(t) = (\Gamma(t))^{-1} \int_{t-T'}^{t} \left(\mathbf{w}^{\mathrm{T}}\hat{\theta} + \mathbf{Z} \right) \tag{6.25}$$

where matrix $\mathbf{w}$ is defined as before in 6.24, while $\mathbf{Z}$ and Γ are described below:

$$\mathbf{Z} = \begin{bmatrix} \int_{t-T}^{t} \dot{\varphi}_1(\tau)y_1(\tau)d\tau + \frac{1}{S}\int_{t-T}^{t} \varphi_1(\tau)u_1(\tau)d\tau \\ \int_{t-T}^{t} \dot{\varphi}_2(\tau)y_2(\tau)d\tau + \frac{1}{S}\int_{t-T}^{t} \varphi_2(\tau)u_2(\tau)d\tau \\ \int_{t-T}^{t} \dot{\varphi}_3(\tau)y_3(\tau)d\tau \end{bmatrix} \quad \Gamma = \begin{bmatrix} \varphi_1(t) & 0 & 0 \\ 0 & \varphi_2(t) & 0 \\ 0 & 0 & \varphi_3(t) \end{bmatrix}$$

Figures 6.1 and 6.2 illustrate the parameters and states estimation. The simulation have been performed by using an initial horizon $T = 2$ seconds and it is at this time when both, estimated parameters and estimated states converge to their corresponding real values.
Now, in the following simulations some faults will be considered. The first ones are leakages in the tanks which appear in different instants of time as it was described before in equation (5.10). The residuals generated when these faults have taken place are shown in Figures 6.3 and 6.4. Each figure represent the set of residual based on the estimated parameters and in the estimated states, respectively. From

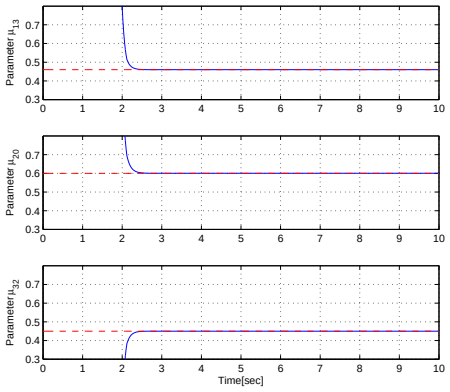

Figure 6.1: Estimated parameters

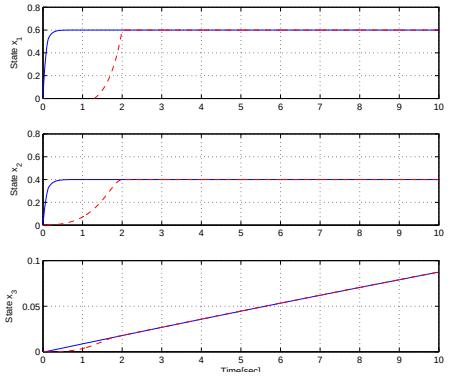

Figure 6.2: Estimated states

these figure one can see that residual present a remarkable deviation from zero when a fault has happened and in the case of Figure 6.4, from these residuals it is possible to know in which tank the fault has been occurred.

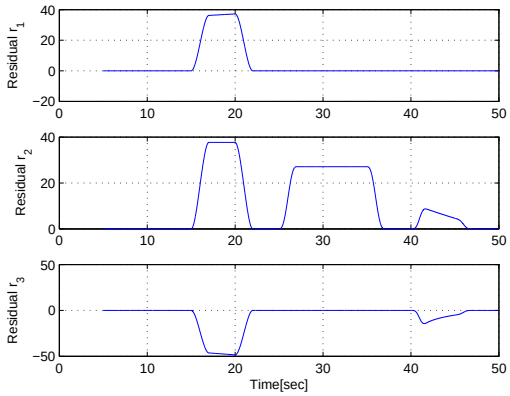

Figure 6.3: Parameter based residuals

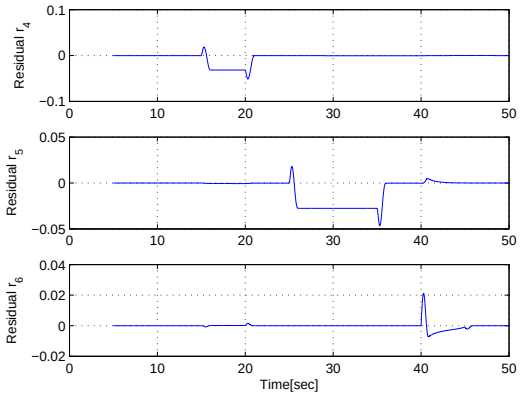

Figure 6.4: States based residuals

The next considered faults are a malfunction in the actuators, which behavior is depicted in Figure 6.5, and the corresponding generated residuals are shown in Figures 6.6 and 6.7.

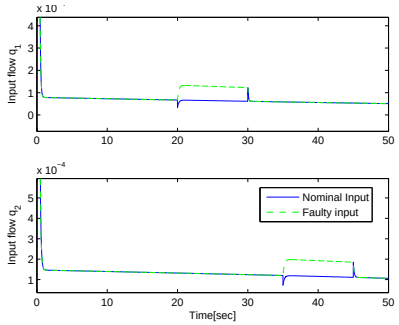

Figure 6.5: Input flows q_1 and q_2

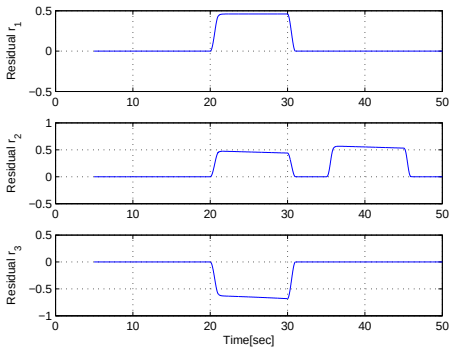

Figure 6.6: Parameter based residuals

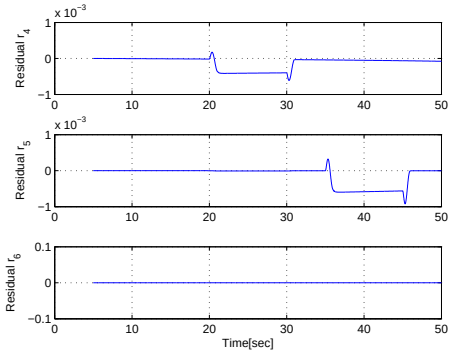

Figure 6.7: States based residuals

In the following case, a parameter change is simulated. The real parameter of the system change with a ramp behavior as it is described in Figure 6.8. Figures 6.9 and 6.10 describe the residual response in front of a change in parameters.

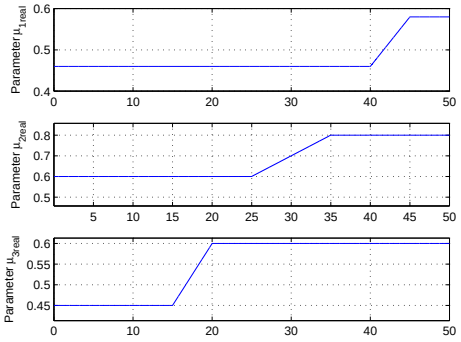

Figure 6.8: Change in the real system parameters

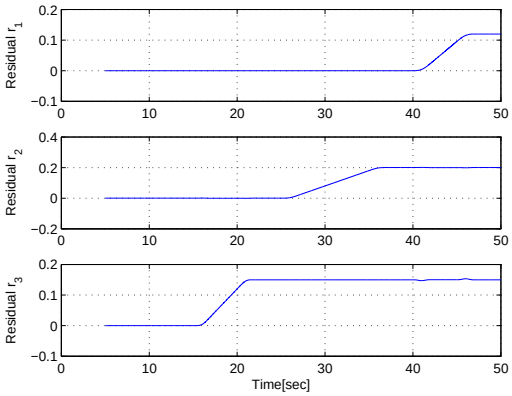

Figure 6.9: Parameter based residuals

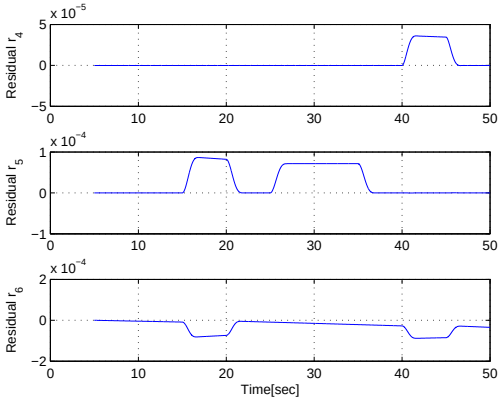

Figure 6.10: States based residuals

Now, leakages will be considered again but this time with a presence of Gaussian noise in the sensor readings. The leaks are the same considered in equation (5.10). The states are illustrated in Figure 6.11 and residuals are shown in Figures 6.12 and 6.13. As it was mentioned before, since modulating functions avoid the direct derivative of the signals, noise issues can be overcome when the estimates are calculated. As show in Figure 6.12 the parameter based residuals do not present a presence of noise since the estimated parameters do not present coupled noise. In Figure 6.13, it can be seen that states based residuals have some coupled noise but this is because the sensed signals are also used to compute the residual signal. However the estimated states do not present presence of noise.

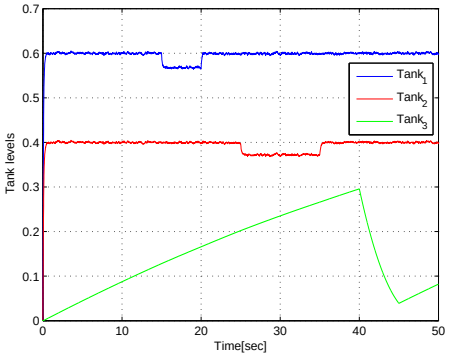

Figure 6.11: Sensor readings with presence of Gaussian noise

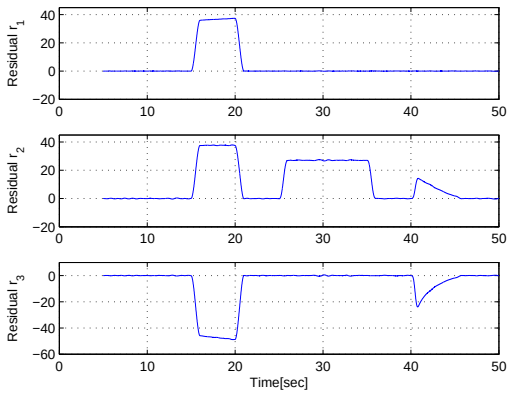

Figure 6.12: Parameter based residuals

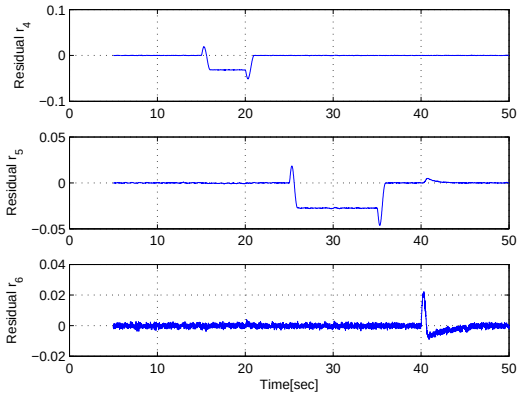

Figure 6.13: States based residuals

6.2.1 Special Cases

In this current section the special cases in which states „jump" from one working region to another and in which states lie in the neighborhood of the *critical points* mentioned in previous sections, will be simulated.
The first simulation will be performed in the way that states are „jumping" between regions as it is illustrated in Figure 6.14. The faults are simulated as leakages and they occur around the time in which states lie close to the critical points. Additionally, presence of Gaussian noise is considered. Figures 6.15 and 6.16 show the residual generated by using the estimated parameters and states by applying modulating functions approach.

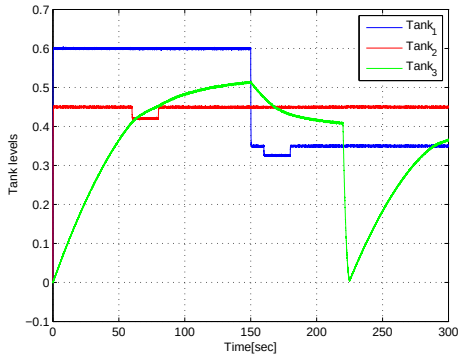

Figure 6.14: System states in the four possible working regions

One can see that residuals can be used to detect faults since they present a remarkable response each time and while a fault has occurred. However, it is also

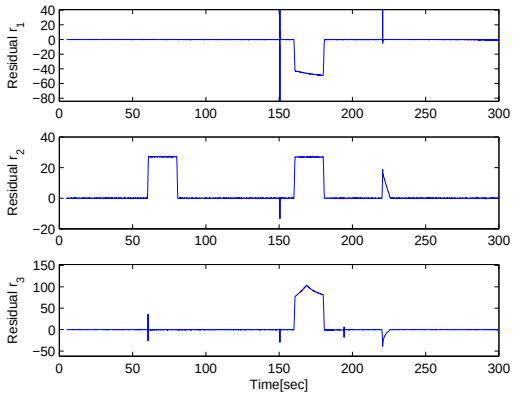

Figure 6.15: Parameters based residuals

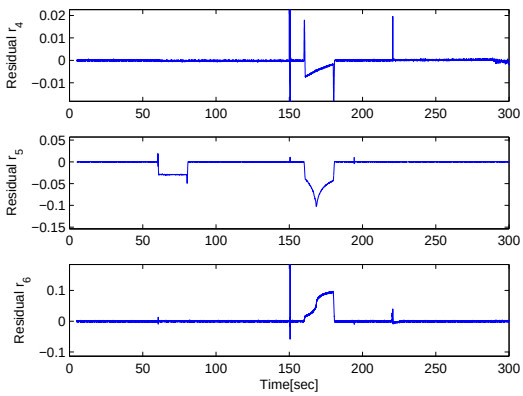

Figure 6.16: States based residuals

possible to see that there exist some peaks in the residuals signals, mostly in the first residual based on estimated states (r_4). This peaks are generated in the instant when the states cross each other reaching the critical points where exist singularities. Although the presence of peaks, it is still possible to achieve a fault detection using the two groups generated residuals.

The next simulation is considered when the states are equal and the system works in the axis region as explained in previous chapters. The system response in front of presence of leaks as faults and Gaussian noise is showed in Figure 6.17. Leaks

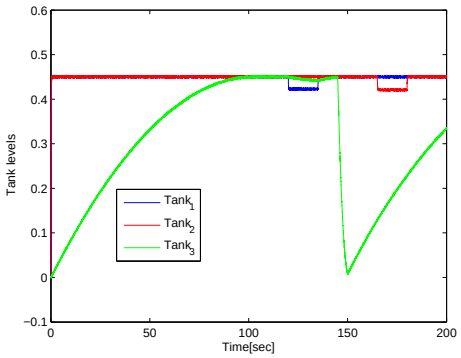

Figure 6.17: System behavior in front of leaks

occurrence is depicted in Figure 6.18 and the residuals generated in Figure 6.19 and 6.20. It can be seen that residuals r_2, r_3, r_5 and r_6 present some peaks when the states are closely equal and cross each other continuously because of the noise presence, but they still present a response when the leaks have occurred. In the case of residuals r_1 and r_4, they do not present peaks but a clear response when leaks have occurred. Then, fault detection can be still achieved by using residuals

signals generated by using a modulating function approach.

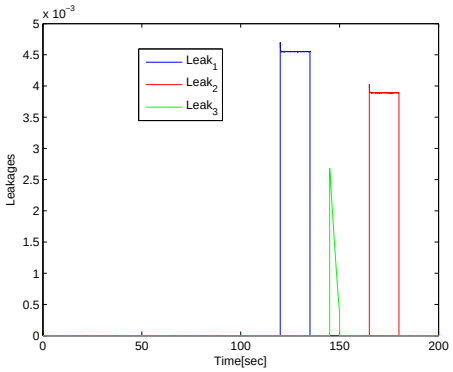

Figure 6.18: Leakages occurrence in time

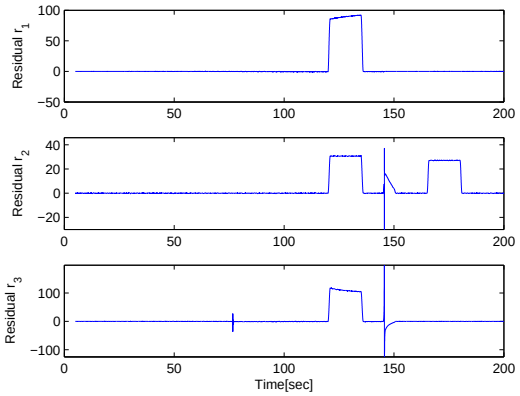

Figure 6.19: Parameters based residuals

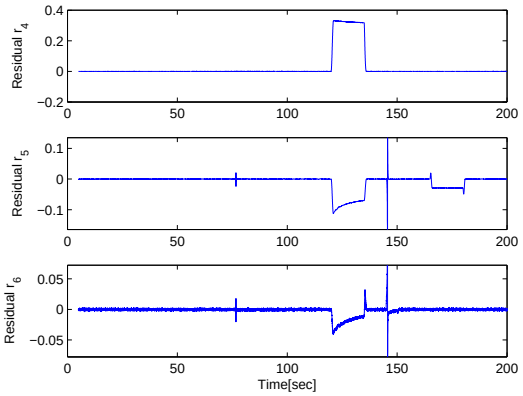

Figure 6.20: States based residuals

7 Practical Implementation in the Real Three Tank System

In the current Chapter, a practical implementation of the studied approaches explained in the previous chapters will be performed. The real system is a Three Tank System which is provided by the Department of Computer Science and Automation of the Technische Universität Ilmenau. The real system will be subjected to some kind of faults, as long as it is possible to simulate the faults considered in Chapter 4. First, a brief description of the real system is presented.

7.1 Description of the Real System

The Three Tank system is not a commercial system. The system has been made by a research group conformed by students, workers and with the supervision of a scientist in charge. The components of the system, almost all have been obtained from other pieces of projects that are not more used. However, components such as sensors, pumps and other measurement instruments are new.
Then, some crucial components and details of the system will be described.

(1) **Tanks:** In terms of geometry, the used tanks are not as usual in this kind of system since they are not cylinders and the transversal area of them is not a constant. The bottom part of the tank, whose height is around $0.10m$, has the geometry of a cone with a pronounced slope around 50 degrees. After that part, the slope in the cone geometry is greater and it is not too decisive. It is important to take in account the geometry of the tanks since it plays an important role in equations which described the system. For control and fault detection purpose, the work region of the system will be greater than $0.10m$.

(2) **Pumps:** The system is made of two pumps, each one supplying water to the correspondent tank 1 and 3. The pumps have a maximal rate of flow of $400l/h$, which is also delimited by the control signal of $10V$. Because of

the characteristic curve of the pump's behavior, the minimal voltage which is needed by the pumps to beat the hysteresis phenomenon is around 5.60 Volts. With this minimal voltage, the pump is able to begin to provide water to the respective tank.

(3) **Input flow to the tanks:** The input flow of each tank is supplied by the two pumps described before and the location of the entry point is at the top of the tanks. Because of the location of the entry point, the input flow enters into the tank performing a free fall behavior. As a result of the collision between the input flow and the water surface in the tank, a water dispersion that can be visualized as bubbles or splashes occurs. This dispersion phenomenon has been solved by using a flexible pipe which connect the top of the tank and the bottom of it. In this way, the input flow now collides directly with the bottom or with the tank wall and there is no more a dispersion phenomenon.

(4) **Level sensors:** The level sensors of the system are located in the top part of each tank. Instead of other systems, the sensors do not work with a mean of measured pressure in each tank, which is used to calculate then the height of the water. Sensors used in the real system are ultrasonic sensors. The sensor transmits pulses which will be used then to compute and obtain the tank level. Also, because of technical characteristics of the sensors, the minimum well measured distance between an object an the sensor is $50mm$, which also restricts the upper limit of the system work region. The most important technical characteristics of the sensor are shown as following:

- Analog range: $50 - 300mm$
- Measuring rate: $25ms$ $(40Hz)$
- Resolution : 12 bits
- Accuracy: $+/-2.5\%$
- Ultrasonic frequency : $400kHz$

(5) **Pipes:** The used pipes are not the same for the whole system, that means, are at least two different kinds of pipes connecting the different parts and components. As a consequence, it is possible that the resistance applied to the flows are not the same.

(6) **Valves:** There exist two types of valves in the system: proportional and on/off valve. The proportional valves are used to interconnect the tanks and also to

regulate the output flow from the tank 3 (the last one) to the container. These proportionally valves are manipulated manually and are usually completely open. The on/off valves, on the other hand, are used as an additionally out coming flow but only for the tanks 1 and 3. These electrical vales will be used in order to simulate leaks in the tanks.

The real system is depicted in Figure 7.1, where each one of its parts is indicated which the corresponding number as in the list above.

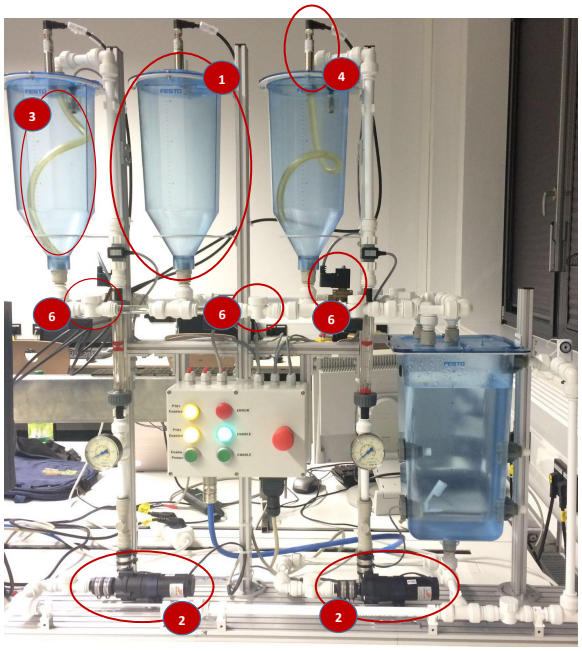

Figure 7.1: Real Three Tank System

Additionally, for a better knowledge of the real system structure, the $P\&ID$ diagram of the system is shown in Figure 7.2.

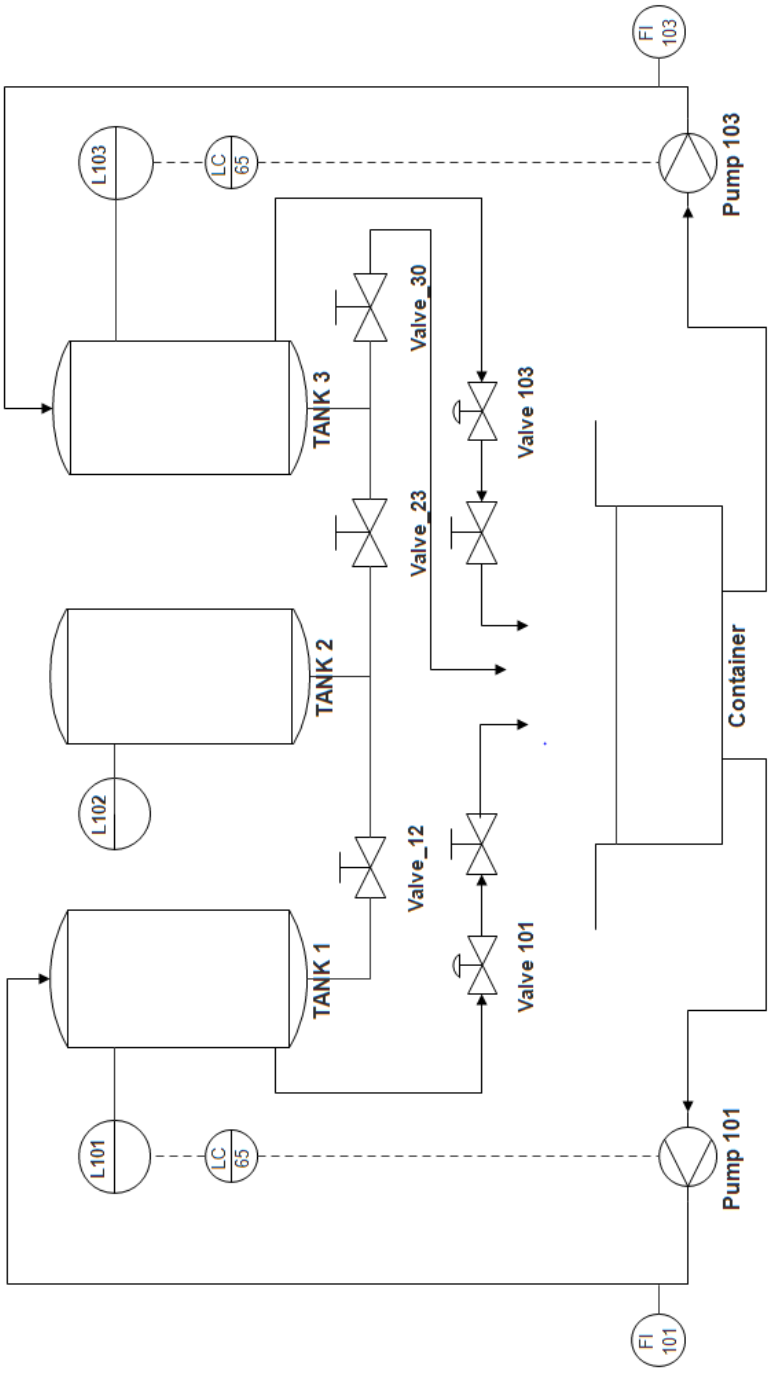

Figure 7.2: *P&ID* diagram of the real Three Tank System

7.1.1 System Model

The distribution and order of the tanks in the real system is not the same established in the model used in the previous chapters. In Figure 7.2 it can be seen the order of the tanks, which is now consecutive.
So, due to the particular characteristics of some system components such as tanks geometry, the equations which are used to model the system have been changed. The model of the real system, which has been obtained by a research group of the university (Sebastian Zehnter) is described as follows:

$$\begin{aligned}
\dot{x_1} &= \tfrac{1}{S_1}(-az_{12}sign(x_1 - x_2)\sqrt{2g|x_1 - x_2|} + u_1) \\
\dot{x_2} &= \tfrac{1}{S_2}(az_{12}sign(x_1 - x_2)\sqrt{2g|x_1 - x_2|} - az_{23}sign(x_2 - x_3)\sqrt{2g|x_2 - x_3|}) \\
\dot{x_3} &= \tfrac{1}{S_3}(az_{23}sign(x_2 - x_3)\sqrt{2g|x_2 - x_3|} - az_{30}sign(x_3)\sqrt{2g|x_3|} + u_3) \\
\vec{y} &= \begin{bmatrix} x_1 & x_2 & x_3 \end{bmatrix}^{\mathrm{T}}.
\end{aligned} \tag{7.1}$$

where $x_i(t)$ is the water level in each tank i and S_i is the transversal area of the corresponding tank, which is a function of the water height:

$$S_i = A_i + \partial A_i \tag{7.2}$$

and A_i and its deviation ∂A_i are described by:

$$\begin{aligned}
A_i &= |a(h_i - h_{offset})| + b \\
\partial A_i &= ah_i
\end{aligned}$$

where h_{offset} is a initial value when there is any water in the tanks and $a \geq 0$ and $b \geq 0$ are constants which have been calculated by the research group who made the system model.
The system parameters az_{12}, az_{23} and az_{30} have been calculated by a system identification and represent the coefficients between the interconnected tanks and the outgoing flow from the last tank to the container. The obtained parameter values after the identification process are shown in Table 7.1.

PARAMETER	VALUE
az_{12}	$2.015422784 \times 10^{-5}$
az_{23}	$1.912356759 \times 10^{-5}$
az_{30}	$2.147795934 \times 10^{-5}$

Table 7.1: Real system parameters

7.1.2 Controller Design

As in Chapter 4 , the controller design will be designed in the same way, using a first order sliding mode controller and using a saturation function in order to avoid the chattering phenomenon. Considering that all the states will be measured, but only two of them are controlled, the system present three errors that are defined by:

$$\begin{aligned} e_1 &= x_1 - x_{1d} \\ e_2 &= x_3 - x_{3d} \\ e_3 &= x_2 \end{aligned} \tag{7.3}$$

where x_{id} is the desired value of the height h_1 and h_3 respectively, $i = 1, 3$. The manifolds are defined as follows:

$$s = \begin{bmatrix} s_1 \\ s_2 \end{bmatrix} = \begin{bmatrix} f(e_1, e_3) \\ f(e_2, e_3) \end{bmatrix} \tag{7.4}$$

where:

$$\begin{aligned} f(e_1, e_3) &= a_1 e_1 + a_2 e_3 \\ f(e_2, e_3) &= b_1 e_2 + b_2 e_3 \end{aligned} \tag{7.5}$$

The control signals which make the manifolds converge to zero $s = 0$ are described by:

$$u(t) = \begin{bmatrix} u_1 \\ u_3 \end{bmatrix} = \begin{bmatrix} u_{1eq} - k_1 sign(s_1) \\ u_{3eq} - k_2 sign(s_2) \end{bmatrix} \tag{7.6}$$

where u_{1eq} and u_{3eq} are the equivalent control for each signal u_1 and u_3. These equivalent control signals are obtained from the dynamics of the manifold, making $\dot{s} = 0$, and are defined by:

$$\begin{aligned} u_{1eq} &= \tfrac{S}{a_1}[-a_2(C_1 f(x_1, x_2) - C_2 f(x_2, x_3)) + a_1(C_1 f(x_1, x_2))] \\ u_{3eq} &= \tfrac{S}{b_1}[-b_2(C_1 f(x_1, x_2) - C_2 f(x_2, x_3)) + b_1(C_3 f(x_3) - C_2 f(x_2, x_2))] \end{aligned} \tag{7.7}$$

where:

$$\begin{aligned} C_1 f(x_1, x_3) &= \tfrac{az_{12}}{S_1} sign(x_1 - x_2)\sqrt{|x_1 - x_2|} \\ C_2 f(x_2, x_3) &= \tfrac{az_{23}}{S_2} sign(x_2 - x_3)\sqrt{|x_2 - x_3|} \\ C_3 f(x_3) &= \tfrac{az_{30}}{S_3} sign(x_3)\sqrt{|x_3|} \end{aligned} \tag{7.8}$$

Then, a saturation function, as in equation 4.24 is also used here to avoid the chattering phenomena in the controller signal. It is important to take into account that the control signal is limited by the maximal flow which the pump is able to

supply.
Figure 7.3 and 7.4 illustrate the measured tank levels and the control signal applied to the real system. The desired heights are fixed to $0.25m$ and $0.20m$ for tank 1 and 3, respectively.

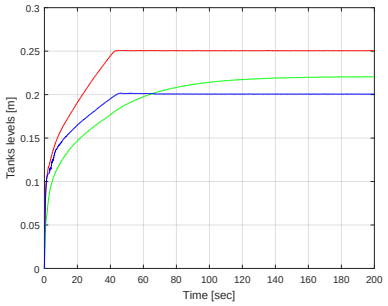

Figure 7.3: Tank levels behavior

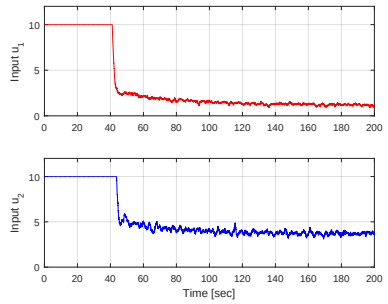

Figure 7.4: Sliding mode Control signal u_1 and u_3

In Figure 7.3 it can be seen the saturation behavior of the control signal at the beginning and after around 45 seconds tanks 1 and 3 reach the desired height and control signals start to decrease until reaching a stable value. However, from Figure 7.4, even after a saturation function has been used, the control signals present a kind of chattering around the stable value. This behavior may be produced due to the own characteristic of the pumps. Figure 7.5 shows manifolds behavior and both converge to zero, once each control signal converges around the stable value.
Additionally, in Figure 7.6 a zoomed view is shown and it can be seen that the measured signal, even after the use of a filter in the simulink model, there is a presence of noise. Due to the own noise in each sensor reading, all simulations consider a presence of noise in the readings.

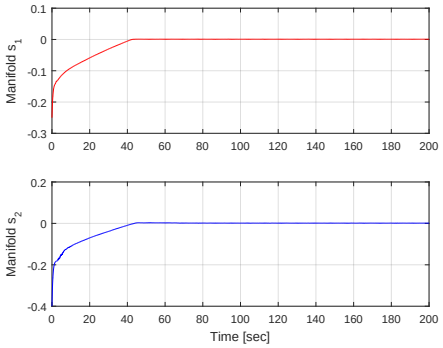

Figure 7.5: Manifolds of the sliding mode controller

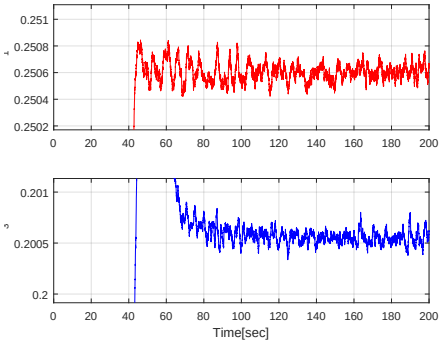

Figure 7.6: Zoomed view of the tank levels

7.2 Implementation of the Studied Approaches

In this section, the approaches used before will be implemented in the real system. The residual generation will be done considering some faults, as long as they can be simulated in the real system.

7.2.1 Observer-based Approach

The real system described in equation 7.1 may be expressed in the following form:

$$\dot{x} = f(x,t) + g(x,t)u(t) \tag{7.9}$$

where x is the state vector which represents the levels and $u = \begin{bmatrix} u_1 & u_3 \end{bmatrix}^{\mathrm{T}}$. Functions $f(x,t)$ and $g(x,t)$ are defined as:

$$f(x,t) = \begin{bmatrix} \frac{1}{S_1}(-az_{12}sign(x_1-x_2)\sqrt{2g|x_1-x_2|}) \\ \frac{1}{S_2}(az_{12}sign(x_1-x_2)\sqrt{2g|x_1-x_2|} - az_{23}sign(x_2-x_3)\sqrt{2g|x_2-x_3|}) \\ \frac{1}{S_3}(az_{23}sign(x_2-x_3)\sqrt{2g|x_2-x_3|} - az_{30}sign(x_3)\sqrt{2g|x_3|}) \end{bmatrix} \tag{7.10}$$

$$g(x,t) = \begin{bmatrix} \frac{1}{S_1} & 0 \\ 0 & 0 \\ 0 & \frac{1}{S_3} \end{bmatrix}$$

Then, considering state x_1 as an output and as in Chapter 5, analyzing its observability, the system is uniformly observable since each state can be determined as a function of the output, inputs and its derivative. So, since the system is uniformly observable, the system can be transformed into a triangular form by using a observable mapping of the form $\mathcal{O}_1(x) = \begin{bmatrix} h(x) & L_f h(x) & L_f^2 h(x) \end{bmatrix}^{\mathrm{T}}$ which is described as follows:

$$\mathcal{O}_1(x) = \begin{bmatrix} h(x) \\ L_f h(x) \\ L_f^2 h(x) \end{bmatrix} = \begin{bmatrix} x_1 \\ -\frac{az_{12}\sqrt{2g}}{S_1} sign(x_1-x_2)\sqrt{|x_1-x_2|} \\ (\frac{az_{12}\sqrt{2g}}{S_1})^2 sign(x_1-x_2) - \frac{az_{12}az_{23}2g}{2S_1S_2}\frac{sign(x2-x3)\sqrt{|x_2-x_3|}}{\sqrt{|x_1-x_2|}} \end{bmatrix} \tag{7.11}$$

And the inverse of its Jacobian matrix is defined as:

$$\left[\frac{\partial \mathcal{O}_1(x)}{\partial x}\right]^{-1} = \begin{bmatrix} 1 & 0 & 0 \\ 1 & \frac{2S_1}{az_{12}\sqrt{2g}}\frac{1}{\alpha} & 0 \\ 1 & \frac{2S_1}{az_{12}\sqrt{2g}}(\frac{1}{\omega}+\frac{\beta}{\alpha\omega}) & \frac{4S_1S_2}{az_{12}az_{23}2g}\frac{1}{\omega} \end{bmatrix} \tag{7.12}$$

where:

$$\alpha = \frac{1}{\sqrt{|x_1-x_2|}}$$
$$\beta = \frac{sign(x_2-x_3)\sqrt{|x_2-x_3|}}{sign(x_1-x_2)|x_1-x_2|^{3/2}}$$
$$\omega = \frac{1}{\sqrt{|x_1-x_2|}\sqrt{|x_2-x_3|}}$$

From Equation 7.12 it is important to notice that when the term $\frac{4S_1S_2}{az_{12}az_{23}2g}\frac{1}{\omega}$ is equal to zero, there is a complete column of zeros and as a consequence, that may leads to a divergence or oscillation of the observer due to a rank deficiency in the matrix $(\partial\mathcal{O}/\partial x)^{-1}$. This issue can take place when S_1 or S_2 are equal to zero or α or ω tends to infinite. However, S_1 and S_2 can not be equal to zero since $S_i = |a(x_i - x_{offset})| + b + ax_1$ presents an absolute value function and $a \geq 0$, $b \geq 0$.

So, the system becomes non observable when α or ω tends to infinite, that means, when the system states tend to be the same, $x_1 = x_2$ and $x_2 = x_3$, and it is at this points when the system presents a singularity.
This *critical points* in which system presents singularity will be analyzed later. Now, continuing with the observer design, the observer of the system will finally have the following form, as in equation 5.8:

$$\dot{\hat{x}} = f(\hat{x}(t)) + g(\hat{x}(t))u(t) + \left[\frac{\partial \mathcal{O}_1(x)}{\partial x}\right]^{-1}_{x=\hat{x}} L(y(t) - h(\hat{x}(t))) + P\rho \begin{bmatrix} sign(\hat{x_1} - x_1) \\ sign(\hat{x_2} - x_2) \\ sign(\hat{x_3} - x_3) \end{bmatrix} \tag{7.13}$$

where the matrix $P = diag(1, 1, 1)$ and the constant $\rho = diag(\rho_1, \rho_2, \rho_3)$.
The residuals will be generated from the reconstructed disturbances signals and are described by:

$$r_i(t) = \hat{d}_i(x, t) = \rho_i sign(e_i)$$

In the implementation of the observer, a low pass filter has been used instead of a saturation function as in Chapter 4.
The first fault case has been made considering leakages in the tanks 1 and 3, using the on/off valves in order to simulate the faults. Figure 7.7 shows the behavior of both, the real system (blue entire line) and the estimated states (red dotted line), in front of the leaks described in Figure 7.8. It can be seen that estimated states follow the real ones very close. Signals shown in Figure 7.8 do not correspond to the out flow of the leaks, but to the boolean signal which activate the on/off valves.

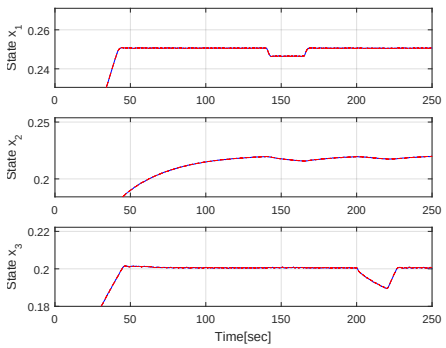

Figure 7.7: Comparison of real and estimated states

Fault detection can be achieved by the generated residual signals, which present a deviation from zero in the instants when a fault has occurred, as shown in Figure 7.9.

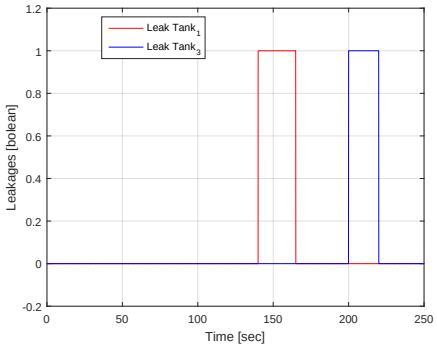

Figure 7.8: Leakage faults occurrence

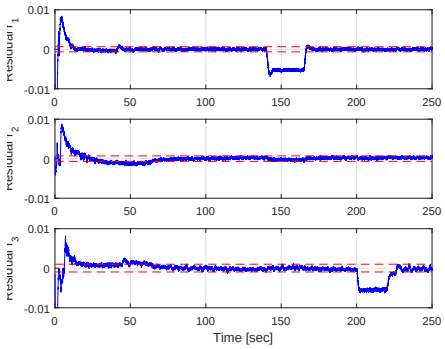

Figure 7.9: Residual signals in a leakage faults case

The second considered case is about a malfunction in the interconnected valves between tanks. Faults have been simulated by closing manually the interconnected valves for an interval of time. Their behavior is described by the following equation:

$$Valve_{12} = \begin{cases} \neq 0, & for\ t < 130 \\ 0, & for\ 130 \leq t \leq 155 \\ \neq 0, & for\ t > 155 \end{cases} \qquad Valve_{23} = \begin{cases} \neq 0, & for\ t < 200 \\ 0, & for\ 200 \leq t \leq 220 \\ \neq 0, & for\ t > 220 \end{cases} \tag{7.14}$$

Residual generated signals are shown in Figure 7.10 and it can be seen that residuals exceed the threshold when faults have occurred. It is important to note that residuals will be used after a period around 80 seconds, which is the time when the system becomes stable and the period before is considered a fault-free case.

Now, for the following simulation, a failure in the actuator is considered. The fault consists in a not corresponding actuator response for a certain control signal from the controller. The behavior of the fault may be described as follows and it is illustrated in Figure 7.11 but as a boolean value, where „1" indicates when the fault

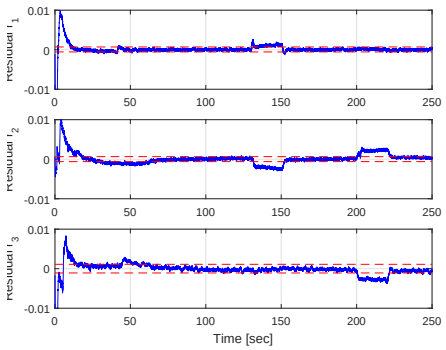

Figure 7.10: Residual signals in valve faults case

occurs and „0" when it does not.

$$u_{1-sys} = \begin{cases} u_1, & for\ t < 140 \\ \alpha u_1, & for\ 140 \leq t \leq 160 \\ u_1, & for\ t > 160 \end{cases} \qquad u_{3-sys} = \begin{cases} u_3, & for\ t < 200 \\ \beta u_3, & for\ 200 \leq t \leq 220 \\ u_3, & for\ t > 220 \end{cases} \tag{7.15}$$

where u_{i-sys} and u_i represent the actuator response and the control signal generated by the controller, respectively. Also, α and β are positive and lower than 1.

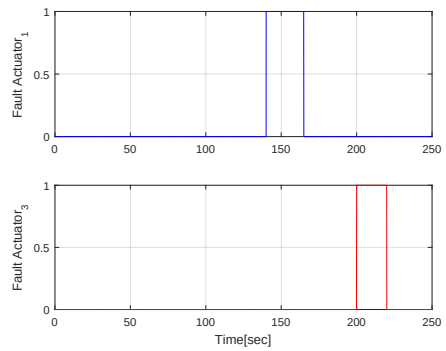

Figure 7.11: Actuator fault occurrence

Residuals signals are illustrated in Figure 7.12 and from them it is possible to achieve the fault detection for each fault.

Another important fact to mention is regarding the control signal, which in front of an actuator fault tries to compensate the fault in order to hold the states in their respective desired values. Figure 7.13 illustrates how the control signals respond to the fault and Figure 7.14 shows the actuators response, which hold almost continuously except for a brief presence of peaks. Due to this compensation, states are almost not affected by the faults, as is illustrated in Figure 7.15

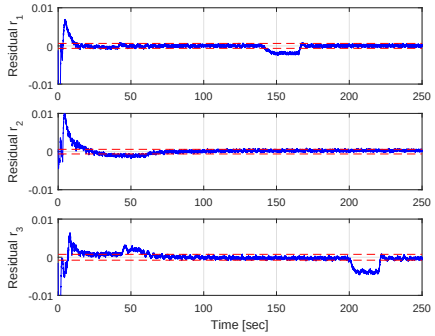

Figure 7.12: Residual signals in front of actuator faults

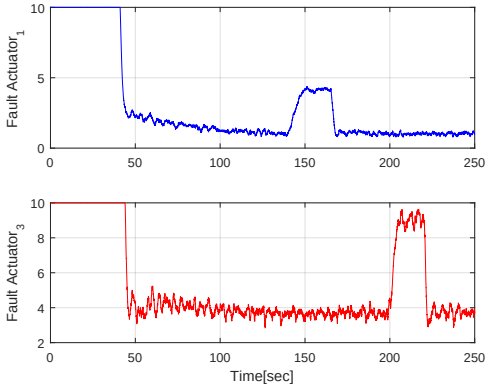

Figure 7.13: Control signal effort in front of actuator fault

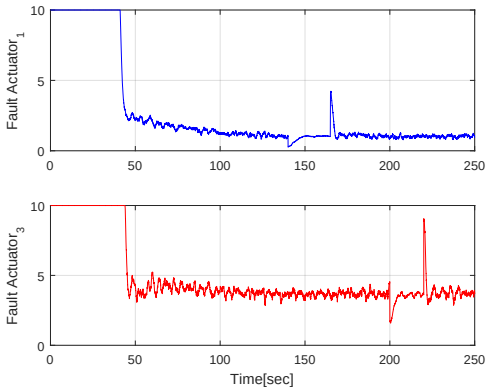

Figure 7.14: Actuators response when faults occur

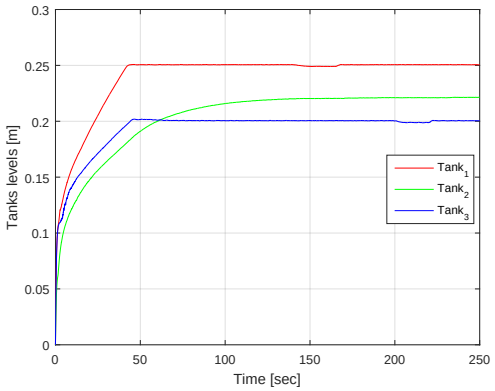

Figure 7.15: System states in front of actuator fault

7.2.2 Structural Analysis Approach

As in the previous chapter, constraints have been made from the model equations. In the same way, from the new model equations of the real system, constraints are described as follows, considering leaks as faults:

$$
\begin{aligned}
&C_1 : \dot{x_1} = \tfrac{1}{S_1}(-q_{12} - q_{L1} + q_1)\\
&C_2 : \dot{x_1} = \tfrac{dx_1}{dt}\\
&C_3 : \dot{x_2} = \tfrac{1}{S_2}(q_{12} - q_{23} - q_{L2})\\
&C_4 : \dot{x_2} = \tfrac{dx_2}{dt}\\
&C_5 : \dot{x_3} = \tfrac{1}{S_3}(q_{23} - q_{L3} + q_3 - q_{30})\\
&C_6 : \dot{x_3} = \tfrac{dx_3}{dt}\\
&C_7 : q_{12} = az_{12} sign(x_1 - x_2)\sqrt{2g|x_1 - x_2|}\\
&C_8 : q_{23} = az_{23} sign(x_2 - x_3)\sqrt{2g|x_2 - x_3|}\\
&C_9 : q_{30} = az_{30} sign(x_3)\sqrt{2g|x_3|}\\
&C_{10} : q_1 = u_1(t) = f(x_1)\\
&C_{11} : q_3 = u_3(t) = f(x_3)\\
&C_{12} : q_{L1} = az_{L1}\sqrt{|x_1|}\\
&C_{13} : q_{L2} = az_{L2}\sqrt{|x_2|}\\
&C_{14} : q_{L3} = az_{L3}\sqrt{|x_3|}\\
&C_{15} : x1 = h_1 km_1\\
&C_{16} : x2 = h_2 km_2\\
&C_{17} : x3 = h_3 km_3
\end{aligned}
\tag{7.16}
$$

where km_i is the constant gain of each level sensor and h_i are the measured signals. The ranked incidence matrix constructed from the constraints is shown in Table 7.2. Residuals are made by using the higher rank constraints and they are described by the following equations:

$$
\begin{aligned}
r_1 &= ZERO_1 = S_1\dot{x_1} + q_{12} + q_{L1} - q_1\\
r_2 &= ZERO_2 = S_2\dot{x_2} - q_{12} + q_{23} + q_{L2}\\
r_3 &= ZERO_3 = S_3\dot{x_3} - q_{23} + q_{L3} - q_3 + q_{30}
\end{aligned}
\tag{7.17}
$$

Now some simulations will be shown, in which different kinds of faults are considered. For the first case, as in the previous approach, a presence of leaks in tank 1 and 3 is considered and their behavior in time is illustrated in Figure 7.16. Residuals signals are described in Figure 7.17

Fault detection can be well performed from the residual signals since they exceed

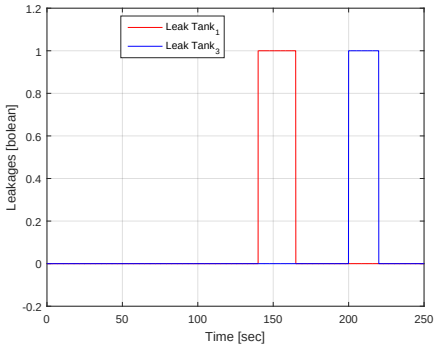

Figure 7.16: Leakage fault behavior

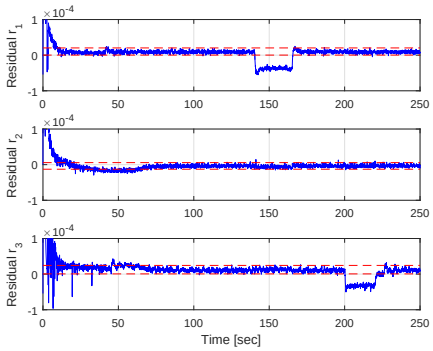

Figure 7.17: Residual signals in front of leakages

the threshold every time a fault occurs.

CONS	$\dot{x}_1$	q_1	q_{12}	x_1	$\dot{x}_2$	x_2	q_3	q_{23}	q_{30}	$\dot{x}_3$	x_3	q_{L1}	q_{L2}	q_{L3}		RANK	RESIDUAL
1	1	1	1									1				②	**ZERO**
2	[1]			1												1	
3			1		1			1					1			②	**ZERO**
4					[1]	1										1	
5							1	1	1	1				1		②	**ZERO**
6										[1]	1					1	
7			[1]	1		1										1	
8						1		[1]			1					1	
9									[1]		1					1	
10		[1]		1												0	
11							[1]				1					0	
12				1								[1]				1	
13						1							[1]			1	
14											1			[1]		1	
15				[1]												0	
16						[1]										0	
17											[1]					0	

Table 7.2: Ranked Incidence Matrix

The following simulated case is the same described in equation 7.14 relative to a malfunction in the interconnecting valves, but the faults have been occurred in different times as in equation 7.14. Figure 7.18 illustrates the states behavior, where it is indicated the intervals of time when each fault occurs. The first fault is indicated between the yellow dotted lines and the second fault is pointed by the purple dotted lines. Residuals are shown in Figure 7.19.

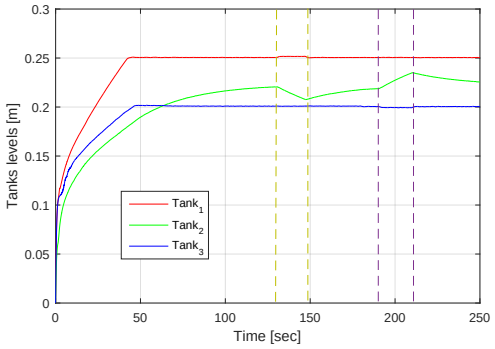

Figure 7.18: Tank levels indicating the occurrence of valves malfunction

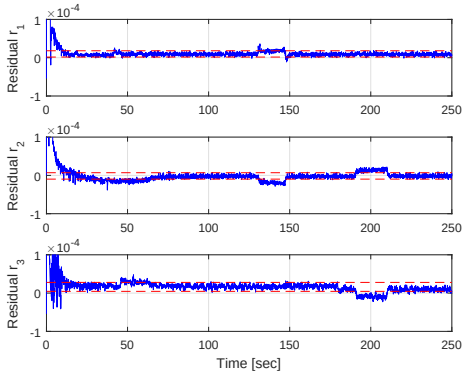

Figure 7.19: Residual signal in front of valve malfunction

From Figure 7.19 it can be seen that residuals present a response in front of the considered faults. However, residual r_1 although presents a not too big deviation it still exceeds the threshold and together with residual r_2, the fault detection can be achieved. In the case of residual r_3, fault detection in $valve_{23}$ can be performed since residual exceeds the threshold, with a clearly amplitude, when the fault occurs.
In the following case, an actuator fault is presented. Faults have appeared as the following equation indicates and each actuator presents a not corresponding response for a certain control signal. Here it is assumed that in normal operation, the actuator

response is equal to the controller signal.

$$u_{1-sys} = \begin{cases} u_1, & for\ t < 140 \\ \alpha u_1, & for\ 140 \leq t \leq 160 \\ u_1, & for\ t > 160 \end{cases} \qquad u_{3-sys} = \begin{cases} u_3, & for\ t < 200 \\ \beta u_3, & for\ 200 \leq t \leq 220 \\ u_3, & for\ t > 220 \end{cases}$$

Figures 7.20 and 7.21 illustrate the moment in which each fault occurs and the residual signals generated in presence of these faults, respectively. Residuals r_1

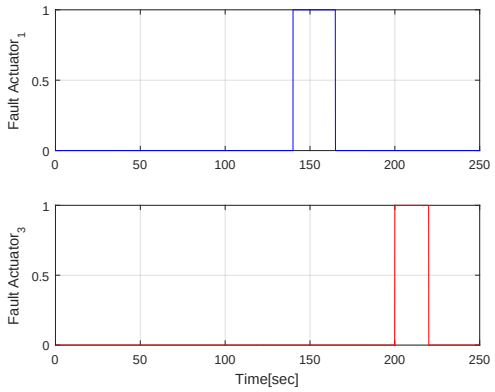

Figure 7.20: Actuator faults behavior in time

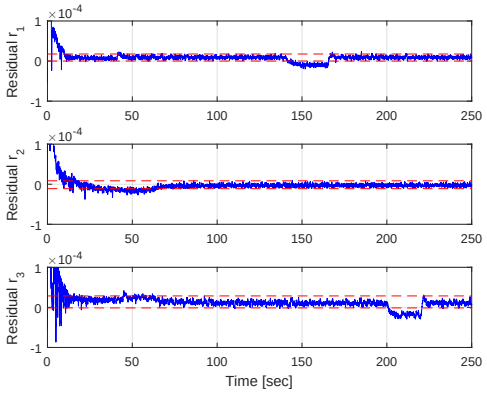

Figure 7.21: Residual signals response in front of actuator faults

and r_3 show the instant of time in which a fault in the control signal u_1 and u_3 have occurred respectively. In this case, with this kind of residual it is possible to isolate the fault directly and to know where the fault has occurred, if in the first or third actuator.

7.2.3 Parameter Estimation Approach

In this section, residual generation is performed by using a parameter estimation approach in the real three tank system. First of all, the identifiability of parameters will be tested. The real system can be reorganized and presented in the following form:

$$\dot{x} = f(x,t) + g(x,t)u(t)$$

with the functions $f(x,t)$ and $g(x,t)$ defined as in equation 7.10:

$$f(x,t) = \begin{bmatrix} \frac{1}{S_1}(-az_{12}sign(x_1 - x_2)\sqrt{2g|x_1 - x_2|}) \\ \frac{1}{S_2}(az_{12}sign(x_1 - x_2)\sqrt{2g|x_1 - x_2|} - az_{23}sign(x_2 - x_3)\sqrt{2g|x_2 - x_3|}) \\ \frac{1}{S_3}(az_{23}sign(x_2 - x_3)\sqrt{2g|x_2 - x_3|} - az_{30}sign(x_3)\sqrt{2g|x_3|}) \end{bmatrix}$$

$$g(x,t) = \begin{bmatrix} \frac{1}{S_1} & 0 \\ 0 & 0 \\ 0 & \frac{1}{S_3} \end{bmatrix}, \quad u = \begin{bmatrix} u_1 \\ u_3 \end{bmatrix}, \quad y(t) = h(x) = \begin{bmatrix} x_1 \\ x_2 \\ x_3 \end{bmatrix}$$

From function $f(x,t)$, *Assumption 3.1* and *Assumption 3.2* mentioned in Chapter 3, can be easily fulfilled. Then, in order to check *Assumption 3.3*, the Jacobian identifiability matrix

$$J_I = \frac{\partial}{\partial az_j} L_f h_i$$

is obtained, where j can takes the combinations 12, 23 or 30 which indicate the parameter belonging to the interconnected pipe between two tanks or between the last tank and the container.

$$J_I = \begin{bmatrix} \frac{\partial}{\partial az_{12}} L_f h_1 & \frac{\partial}{\partial az_{23}} L_f h_1 & \frac{\partial}{\partial az_{30}} L_f h_1 \\ \frac{\partial}{\partial az_{12}} L_f h_2 & \frac{\partial}{\partial az_{23}} L_f h_2 & \frac{\partial}{\partial az_{30}} L_f h_2 \\ \frac{\partial}{\partial az_{12}} L_f h_3 & \frac{\partial}{\partial az_{23}} L_f h_3 & \frac{\partial}{\partial az_{30}} L_f h_3 \end{bmatrix}$$

After computing Lie derivatives and the partial derivatives respect to each parameter, the Jacobian identifiability matrix is:

$$J_I = \begin{bmatrix} \frac{\partial}{\partial az_{12}} L_f h_1 & 0 & 0 \\ \frac{\partial}{\partial az_{12}} L_f h_2 & \frac{\partial}{\partial az_{23}} L_f h_2 & 0 \\ 0 & \frac{\partial}{\partial az_{23}} L_f h_3 & \frac{\partial}{\partial az_{30}} L_f h_3 \end{bmatrix}$$

Now in order to check the matrix rank, its determinant is calculated:

$$det(J_I) = \left(\frac{\partial}{\partial az_{12}} L_f h_1\right)\left(\frac{\partial}{\partial az_{23}} L_f h_2\right)\left(\frac{\partial}{\partial az_{30}} L_f h_3\right) \tag{7.18}$$

$$det(J_I) = -\left(\frac{(2g)^{3/2}}{S_1 S_2 S_3}\right)\left(sign(x_1 - x_2)\sqrt{|x_1 - x_2|}\right)\left(sign(x_2 - x_3)\sqrt{|x_2 - x_3|})(sign(x_3)\sqrt{|x_3|}\right)$$

The Jacobian identifiability matrix will have full rank as long as its determinant be different from zero. That means, while states be different from each other, $x_1 \neq x_2 \neq x_3$, the identifiability of parameters az_{12},az_{23} and az_{30} is insured.
Once the identifiability has been checked, the residual generation by using the parameter estimation approach can be performed. Residual signals are described as:

$$r_i = \hat{az}_j - az_j \tag{7.19}$$

with $j = 12, 23, 30$ and the estimated parameters are calculated as follows:

$$\begin{aligned} \hat{az}_{12} &= \frac{-S_1\hat{y}_1 + u_1}{sign(y_1 - y_2)\sqrt{2g|y_1 - y_2|}} \\ \hat{az}_{23} &= \frac{-S_1\hat{y}_1 - S_2\hat{y}_2 + u_1}{sign(y_2 - y_3)\sqrt{2g|y_2 - y_3|}} \\ \hat{az}_{30} &= \frac{-S_1\hat{y}_1 - S_2\hat{y}_2 - S_3\hat{y}_3 + u_1 + u_3}{sign(y_3)\sqrt{2g|y_3|}} \end{aligned} \tag{7.20}$$

where y_i corresponds to the sensed state x_i and the estimated derivatives $\hat{y}_i$ are estimated by using Levant's Differentiator as explained in Chapter 3.
The estimated parameters in a free fault case are illustrated in Figure 7.22. From a zoomed view, as in Figure 7.23, it can be seen that the estimated parameters present a coupled noise, but their values are around 1×10^{-5} and 2×10^{-5} which are very close to the values parameters in Table 7.1.
Now, as for the other approaches, some simulations are shown considering different faults. The first faults are leakages in tanks 1 and 3 and their occurrence in time is shown in Figure 7.24. The residual signals are described in Figure 7.25 and it may be seen that residuals exceed the thresholds every time a fault has occurred, however

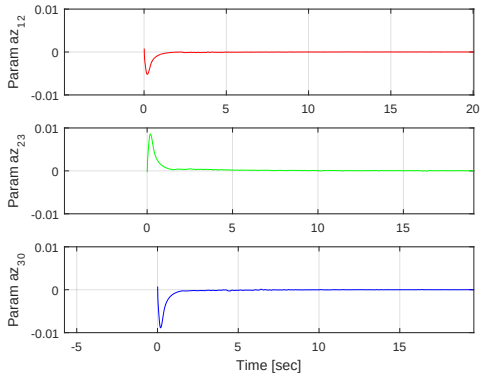

Figure 7.22: Convergence of parameter estimation

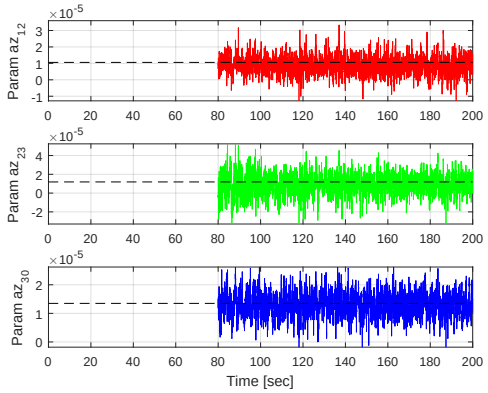

Figure 7.23: Zoomed view of estimated parameters

around time $t = 65-70sec$ there is a presence of a peak which is produced due to the intersection between states x_2 and x_3, that means near the moment when $x_2 = x_3$. This behavior will be take into account in the following section, where singularities are analyzed. From now, considering that before instant $t = 80$ seconds the system lies in a free fault case, residuals will be shown from that instant onwards. Figure 7.26 illustrates the residual after time $t = 80$ seconds.

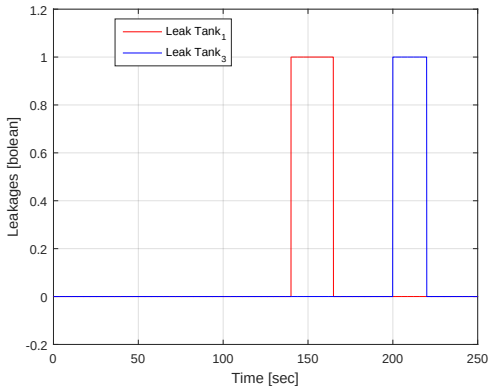

Figure 7.24: Leakage faults in Tank 1 and Tank 3

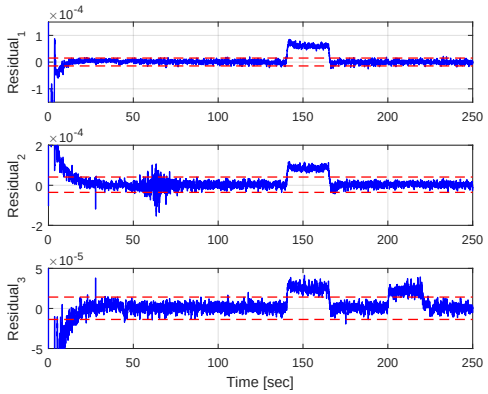

Figure 7.25: Residual behavior in leakage faults case

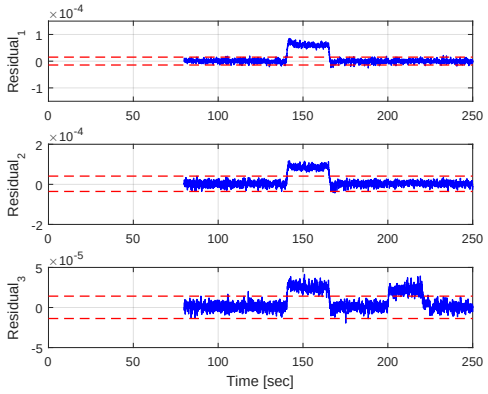

Figure 7.26: Residual behavior after system stabilization

The next case considers actuator faults described by the following equation:

$$u_{1-sys} = \begin{cases} u_1, & for\ t < 140 \\ \alpha u_1, & for\ 140 \leq t \leq 160 \\ u_1, & for\ t > 160 \end{cases} \qquad u_{3-sys} = \begin{cases} u_3, & for\ t < 200 \\ \beta u_3, & for\ 200 \leq t \leq 220 \\ u_3, & for\ t > 220 \end{cases}$$

Figures 7.27 and 7.28 illustrates the occurrence of each actuator fault in time and the residual signals generated, respectively.

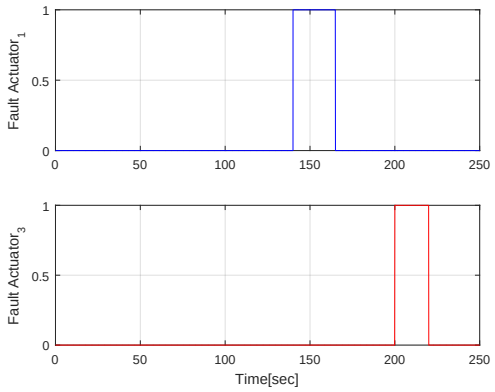

Figure 7.27: Occurrence of actuators failure

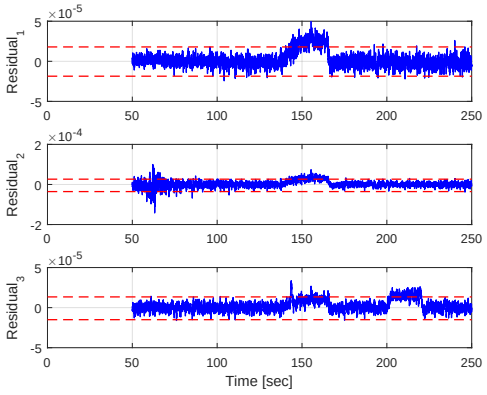

Figure 7.28: Residual behavior in front of actuator partial failure

7.2.4 Modulating Functions Approach

In this section, residuals for the real system will be generated by using the modulating function approach. As in Chapter 6, parameters and states will be estimated and then they will be used to generate the residuals. Considering that

the three tank levels are measured, $y = \begin{bmatrix} x_1 & x_2 & x_3 \end{bmatrix}^{\mathrm{T}}$, and the system is described as follow:

$$\begin{aligned}
\dot{x}_1 &= \tfrac{1}{S_1}(-az_{12}sign(x_1 - x_2)\sqrt{2g|x_1 - x_2|} + u_1) \\
\dot{x}_2 &= \tfrac{1}{S_2}(az_{12}sign(x_1 - x_2)\sqrt{2g|x_1 - x_2|} - az_{23}sign(x_2 - x_3)\sqrt{2g|x_2 - x_3|}) \\
\dot{x}_3 &= \tfrac{1}{S_3}(az_{23}sign(x_2 - x_3)\sqrt{2g|x_2 - x_3|} - az_{30}sign(x_3)\sqrt{2g|x_3|} + u_3)
\end{aligned}$$

The parameter estimation is made using complete modulating functions of the form $\varphi_k(t) = (t-T)^k t^k$ and an horizon T is considered. Then the parameters are estimated as:

$$\hat{\theta}(t) = \begin{bmatrix} C_{12} \\ C_{23} \\ C_{30} \end{bmatrix} = \left(\int_{t-T}^{t} \mathbf{w}(\tau)\mathbf{w}^{\mathrm{T}}(\tau)d\tau \right)^{-1} \int_{t-T}^{t} \mathbf{w}(\tau)\mathbf{z}(\tau)d\tau$$

where:

$$\begin{bmatrix} \hat{C}_{12} \\ \hat{C}_{23} \\ \hat{C}_{30} \end{bmatrix} = \begin{bmatrix} \frac{1}{S_1}\sqrt{2g}\hat{az}_{12} \\ \frac{1}{S_2}\sqrt{2g}\hat{az}_{23} \\ \frac{1}{S_3}\sqrt{2g}\hat{az}_{30} \end{bmatrix}$$

and the matrices $\mathbf{w}$ and $\mathbf{z}$ are defined in the same way as it was explained in Chapter 6.

$$\mathbf{z}(t) = \begin{bmatrix} -\int_{t-T}^{t} \dot{\varphi}_1(\tau)y_1(\tau)d\tau - \frac{1}{S_1}\int_{t-T}^{t} \varphi_1(\tau)u_1(\tau)d\tau \\ -\int_{t-T}^{t} \dot{\varphi}_2(\tau)y_2(\tau)d\tau \\ -\int_{t-T}^{t} \dot{\varphi}_3(\tau)y_3(\tau)d\tau - \frac{1}{S_3}\int_{t-T}^{t} \varphi_2(\tau)u_3(\tau)d\tau \end{bmatrix}$$

$$\mathbf{w}(t) = \begin{bmatrix} -\int_{t-T}^{t} \varphi_1(\tau)f_1(\tau)d\tau & 0 & 0 \\ \int_{t-T}^{t} \varphi_1(\tau)f_1(\tau)d\tau & -\int_{t-T}^{t} \varphi_2(\tau)f_2(\tau)d\tau & 0 \\ 0 & \int_{t-T}^{t} \varphi_3(\tau)f_2(\tau)d\tau & -\int_{t-T}^{t} \varphi_3(\tau)f_3(\tau)d\tau \end{bmatrix}$$

with f_1, f_2, f_3 described as:

$$f_1 = sign(x_1 - x_2)\sqrt{|x_1 - x_2|}$$
$$f_2 = sign(x_2 - x_3)\sqrt{|x_2 - x_3|}$$
$$f_3 = sign(x_3)\sqrt{|x_3|}$$

Once the parameters have been estimated, they are used in the estimation of states using now left modulating functions of the form $\varphi_k(t) = t^k e^{-t}$. Estimated states are calculated by:

$$\hat{y}(t) = \begin{bmatrix} \hat{x}_1 \\ \hat{x}_2 \\ \hat{x}_3 \end{bmatrix} = (\Gamma(t))^{-1} \int_{t-T'}^{t} \left(\mathbf{w}^{\mathrm{T}} \hat{\theta} + \mathbf{Z} \right)$$

where, the matrix $\mathbf{w}$ is the same as defined above for the estimation of parameters and matrices $\mathbf{Z}$ and Γ are defined as:

$$\mathbf{Z} = \begin{bmatrix} \int_{t-T}^{t} \dot{\varphi}_1(\tau) y_1(\tau) d\tau + \frac{1}{S} \int_{t-T}^{t} \varphi_1(\tau) u_1(\tau) d\tau \\ \int_{t-T}^{t} \dot{\varphi}_2(\tau) y_2(\tau) d\tau + \frac{1}{S} \int_{t-T}^{t} \varphi_2(\tau) u_2(\tau) d\tau \\ \int_{t-T}^{t} \dot{\varphi}_3(\tau) y_3(\tau) d\tau \end{bmatrix} \quad \Gamma = \begin{bmatrix} \varphi_1(t) & 0 & 0 \\ 0 & \varphi_2(t) & 0 \\ 0 & 0 & \varphi_3(t) \end{bmatrix}$$

In Figure 7.29 and 7.30 the estimated parameters and states are depicted, respectively. In Figure 7.29 it can be seen that the estimated parameters values are close to the parameter values in Table 7.1. Also, in Figure 7.30 it is possible to

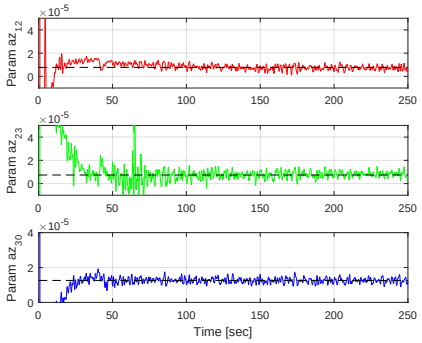

Figure 7.29: Estimated parameters

see that the estimated states, described by the red dotted lines, are the same as

the real measured states re presented by the blue lines. Then, the residuals are

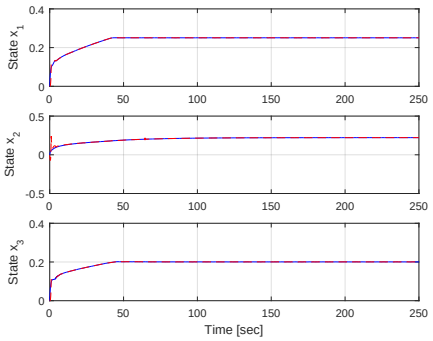

Figure 7.30: Estimated states

generated based on both, the estimated parameters and states. The first considered scenario is when there is presence of leakages in the system. Figure 7.31 shows the occurrence of the leaks in tanks 1 and 3 and the residuals are shown in Figure 7.32 and 7.33. The first residuals are generated based on the estimated parameters and the second ones based on the estimated states.

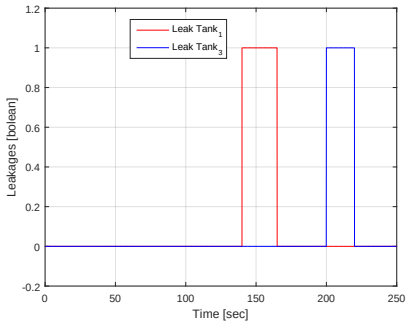

Figure 7.31: Behavior of leaks in tank 1 and 3

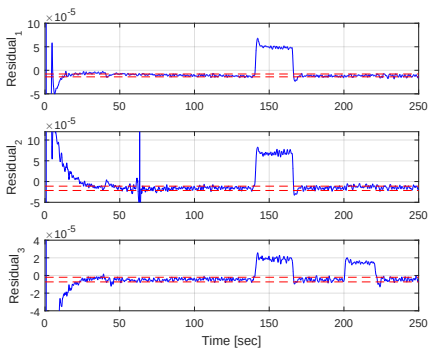

Figure 7.32: Based on estimated params.

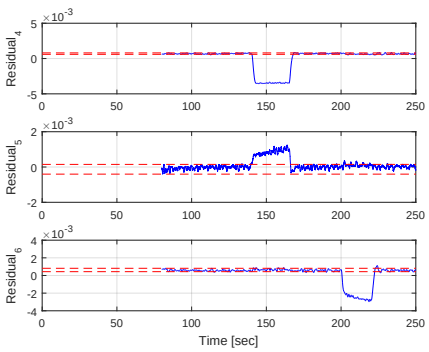

Figure 7.33: Based on estimated states

From Figures 7.32 and 7.33 one can see that faults can be detected since residuals present a deviation from the zero range in each moment when a fault has occurred. In the next scenario faults in the valves which interconnect tanks 1-2 and 2-3 are considered. The behavior of these faults are described in the following equation:

$$Valve_{12} = \begin{cases} \neq 0, & for\ t < 130 \\ 0, & for\ 130 \leq t \leq 150 \\ \neq 0, & for\ t > 155 \end{cases} \qquad Valve_{23} = \begin{cases} \neq 0, & for\ t < 200 \\ 0, & for\ 200 \leq t \leq 220 \\ \neq 0, & for\ t > 220 \end{cases}$$

Figures 7.34 and 7.35 show the residual behavior in front of the valve malfunction and also in this case, faults are able to be detected by using the two pair of generated residuals.

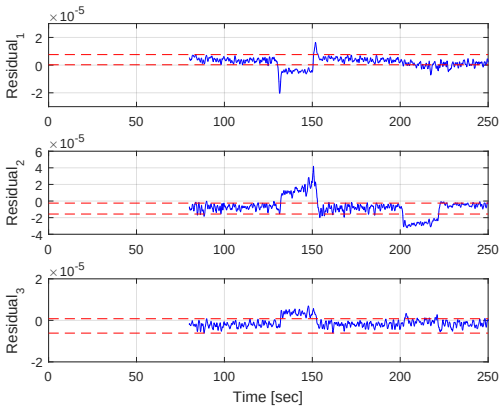

Figure 7.34: Based on estimated params.

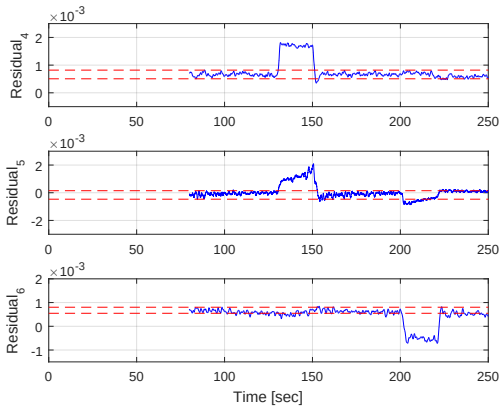

Figure 7.35: Based on estimated states

Now, in the next scenario actuator faults are considered and its occurrence behavior is described in the following equation and it is depicted in Figure 7.36.

$$u_{1-sys} = \begin{cases} u_1, & for\ t < 140 \\ \alpha u_1, & for\ 140 \leq t \leq 160 \\ u_1, & for\ t > 160 \end{cases} \qquad u_{3-sys} = \begin{cases} u_3, & for\ t < 200 \\ \beta u_3, & for\ 200 \leq t \leq 220 \\ u_3, & for\ t > 220 \end{cases}$$

The generated residuals are shown in Figures 7.37 and 7.38. It is possible to see that with the first group of residuals it is possible to detect the faults but the isolation can not be made directly. However, by using the second group of residuals, it is possible to perform a direct isolation of the faults since the residuals r_4 and r_6 present a deviation when there is a fault which affect the tank 1 and tank 3, respectively.

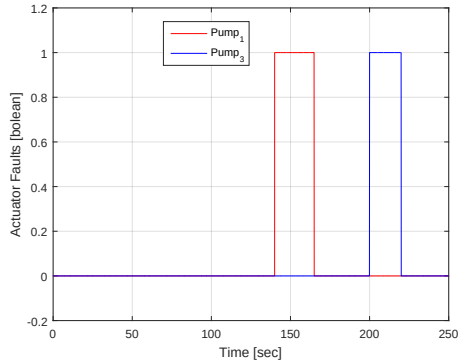

Figure 7.36: Occurrence of actuator faults in each pump

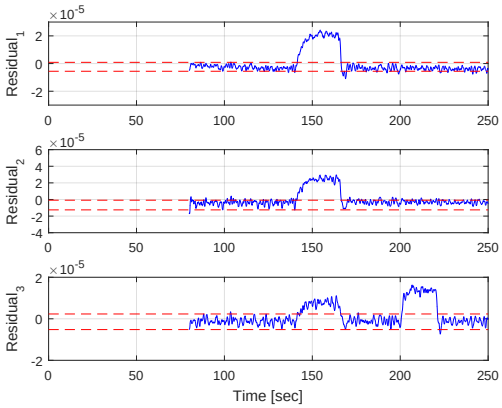

Figure 7.37: Based on estimated params.

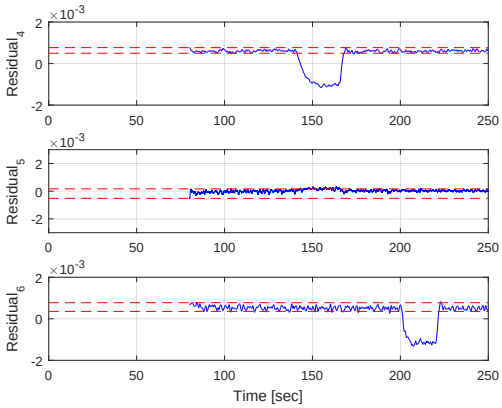

Figure 7.38: Based on estimated states

7.3 Singularity Cases

The real three tank system is described by the following equations:

$$\begin{aligned}
\dot{x_1} &= \frac{1}{S_1}(-az_{12}sign(x_1 - x_2)\sqrt{2g|x_1 - x_2|} + u_1) \\
\dot{x_2} &= \frac{1}{S_2}(az_{12}sign(x_1 - x_2)\sqrt{2g|x_1 - x_2|} - az_{23}sign(x_2 - x_3)\sqrt{2g|x_2 - x_3|}) \\
\dot{x_3} &= \frac{1}{S_3}(az_{23}sign(x_2 - x_3)\sqrt{2g|x_2 - x_3|} - az_{30}sign(x_3)\sqrt{2g|x_3|} + u_3) \\
y &= \begin{bmatrix} x_1 & x_2 & x_3 \end{bmatrix}^{\mathrm{T}}.
\end{aligned}$$

From the equation shown above, as in the previous chapter, states can be located in four working regions depending in the relations between tank levels. Figure 7.39 shows the different possible state locations.

In this section, two special cases will be analyzed. The first one is about the residual generation when states „jump" from one working region to another. The second case consist in the residual generation when desired states are equal, that

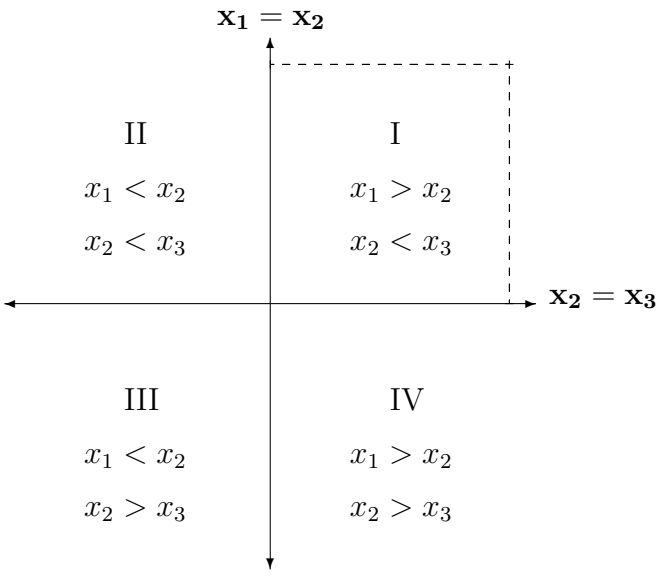

Figure 7.39: Possible working regions of states

means the case when states are located in the axis in Figure 7.39. For the following simulations only leakage faults will be considered since the main point is the analysis of singularity cases.

In order to overcome singularity problems during the residual generation, an algebraic approximation will be performed when the system states lie around the critical points. The algebraic approximation is described by:

$$\begin{aligned}
\frac{1}{sign(x_1-x_2)\sqrt{|x_1-x_2|}} &\approx \frac{1}{sign(x_1-x_2+\varepsilon)\sqrt{|x_1-x_2|+\varepsilon}} \\
\frac{1}{sign(x_2-x_3)\sqrt{|x_2-x_3|}} &\approx \frac{1}{sign(x_2-x_3+\varepsilon)\sqrt{|x_2-x_3|+\varepsilon}} \\
\frac{1}{sign(x_3)\sqrt{|x_3|}} &\approx \frac{1}{sign(x_3+\varepsilon)\sqrt{|x_3|+\varepsilon}}
\end{aligned} \tag{7.21}$$

By using this algebraic approximation the rank deficiency in the inverse of the Diffeomorphism Jacobian matrix mentioned in Chapter 5 is avoided. Also, the condition of full rank shown in equation 7.18 is fulfilled due to the determinant of the Jacobian identifiability matrix will not be equal to zero even at critical points, $x_1 = x_2 = x_3$. In this way, the parameter identification when the system states lie around the singularities will be possible to achieved.

7.3.1 Changing Regions

In this first situation, when states „jump" from one region to another, the system goes through *critical points*, $x_1 = x_2$ or $x_2 = x_3$, in which the system presents singularities. The idea for the next simulations is to analyze the residual generation when the system states are around this *critical points*. In order to perform a changing region behavior, a change in the desired state x_1 has been made. Due to the behavior of the system, it was not possible to go through the four working regions, but at least two of them were able to be performed. Figure 7.40 illustrates the system behavior, which in terms of the working regions can be described as follow:

$$Stateslocation = \begin{cases} I, \quad for\ t < 95 \\ I - IV\ through\ Axis\ x_1 = x_2, \quad for\ 95 \leq t \leq 200 \\ IV, \quad for\ t > 220 \end{cases}$$

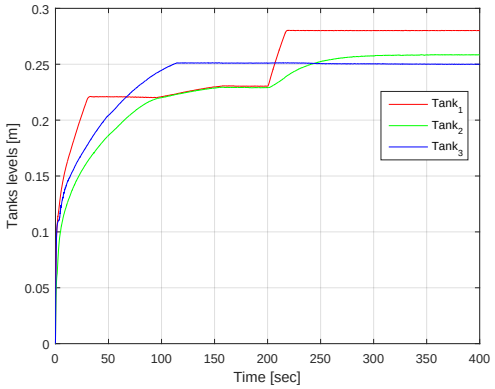

Figure 7.40: States behavior through different working regions

In Figure 7.40 it is noted a region changed, from I to IV, crossing very close the axis region $x_1 = x_2$.
The tank leakages will take place right around the instants where states cross each other. Figure 7.41 describes the leakages occurrence in time, in which „1" and „0" indicate the activation and deactivation, respectively of on/off valves used to simulate the faults.
Figure 7.42 shows the system behavior in front of faults described above.

Figures 7.43, 7.44, 7.45 and 7.46-7.47 describe the residual signals by using the observer-based, structural analysis, parameter estimation and modulating function approaches, respectively. In case of residuals generated by using the observer or

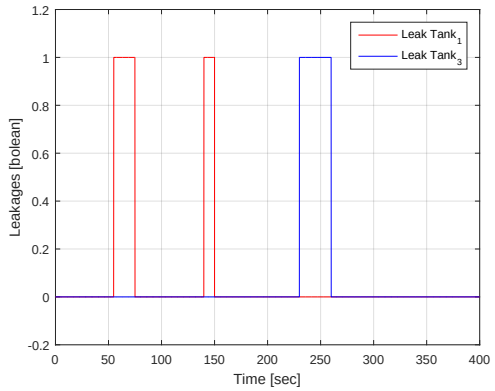

Figure 7.41: Occurrence of leakage faults in Tanks 1 and 3

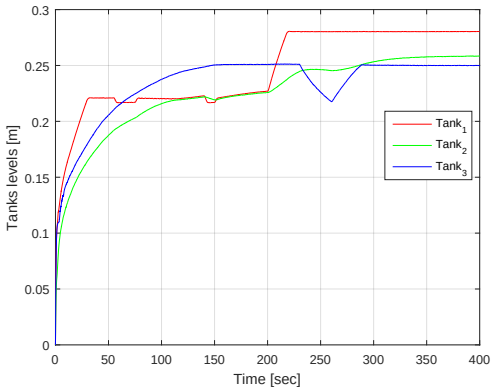

Figure 7.42: System states behavior due to leakages presence

structural analysis approach, the fault detection can be well performed since each residual presents a noteworthy response every time a fault has been occurred and this response exceeds the threshold sufficiently in terms of amplitude.

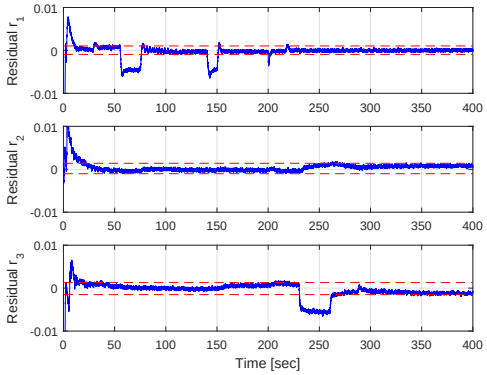

Figure 7.43: Observer based approach

On the other hand, residuals generated by using the parameters estimation approach

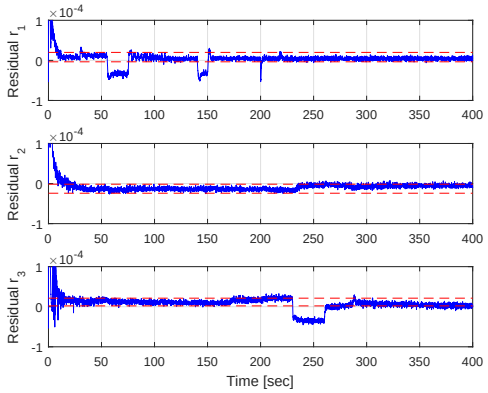

Figure 7.44: Structural analysis approach

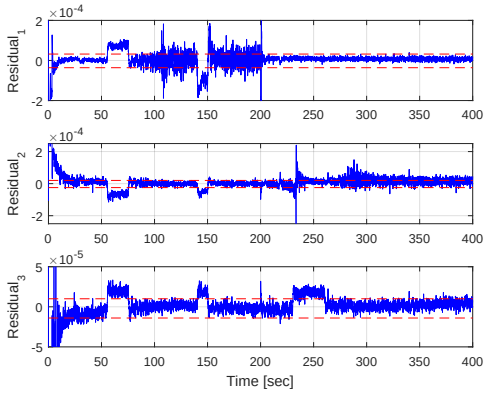

Figure 7.45: Parameter estimation approach

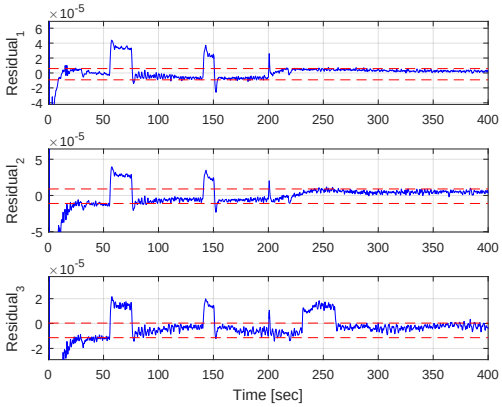

Figure 7.46: Based on estimated params.

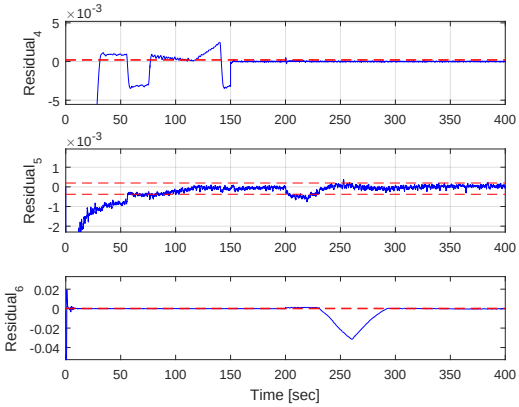

Figure 7.47: Based on estimated states

show some possible false detection. Residual r_1 presents a more noisy response between the period of time 120 and 180 seconds, in which states x_1 and x_2 are very close to each other. Even in presence of this behavior, the residual still shows a noteworthy response when a fault has occurred. Analyzing residual r_2, the first and

second fault can be detected but it is possible to note two peaks presence around instants $t = 130$ and $t = 180$ seconds, in which a cross between states x_2 and x_3 has happened. Due to these peaks, a false detection is achieved. In the case of residual r_3, all faults can be detected without possible false detections since no peak has occurred and the residual response describes well the faults occurrence. So, although there could be the possibility to make a false detection using residuals r_1 and r_2, the use of each of them with residual r_3 together, may achieve a good fault detection of each fault.

In the case of generated residuals based on the modulating functions approach, a good fault detection can be performed. Other than the parameter estimation approach, it is possible to notice that residuals based on the estimated parameters using modulating functions present less coupled noise, in terms of amplitude. Also, and what it is more important, these residuals do not present peaks which can be interpreted or can lead to a false fault detection. Additionally, with the second group of residuals based on the estimated states, it is possible to perform a direct isolation of the faults in each tank since it is easy to see that the two first leaks have occurred in the tank 1 and he last one has taken place in the tank 3.

7.3.2 Axis Region

In this section, the special case in which the desired level tanks are equal (consequently the states are also equal), will be analyzed. Physically, in the laboratory system, these singularities take place when the three tank levels are the same, that means $x_1 = x_2 = x_3$ and also, considering that the levels are stable at this equilibrium point $\dot{x}_1 = \dot{x}_2 = \dot{x}_3 = 0$. So, from the system equations in (7.1) it is possible to see that once the desired levels are reached, only the Pump 103, relating to the control signal u_3, is being used in order compensate the outflow from the tank 3. While there is no more visual effects in the system when the states are equal, these singularities lead to a non-observability of the system and also a non-identifiability of the system parameters. The non-observability takes place since, in case of the singularities, a rank deficiency in the inverse of the diffeomorphism Jacobian matrix is presented. In the same way, the non-identifiability is presented since the determinant of the identifiability Jacobian matrix is equal to zero when the states are the same.

Then, for the following simulations, the desired level for both tanks 1 and 3 is $x_1 = x_3 = 0.25m$ and simulated faults will take place when the two desired level are

reached and are the same. Valves behavior, which simulate leakages in tanks 1 and 3 are shown in Figure 7.48 and the system response is illustrated in Figure 7.49.

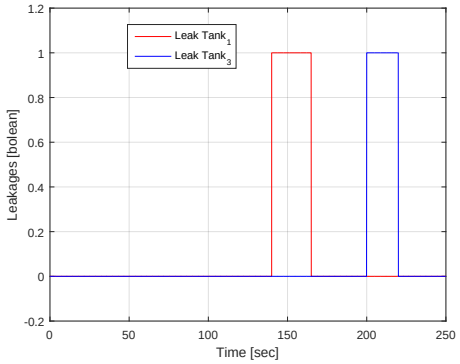

Figure 7.48: Leakage faults behavior

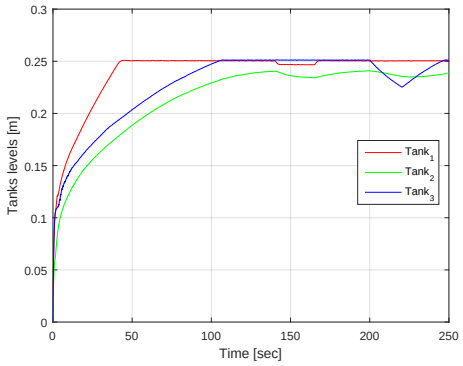

Figure 7.49: States behavior due to leakages presence

Residual signals generated by using observer based, structural analysis, parameter estimation and modulating functions approaches are depicted in Figures 7.50, 7.51, 7.52 and 7.53-7.54, respectively.

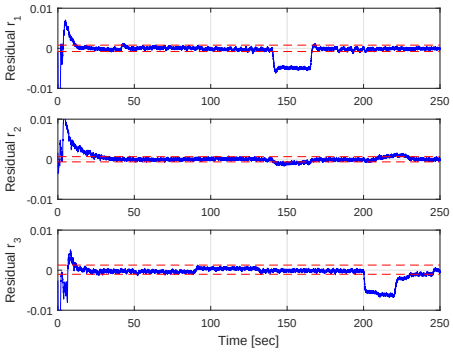

Figure 7.50: Observer based approach

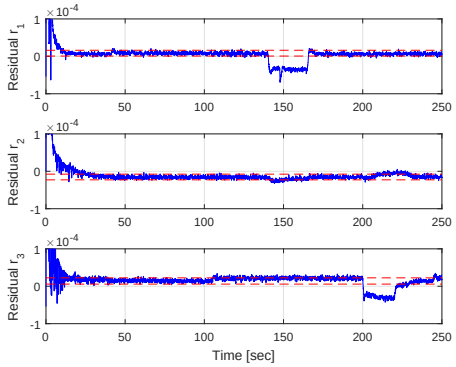

Figure 7.51: Structural analysis approach

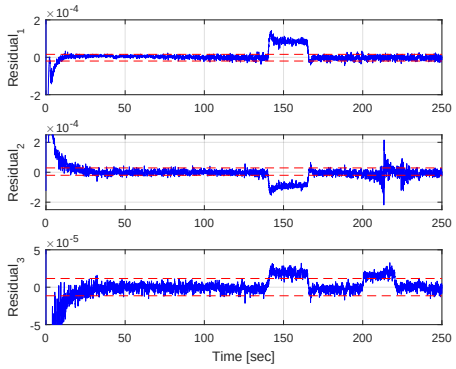

Figure 7.52: Parameter estimation approach

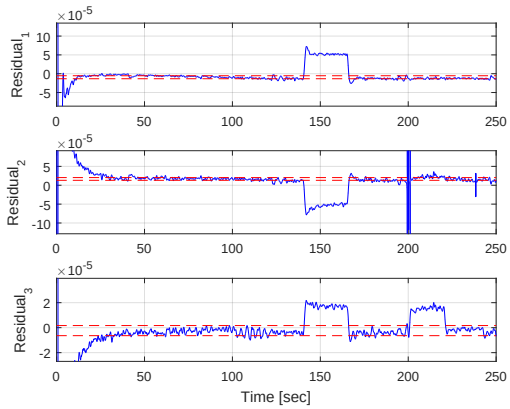

Figure 7.53: Based on estimated params.

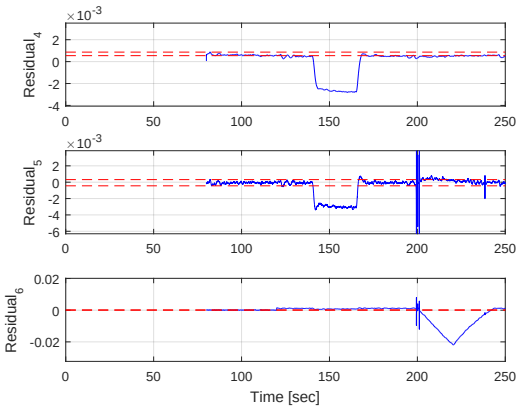

Figure 7.54: Based on estimated states

From these figures it can be noted that residual generated by each approach can be used to achieve a fault detection task. In the first two approaches and in the last one residuals have a notorious response whenever a fault has occurred and they can be used directly for an isolation task. That means, it is possible to know in which tank a fault appeared since r_i represents a leakage fault in tank i. In the case

of parameter estimation approach it is not possible to isolate a fault by using the residuals independently since, for example, more than one residual exceeds the fixed threshold when a fault in the first tank has taken place. Also, at residual r_2, there is a presence of a pair of peaks around the instants in which states x_2 and x_3 cross each other. As a consequence, there is a likelihood performing a false detection. However, fault detection may still be achieved by using this residual with the other two.

8 Conclusions

Different residual generation approaches have been developed and implemented for both, simulation model and a real three tank system, considering in each case different possible faults with and without the presence of noise.

In the case of structural analysis approach, presence of noise can make a good residual generation difficult, but it can be overcome by processing the measured signals before they will be used to generate the residuals. Also, it is necessary to model and consider all the possible faults in order to make the generator system sensitive to all the possible faults. However, in the performed tests, it can be relatively simple to isolate the faults directly from the residuals, which can not be done by using a parameter estimation approach. This technique has been capable to detect all the considered faults and it does not have many problems when subject to noise, since the derivatives are not directly computed, but estimated by using Levant's differentiator. In the case of observer based approach, the use of a sliding mode concept has made the reconstruction of the fault possible which may be used then as important information for a reconfiguration of the control system in case of faults.

Additionally to the approaches mentioned, a modulating function approach has been used in this thesis work. By using this technique it can be achieved a finite and simultaneous parameter and state estimation. Since both can be estimated, a bigger set of residuals based on the estimated parameters and estimated states is made possible. In the performed simulations it was possible to see that residuals are well generated and can be used for a well fault detection. Also, since this approach does not compute the derivatives from the measured signals, the noise issues are avoided and as it was shown, the estimation of both, parameters and states does not present a detrimental amplitude of coupled noise.
An important addressed issue is the residual generation for the three tank system not only in one of its working regions, but in the four possible ones. Most

literature has developed and implemented the approaches in only one working region but in this work all of them have been taken into account and it was possible to see that the residual generation was well done independently of the working region and the residual could be used to achieve a fault detection.
The change on the states location leads to intersections of the states in which the three tank system presents singularities. Hence, it was seen that in these critical points the observable mapping may be not well defined and the Jacobian of the inverse of the observable mapping may present a column of zeros which leads to a non-observation of the states. In the same way, the identifiability analysis of the parameters showed that in this critical points the parameters are not identifiable since the Jacobian identifiability matrix has not a full rank. As a consequence, it is possible that when states lie near these critical points, the residual generation can not be well performed. In order to overcome this problem, an algebraic approximation around the critical points has been done and then residuals can be generated so the fault detection can still be achieved. However, the problem is not totally avoided since there is a presence of peaks or a series of peaks in the residuals which may be lead to a false fault detection. Though by using the residuals signals together it is still possible to perform the fault detection.
In the case of the modulating function approach, residuals present some peaks around the critical points which can also lead to a false detection, but since there is a residual which has no presence of peaks, fault detection can be performed.

In the implementation of the studied approaches in the real system, the residuals are generated and they can be used then for a fault detection. Although not all the possible studied faults were able to be simulated in the real system, the simulated ones could be detected. Because of own characteristics of the system, it was not possible or it turns complicated to perform a state location change through the four possible regions but in the two considered regions the fault detection was able to be achieved. However, by using the parameter estimation approach, residuals are not very clear when the states are around the critical points, presenting some peaks or a series of peaks which can also lead to a false detection. In other cases, there was not a clearly presence of peaks and the residuals can be used to perform a fault detection.
It is also important to notice that using the modulating functions approach, residuals generated based on the estimated parameters has a clear less presence of noise than the residuals generated based on the parameters estimated approach. This effect

corresponds directly to the own property of modulating function approach which does not compute directly the derivatives of the measured signals, avoiding most of the issues that take place when exist a presence of noise in the sensor readings. Also, since these residuals based on the estimated parameters do not present a chain of peaks which can lead to a false detection of the fault, like in the case of the parameter estimation approach, the fault detection can be performed well.
From the practical implementation in the real system it can be noticed that each approach has advantages and at the same time some problems, so it could be better to use a particular one in a specific case, depending on the possible faults in the system and its own characteristics.

Bibliography

[1] R. Isermann, *Fault-diagnosis applications: model-based condition monitoring: actuators, drives, machinery, plants, sensors, and fault-tolerant systems*. Springer Science & Business Media, 2011.

[2] E. Sobhani-Tehrani and K. Khorasani, *Fault diagnosis of nonlinear systems using a hybrid approach*, vol. 383. Springer Science & Business Media, 2009.

[3] R. Isermann, *Fault-diagnosis systems: an introduction from fault detection to fault tolerance*. Springer Science & Business Media, 2006.

[4] M. Blanke, M. Kinnaert, J. Lunze, M. Staroswiecki, and J. Schrder, *Diagnosis and fault-tolerant control*. Springer Publishing Company, Incorporated, 2010.

[5] S. Ding, *Model-based fault diagnosis techniques: design schemes, algorithms, and tools*. Springer Science & Business Media, 2008.

[6] J. Chen and R. J. Patton, *Robust model-based fault diagnosis for dynamic systems*, vol. 3. Springer Science & Business Media, 2012.

[7] S. Simani, C. Fantuzzi, and R. J. Patton, *Model based Fault Diagnosis in Dynamic System using Identification Techniques*. Springer, 2003.

[8] C. Join, H. Sira-Ramirez, and M. Fliess, "Control of an uncertain three tank system via on-line parameter identification and fault detection," *Proceedings of 16th IFAC World Congress, Prague*, 2005.

[9] S. X. Ding, *Data-driven design of fault diagnosis and fault-tolerant control systems*. Springer, 2014.

[10] H. Noura, D. Theilliol, J.-C. Ponsart, and A. Chamseddine, *Fault-tolerant control systems: Design and practical applications*. Springer Science & Business Media, 2009.

[11] R. Isermann and P. Balle, "Trends in the application of model-based fault detection and diagnosis of technical processes," *Control engineering practice*, vol. 5, no. 5, pp. 709–719, 1997.

[12] S. K. Kanev, *Robust fault-tolerant control*. PhD thesis, University of Twente, 2004.

[13] A. Q. Khan, *Observer-based fault detection in nonlinear systems*. PhD thesis, Universität Duisburg-Essen, Fakultät für Ingenieurwissenschaften» Elektrotechnik und Informationstechnik, 2011.

[14] M. Witczak, *Fault Diagnosis and Fault-Tolerant Control Strategies for Non-Linear Systems: Analytical and Soft Computing Approaches*, vol. 266. Springer Science & Business Media, 2014.

[15] M. Witczak, *Modelling and estimation strategies for fault diagnosis of non-linear systems: from analytical to soft computing approaches*, vol. 354. Springer Science & Business Media, 2007.

[16] L. Chen, *Model-based fault diagnosis and fault-tolerant control for a nonlinear electro-hydraulic system*. PhD thesis, Kaiserslautern, Techn. Univ., Diss., 2010, 2010.

[17] R. Martinez-Guerra and J. L. Mata-Machuca, *Fault detection and diagnosis in nonlinear systems*, vol. 10. Springer, 2014.

[18] M. Zeitz, "The extended luenberger observer for nonlinear systems," *Systems & Control Letters*, vol. 9, no. 2, pp. 149–156, 1987.

[19] E. Ergueta, R. Seifried, R. Horowitz, and M. Tomizuka, "Extended luenberger observer for a mimo nonlinear nonholonomic system," *Proceedings of the 17th World Congress of the International Federation of Automatic Control, Seoul, Korea*, 2008.

[20] C. Christophe, V. Cocquempot, and B. Jiang, "Link between high gain observer-based residual and parity space one," *Proceedings of the American Control Conference*, vol. 3, pp. 2100–2105, 2002.

[21] H. Hammouri, M. Kinnaert, and E. El Yaagoubi, "Observer-based approach to fault detection and isolation for nonlinear systems," *IEEE Transactions on Automatic Control*, vol. 44, no. 10, pp. 1879–1884, 1999.

[22] C. De Persis and A. Isidori, "A geometric approach to nonlinear fault detection and isolation," *IEEE Transactions on Automatic Control*, vol. 46, no. 6, pp. 853–865, 2001.

[23] C. P. Tan and C. Edwards, "Sliding mode observers for detection and reconstruction of sensor faults," *Automatica*, vol. 38, no. 10, pp. 1815–1821, 2002.

[24] X.-G. Yan and C. Edwards, "Nonlinear robust fault reconstruction and estimation using a sliding mode observer," *Automatica*, vol. 43, no. 9, pp. 1605–1614, 2007.

[25] X.-G. Yan and C. Edwards, "Robust sliding mode observer-based actuator fault detection and isolation for a class of nonlinear systems," *International Journal of Systems Science*, vol. 39, no. 4, pp. 349–359, 2008.

[26] R. Sharma and M. Aldeen, "Fault detection in nonlinear systems with unknown inputs using sliding mode observer," *American Control Conference*, pp. 432–437, 2007.

[27] R. Hermann and A. J. Krener, "Nonlinear controllability and observability," *IEEE Transactions on automatic control*, vol. 22, no. 5, pp. 728–740, 1977.

[28] J. Gauthier and G. Bornard, "Observability for any u (t) of a class of nonlinear systems," *19th IEEE Conference on Decision and Control including the Symposium on Adaptive Processes*, no. 19, pp. 910–915, 1980.

[29] M. Hou, Y. Xiong, and R. J. Patton, "Observing a three-tank system," *IEEE transactions on control systems technology*, vol. 13, no. 3, pp. 478–484, 2005.

[30] M. Hou, K. Busawon, and M. Saif, "Observer design based on triangular form generated by injective map," *IEEE Transactions on Automatic Control*, vol. 45, no. 7, pp. 1350–1355, 2000.

[31] J. A. Moreno, "Nonlinear Observers : Continuous and Discontinuous," *Fakultätskolloquium*, 2015.

[32] K. Veluvolu, Y. Soh, and W. Cao, "Robust observer with sliding mode estimation for nonlinear uncertain systems," *Control Theory & Applications, IET*, vol. 1, no. 5, pp. 1533–1540, 2007.

[33] V. I. Utkin, *Sliding modes in control and optimization*. Springer Science & Business Media, 2013.

[34] Z. Ke-qin, Z. Kai-yu, S. Hong-ye, C. Jian, and G. Hong, "Sliding mode identifier for parameter uncertain nonlinear dynamic systems with nonlinear input," *Journal of Zhejiang University SCIENCE*, vol. 3, no. 4, pp. 426–430, 2002.

[35] M. Iqbal, A. I. Bhatti, S. I. Ayubi, and Q. Khan, "Robust parameter estimation of nonlinear systems using sliding-mode differentiator observer," *IEEE Transactions on Industrial Electronics*, vol. 58, no. 2, pp. 680–689, 2011.

[36] M. Anguelova, *Observability and identifiability of nonlinear systems with applications in biology*. PhD thesis, Chalmers University of Technology, 2007.

[37] M. Iqbal, A. Bhatti, S. Iqbal, Q. Khan, and I. Kazmi, "Parameter estimation of uncertain nonlinear mimo three tank systems using higher order sliding modes," *IEEE International Conference on Control and Automation*, pp. 1931–1936, 2009.

[38] H. Sira-Ramirez and S. K. Agrawal, *Differentially flat systems*. CRC Press, 2004.

[39] J. Guzinski, M. Digue, Z. Krzemiński, A. Lewicki, and H. Abu-Rub, "Application of speed and load torque observers in high speed train," *13th Power Electronics and Motion Control Conference*, pp. 1382–1389, 2008.

[40] M. Fliess and H. Sira-Ramirez, "Control via state estimations of some nonlinear systems," *IFAC Symposium on Nonlinear Control Systems*, 2004.

[41] B. Bandyopadhyay, S. Janardhanan, and S. K. Spurgeon, *Advances in Sliding Mode Control*. Springer, 2013.

[42] Q. Ahmed, A. Bhatti, and S. Iqbal, "Nonlinear robust decoupling control design for twin rotor system," *7th Asian Control Conference*, pp. 937–942, 2009.

[43] M. Iqbal, A. Bhatti, and Q. Khan, "Dynamic sliding modes control of uncertain nonlinear mimo three tank system," *IEEE 13th International Multitopic Conference*, pp. 1–7, 2009.

[44] M. Shinbrot, "On the analysis of linear and nonlinear systems," *Trans. ASME*, vol. 79, no. 3, pp. 547–552, 1957.

[45] G. Rao and H. Unbehauen, "Identification of continuous-time systems," *IEE Proceedings-Control Theory and Applications*, vol. 153, no. 2, pp. 185–220, 2006.

[46] J. Jouffroy and J. Reger, "Finite-time simultaneous parameter and state estimation using modulating functions," *IEEE Conference on Control Applications (CCA)*, pp. 394–399, 2015.

[47] S. Daniel-Berhe and H. Unbehauen, "Parameter estimation of nonlinear continuous-time systems using hartley modulating functions," *International Conference on Control, UKACC (Conf. Publ. No. 427)*, vol. 1, pp. 228–233, 1996.

[48] S. Daniel-Berhe, "Real-time on-line identification of a nonlinear continuous-time plant using hartley modulating functions method," *Proceedings of IEEE International Conference on Industrial Technology*, vol. 1, pp. 584–589, 2000.

[49] S. Ungarala, K. Miriyala, and B. Tomas, "On the estimation of time-varying parameters in continuous-time nonlinear systems," *Dynamics and Control of Process Systems*, vol. 10, no. 1, pp. 565–570, 2013.